

Development of highly functional microfluidic devices for biochemical analyses

Shishir Kanti Pramanik

February, 2019

Development of highly functional microfluidic devices for biochemical analyses

Shishir Kanti Pramanik

Doctoral Program in Nano-Science and Nano-Technology

Submitted to the Graduate School of
Pure and Applied Sciences
in Partial Fulfillment of the Requirements
for the Degree of Doctor of Philosophy in
Engineering

at the
University of Tsukuba

Abstract

Point-of-care testing (POCT) is indispensable for prompt on-spot diagnosis and treatment of acute diseases by providing diagnostic results rapidly even by non-trained personnel. For contemporary POCT diagnostic systems, the most imperative feature is the short analysis time and high sensitivity, with a “sample-to-answer” format. As a result, the microfluidics technologies have been spotlighted to meet the criterion of the POCT since they have remarkable features of high surface area to volume ratio resulting in fast diagnosis, reduced sample consumption, and a miniaturized format with portability and simplicity. The benefits of the microfluidic technology thus motivated to have widespread research determinations toward the development of clinical diagnostic POCT tools for detecting numerous types of analytes. The multiple functions within the chip are accomplished by the integration all of the functional modules into the devices. But, for the successful application of POCT microfluidic systems as a routine diagnostic tools, the accurate flow control in the integrated device with the automatic or programmed operation is remaining one of the major critical challenges. The fluid control is mostly performed by pumps and valves, which are operated mostly by an external instrument. Regarding the use by non-professional end users, more simplification method and the device function is required for processing of the multiple solutions to the sensing area along with the solution exchange facilities. Therefore, in this study, we presented an integrated microfluidic device with on-chip multiple solutions exchange facility with minimal user intervention for conducting bioassay. To realize the proper function of the integrated device, a novel polymer-based micropumps and conducting polymer-based switchable hydrophobic valves were incorporated into the microfluidic systems and the device applicability was demonstrated by performing immunoassay.

Primarily, a simple valve-less microfluidic device comprising of a reaction chamber and eight flow channels was introduced for the detection of proteins. Efficient exchange of solutions in a reaction chamber was accomplished by creating positive and negative pressure using the plastic syringe in which a solution was introduced into the reaction chamber and subsequently removed the solution from the reaction chamber through the same flow channels one by one. The effect of hydrophobicity of the bottom surface of the reaction chamber and viscosity of a blocking solution on the performance of solution exchange was studied. Using the device, human interleukin 2 (IL-2) can be detected by sandwich fluorescence immunoassay. The immuno-complex formed inside the reaction chamber (cAb-Ag-FITC-dAb) was monitored by fluorescence microscopy. The approach can be capable to detect IL-2 within 30 min. The surface treated with the oxidative solution (37% HCl, 30% H₂O₂ and ultra-pure H₂O with ratio 1:1:5) facilitated reducing non-specific adsorption of proteins. Clear dependence of fluorescence intensity on IL-2 concentration was observed in a range between 125 pg/mL and 2.0 ng/mL, and the detection limit was 105 pg/mL. Toward automation, the exchange of solution was demonstrated by the movement of a PDMS diaphragm to the downward and the upward. However, to achieve an automatic on-chip exchange of

solutions efficiently without end-user intervention, the development and integration of novel pumps were demonstrated.

For this purpose, the integration of a novel micropump based on a sodium polyacrylate polymer was reported for exchanging of solution within a microfluidic device. The pump was constructed with a freeze-dried disc of a superabsorbent polymer (SAP) and four individual PDMS layer. The polymer disc in the actuation chamber was swelled by the absorbing priming solution and the volume change of the disc assists to deflect the diaphragm toward the pump chamber which is provided a driving force to drive the fluid flow from the inlet reservoir to the reaction chamber. With this simple design, the injection flow rate was constant and the average value for deionized water was about 25.8 $\mu\text{L}/\text{min}$. This flow rate can be tuned by modulating the cross-sectional area of the pump chamber and by choosing an appropriate priming solution. The extraction of the solution from the reaction chamber was accompanied by placing the polymer disc into the extraction chamber. The extraction flow rates were varied with the sample solution to be exchanged and on their pH, and the composition of the materials used to prepare polymer disc. The highest extraction flow rate was achieved for a sample solution of DI water (0.70 $\mu\text{L}/\text{min}$) when the disc was prepared with ultra-pure water, sodium polyacrylate, and cellulose acetate at a ratio 1:1.5. Both of the injection and extraction flow rate are also sensitive to the viscosity of the sample solution to be exchanged. Thus, the superabsorbent polymer-based micro-pump, which are effectively applied to exchange a series of solutions in a controlled manner, can be broadly applicable for lab-on-a-chip based bioassays.

Additionally, to demonstrate the exchange of solutions with minimal user intervention, a novel switchable hydrophobic valve based on conducting polymer was developed to integrate the valve into the integrated device. Therefore, a simple tunable microvalve was developed for the control of microfluidic transport of solutions in microchannels. The valve consists of a sodium dodecyl benzenesulfonate-doped polypyrrole (NaDBS-doped PPy) film formed on a platinum electrode. The surface of the doped polymer film changes between hydrophobic and hydrophilic states when it is reduced or oxidized by the application of appropriate potentials. Type of dopant and polymerization time were critical in the wettability change of the coated polymer film. Average switching time was 5 s for the 50- μm long valve. Without applying the potential, the valve could stop the solution stable for more than 10 min even using the 50- μm long valve. The response time of the valve can be reduced by selecting an appropriate dopant concentration. Because of its simple structure and fabrication, many valves could easily be integrated into microfluidic systems and solutions could be transported in a network of flow channels as intended. Efficient exchange of solutions with minimal user intervention was demonstrated by integrating the valve into the integrated device for immunoassay. Since the developed microfluidic immunoassay platform is portable, consumed of minimum power, and provided on-chip solution exchange autonomously, the integrated device could be an effective tool for the POCT measurement of protein biomarkers.

Table of Contents

Abstract	i
Chapter 1: Introduction	1
1.1 Motivation.....	1
1.2 Challenges of point-of-care diagnostic devices in developing countries.....	3
1.3 Advances in microfluidic-based LOC technologies for global health/ POCT	5
1.3.1 On-chip sample preparation	6
1.3.2 Microfluidic immunoassays	7
1.3.3 Nucleic acid analysis on microfluidic platforms	9
1.3.4 Fully integrated microfluidic systems in POCT	11
1.4 Microfluidic components for flow control.....	13
1.4.1 Flow channels and its resistance.....	13
1.4.2 Microvalves	14
1.4.2.1 Active valves	14
1.4.2.2 Passive valves	16
1.4.3 Micropumps	18
1.4.3.1 Active pumping	18
1.4.3.1 Passive pumping	19
1.5 Scope and aim of this thesis	21
1.6 Structure of this dissertation	22
References	23
Chapter 2: Valve-less microfluidic device with push-pull sequential solution exchange function for fluorescence immunoassay	28
2.1 Introduction.....	28
2.2 Solution handling for on-chip sandwich immunoassay	29
2.3 Experimental	30
2.3.1 Reagents and materials.....	30
2.3.2 Fabrication of the microfluidic device	30
2.3.3 Solution exchange procedure	32
2.3.4 Tagging of detection antibodies with FITC.....	32
2.3.5 Procedure for on-chip fluorescence immunoassay	32
2.4. Results and Discussion	34
2.4.1 Optimization of the structure of flow channel.....	34
2.4.2 Exchange of multiple solutions	36

2.4.3	Device application to immunoassay	37
2.4.4	Reducing the non-specific binding of proteins	40
2.4.5	Towards incorporating micropumps	42
2.4.	Conclusions	42
	References	45
Chapter 3: Polymer-based on-chip micro-pump for the exchange of solutions in valve-less microfluidic device		47
3.1.	Introduction	47
3.2.	Objective of the propose study	48
3.3.	Experimental section	49
3.3.1	Reagents and materials	49
3.3.2	Preparation of the freeze-dried polymer disc	49
3.3.3	Design and fabrication of micropumps	51
3.3.4	Working principle and characterizing the pump	52
3.3.5	Calculation of the flow rate	54
3.4.	Results and discussion	54
3.4.1	Optimizing the structure of the pump chambers	54
3.4.2	Pump performance	57
3.4.3	Tuning of the injection and extraction flow rate	61
3.5.	Conclusions	62
	References	64
Chapter 4: Control of microfluidic solution transport by switchable hydrophobic microvalves based on conducting polymer		66
4.1.	Introduction	66
4.2.	Toward development of the novel valve	66
4.3.	Experimental	67
4.3.1	Reagents and Materials	67
4.3.2	Formation of the polypyrrole films	68
4.3.3	Measurement of the wettability of the NaDS or NaDBS-doped PPy film	68
4.3.4	Fabrication and operation of the valve	69
4.4.	Results and discussion	72
4.4.1	Characterizing the wetting behavior of the doped PPy film	72
4.4.2	Characterization of the valve	75
4.4.3	Decreasing the switching time	77
4.4.4	Controlled operation of the valve in microfluidic systems	77
4.4.5	Application to the flow focusing device	81

4.4.6	Application the valve to use repeatedly	84
4.4.7	Application of the valve into the integrated device	84
4.5.	Conclusions.....	85
	References	88
	Chapter 5: Summary	90
	Appendix	94
	List of publications	99
	List of conferences.....	99
	Acknowledgement	100

List of figures

Figure 1.1. Schematic illustration representing an expected POCT diagnostic	2
Figure 1. 2. PubMed documentations for Point-of-care diagnostics.....	4
Figure 1.3. Cell separation and concentration in microfluidic devices..	7
Figure 1.4. Microfluidic immunoassay-based diagnosis toward POCT.....	8
Figure 1.5. Microfluidic-LOC devices for POCT nucleic acid analysis.	10
Figure 1.6. Integrated microfluidic-LOC system for diagnosis of infectious.....	12
Figure 1.7. Active mechanical microvalves for realizing on and off flow	15
Figure 1.8. Active non-mechanical valves. (i) Electrochemical actuated	16
Figure 1.9. Passive valves. (i) SEM image of capillary valve system	17
Figure 1.10. Micropumps classification adapted from Laser & Santiago	18
Figure 1.11. Active microfluidics pump. (i) Structure of PZT type.....	19
Figure 1.12. Passive pumping system for autonomous microfluidic	20
Figure 2. 1. Schematic illustration of the exchange of solutions for	31
Figure 2.2. Microfluidic device for exchange of multiple solutions.	31
Figure 2.3. Schematic illustration of the solution exchange method:	33
Figure 2.4. Schematic illustration of one-step sandwich fluorescence	35
Figure 2.5. (A) & (B) The solution penetrate into the other flow.....	38
Figure 2.6. Images demonstrating sequential exchange of solutions	38
Figure 2.7. (A) Dependence of water contact angle on different reaction chamber	39
Figure 2.8. Detection of IL-2 by sandwich fluorescence immunoassay.	41
Figure 2.9. Efficiency of APTES-based immobilization of capture antibodies.....	41
Figure 2.10. Non-specific adsorption of FITC-dAb on the reaction surface.	43
Figure 2.11. (A) Schematic illustration of push-pull mechanism for	43
Figure 2.12. Exchange of multiple solutions by push-pull of the diaphragm.....	44
Figure 3.1. Mechanism of swelling behavior of SP by absorbing of an aqueous	50
Figure 3.2. Schematic illustration of the preparation of cylindrical.....	50
Figure 3.3. (A) Structure and design of the device with a single.....	53
Figure 3.4. Working principle of the SP polymer actuated micropumps	55
Figure 3.5. (A) Volume change of the polymer discs after absorbing water.....	55
Figure 3.6. Procedures showing the exchange of multiple solutions using the SP polymer actuated pumps.....	56
Figure 3.7. Injection flow rate of the SP polymer actuated pump	58

Figure 3.8. Solution extraction efficiency of the polymer disc using .	58
Figure 3.9. Images shows that exchange of multiple solutions using the SP	60
Figure 3.10. Dependence of the injection and extraction flow rate on	60
Figure 3.11. Dependence of the extraction efficiency of the	62
Figure 3.12. Dependence of the injection flow rate of DI water.	63
Figure 3.13. Dependence of the extraction pump efficiency on the d	63
Figure 4.1. Schematic of three-electrode electrochemical cell:	70
Figure 4.2. (A) Schematic of the microfluidic system with .	71
Figure 4.3. (A) Photograph of the experimental set-up for the formation.	73
Figure 4.4. Change in wettability of the doped PPy by the application of potential.	74
Figure 4.6. (A) Wettability behavior of the NaDBS-doped PPy film.	76
Figure 4.5. Dependence of the wettability changes	76
Figure 4.8. Dependence of switching time on applied.	78
Figure 4.7. (A) Flow control using a 100- μ m long valve.	78
Figure 4.9. (A) Schematic showing the effect of pH on the valve function	79
Figure 4.10. Dependence of the switching time on the storage time .	79
Figure 4.11. (A) Dependence of switching time on the dopant concentration	80
Figure 4.12. Precise solution manipulation and control is demonstrated.	82
Figure 4.13. Controlled microfluidic transport using multiple integrated valves.	83
Figure 4.14. PDMS flow focusing device with NaDBS-doped PPy based microvalve.	83
Figure 4.15. Device structure for the regeneration of the valve.	86
Figure 4.16. Exchange of solutions with minimal user handling steps.	87

Chapter 1: Introduction

1.1 Motivation

As a disease attacks a person, the risk or status of the diseases is evaluated by measuring the level of biomarkers which are the characteristic determinant of normal biological processes, pathogenic processes and pharmacologic responses to therapeutic intervention [1]. These biomarkers including mRNA expression profiles, circulating DNA and tumor cells, proteins, proteomic pattern, lipids, metabolites [2-4] are evaluated from physiological fluids such as urine, blood, tissues, serum or other exudates in relation to the infectious agents. Early diagnosis of the diseases causing biomarkers is important to improve the survival rates of the diseases.

Acute infectious diseases caused by pathogenic organisms have been the main reasons of global mortality and morbidity throughout the civic society [5, 6]. Due to the lack of inexpensive diagnosis, treatment, and unavailability of adequate healthcare infrastructure, people's in developing countries are threatened even with the remediable infectious diseases [7]. Each year around 3.5 million deaths from infectious diseases are caused by an improper diagnostics and treatments, and mostly they were poor and young children who were lived in poor and developing nations (Global report on infectious diseases of poverty (2012), WHO) [8]. Thus, Millennium Development Goals (MDGs) from United Nation (UN) sets a context for rapid diminish of infectious diseases. For the case of malaria infection, the successes have been ascribed to decrease of death rates of more than a quarter [9]. In spite of the positive outcomes, infectious diseases are leading causes of premature deaths in developing countries, for example, diarrhea, HIV/AIDS, tuberculosis, and malaria [10]. As a solution to this issue, total eradication of the infectious diseases will be the ultimate goal to control infectious diseases. A good successful example is observed in the suppression of smallpox [11]. However, some issues such as increases of the antibiotics resistance and the slow progress to find a potential vaccine are remaining the challenges toward the advancement of the effective tools toward complete eradication. Conventional laboratory tests such as enzyme-linked immunosorbent assay (ELISA), immunofluorescence, western blotting, immunodiffusion, polymerase chain reaction (PCR), flow cytometry have been used mostly for detecting infectious diseases and cancer [12, 13]. However, most of these assays are complex, needed long time to complete, require significant volumes of samples and reagents, and rely on bulky and expensive instrumental set-up limiting their wide-scale applications in rural and resource-poor countries. Thus, there is urgent need to develop a simple, inexpensive, portable new diagnostic tool to support point-of-care testing (POCT) that will provide a rapid and effective diagnosis of infectious diseases with high specificity and accuracy. Development of such devices can protect the spread of infectious diseases by detecting the biomarker earlier and taking follow-up treatment. The POCT diagnostic systems are an instrument

that does not involve the use of trained laboratory personnel and facilities to provide the *in vitro* diagnostic test results [14]. In order to satisfy the requirements for POCT, WHO has established a set of requirements toward the development of diagnostic tool in resources poor environments as follows: Affordable, Sensitive, Specific, User friendly, Rapid and robust, Equipment free and Delivered to the end user [15], which are abbreviated as ASSURED. Apparently, a “sample-to-answer” system is an advantageous format as users only required to load a sample to the systems and then the test results obtained after pushing a start button as shown in Fig. 1.1. It should be noted that the demand and market growth for *in-vitro* diagnosis has reached to US\$18 billion in 2016 [16]. Furthermore, Furthermore, the total diagnostic market relating to POCT of infectious diseases was approximately US\$7 billion with annual growth rates of more than 18%. [112].

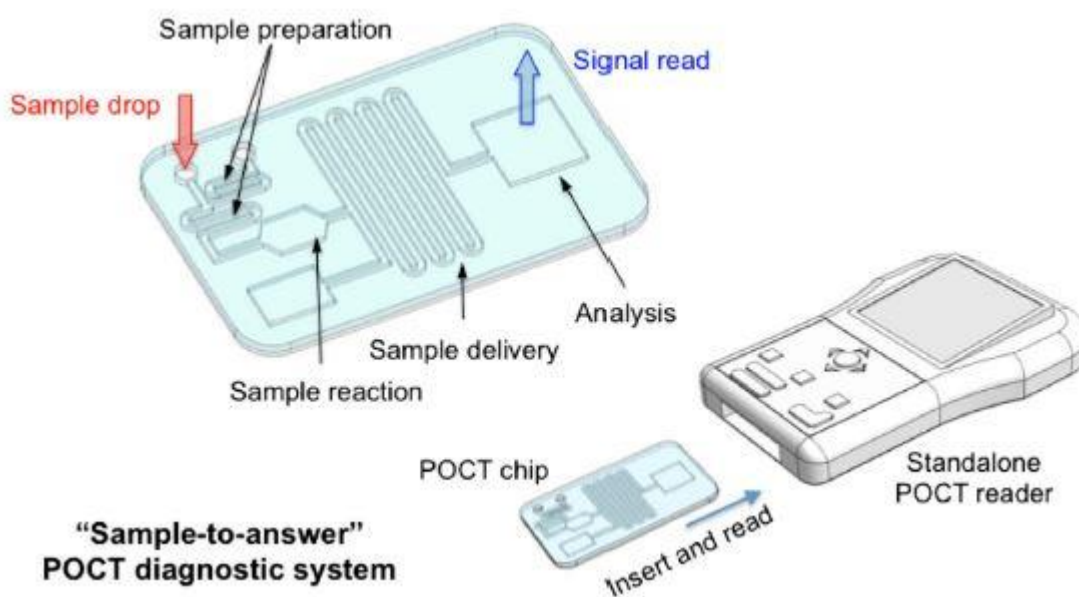


Figure 1.1. . Schematic illustration representing an expected POCT diagnostic system with the “sample-to-answer” competency. Reprinted from the reference [16]. Copyright 2015 Elsevier

In POCT, challenges attributed by typical diagnostic devices could be addressed by microfluidic technologies that meet the ASSURED criteria. These approaches allow on-chip diagnosis and real-time monitoring of infectious diseases from the small volume of bodily fluids [17]. In the development of an independent sensor, the microfluidic devices with the high capacity of integration of different type of assays have been performed routinely for bio-molecular analysis [18-23]. Currently, the lab-on-a-chip (LOC) technologies are promising for biochemical analysis, where microfluidic systems have been actively incorporated for understanding of the highly sophisticated analysis system [24]. However, to fabricate the microfluidic components for analytical devices, the complex micromachining systems [25, 26] have been presented a significant engineering challenge to make the simple device structure. Even though the integration of many mechanical pumps and valves on a chip may be possible, it

is difficult to operate collectively of these components for a certain microfluidic application. With the progress of the semiconductor-related micro-processing technology, the necessary components such as micro-pumps, valves, sensors for the micro total analysis system (μ TAS) can be fabricated by suppressing the configuration of the components for the usable on-device format. Furthermore, simplifying the structure and function of the components is a critical requirement for the high throughput sophisticated micro-analysis systems.

For detection and management of infectious diseases, immunological assay techniques have come to be an excellent candidate. However, immunoassay conducted with minimum equipment is mostly absent. Therefore, there is a growing interest to develop the miniaturized immunoassay into a microfluidic system that could be minimized of the manual operation, external power or pressure management. We expect that microfluidic technology could be enabled to provide more precise and authentic immunoassays than that of test strips system by offering benefits of (i) precise control of the liquid flow in microchannel, (ii) an opportunity of miniaturizing test areas, and (iii) an opportunity to enhance the assay sensitivity by integrating definite microfluidic elements.

This thesis describes the microfluidic platform and methods of exchange of multiple solutions autonomously especially for immunoassay purposes for promising POCT of the detection of infectious diseases. The solution exchange is accompanied by injecting a solution from the inlet to the reaction chamber and subsequently withdrawing the solution from the reaction chamber via the same flow channel. In this introduction, we focus on the necessity of a microfluidic platform for point-of-care testing, especially in resource-poor environments. Furthermore, we describe the basic components of the microfluidic system, and the current state and the technological barrier of lab-on-a-chip (LOC) systems in a routine bioassay in a poor resource area.

1.2 Challenges of point-of-care diagnostic devices in developing countries

LOC and microfluidic technologies have a remarkably advanced toward the development of portable diagnostic system by taking into account its small size, insignificant volume requirement for samples, and quick analysis, however, there is an argument for the benefit of the system to improve the healthcare of the developing nations. With the developments in integrating fluid actuation, sample pre-treatment, sample separation, signal amplification, and signal detection into a single device, truly, portable LOC devices are now using in a remote area with few resources. These devices are not yet applicable in the extreme resource-poor settings of developing countries; but, these developments place the field of LOC research in a leading position to challenge the overwhelming subject of global health. Fig. 1.2 shows an example of the importance and scientific relevance of POC diagnostic. Unlike other settings, LOC devices are experienced significant challenges such as technological, economical, policy-related, and cultural barriers for successful application of the tools in developing countries.

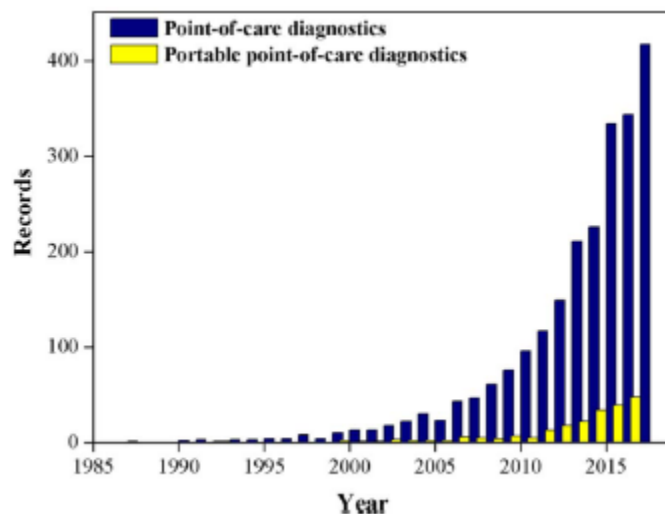


Figure 1. 2. PubMed documentations for Point-of-care diagnostics and Portable point-of-care diagnostic from 1990- 5th December, 2017. Reprinted from the reference [27]. Copyright 2018 Elsevier.

- **Material:** The cost of microfluidic devices can be reduced using an inexpensive component such as plastic instead of using expensive components like glass, quartz, and silicon. However, regarding the use of plastic, some of the challenges include minimization of batch-to-batch variation, improvement in chemical resistance, improvement in control over surface chemistry, and compatibility with fluorescence should be considered [28].
- **Storage and transportation:** Avoiding the controlled research environments, the LOC device will be adapted to diversified environmental conditions. Reagents, which are stored inside the microfluidic chip, must be stable to variations in temperature as well as physical shocks.
- **Sample pre-treatment:** For diagnostic purposes, whole blood and its derivatives (plasma and serum) and non-invasive samples such as saliva, urine are used. Before the analysis, the pretreatment of the sample is indispensable. In the central laboratory pretreatment was carried out with the help of trained staffs or using robots before injection into microfluidic diagnostic chip. In resource-poor area, automation and integration of on-chip sample preparation method with a minimal user intervention is desirable [29].
- **Sample solution transportation and control:** For an ideal LOC device, the fluid flow at a constant flow rate by the inexpensive and compact instrument is necessarily important. For portable devices, pneumatic actuation by battery or hand powered vacuum sources and capillary force could be a promising solution for transporting fluids in portable devices [30]. For complex assay in microfluidic devices, a series of multiple solutions need to be exchanged. In portable devices, passive delivery or on-chip valves operated with low power could be an attractive solution to deliver a series of reagents [31].
- **Signal detection:** Detection of signal generated from a small sensing region is considered a fundamental challenge in microfluidics. For portable devices, this detection should be inexpensive, and preferably, use

compact instrumentation that would be used little power. In this regard, electrical measurements such as current or conductance offers inexpensive and portable detection methods for practice in developing countries [32].

- **Standardization and connectivity:** The POC device can be designed and automated in consideration of communications and GPS recording rather than only for testing, processing, and data analysis. These can be important for secondary analysis. However, collection of test results from non-standard platforms are the most challenges toward the application of POCT devices in remote settings. Therefore, there is a requirement for design of set of widespread operation standards and procedures for telecommunication of test results.
- **Powering:** In POC devices, safe and constant power supply is necessary for diversification, such as, image collection, data handling, data conveying, and sample testing. As a solution, external auxiliary power packs, wireless energy transfer, high-capacity batteries, portable biofuel cells, lithium-ion rechargeable batteries, and piezoelectric materials could be utilized to overcome the constraint of power scarcity in POC devices [33].
- **Environmental impacts:** Several POCT platforms depend on heat-responsive chemicals and biological reagents which are denatured in tropical or harsh environments. Therefore, to solve this problem, improvement of the packaging and the refrigerator facilities are the main challenge for successful application of POCT in in poor-resource areas.
- **Commercialization:** In some cases, the POCT devices are expensive than those of conventional laboratory test. Thus, the cost of the POCT devices discourages the use it in poor countries. Additionally, numerous challenges such as, the patient's acceptance, limited investments, and commercialization can impede of the entry of POCT devices to the specific society or poor nations. With the above mentioned challenges in mind, the ideal POCT devices should be outlined in such a way which render a clear message of device performance and drawback for patients.

1.3 Advances in microfluidic-based LOC technologies for global health/ POCT

A LOC is a platform where complete bioassay protocols including sample collection, sample preparation, sample manipulation, and analysis can be performed. These multiple functions may be accomplished by integrating components including microfluidic micro-channel and active components such as valves, mixers, pump and sensor [34], which are integrated onto miniaturized chip using micro/nano-fabrication technology. LOC offers several benefits such as consumes insignificant volume of sample and reagents, provides rapid and portable analysis facility in an automated fashion [35]. LOC technologies comprised of microfluidic has a long history; it has been started from a basic research to the diagnostic products existing today in hospitals or clinics. In the early stage, the development of the revolutionized techniques such as gas chromatography and capillary electrophoresis was

introduced by manipulating the small liquid with high precision for biochemical analysis [36, 37]. At the same time, the development of continuous inkjet technology relies on precisely fluid control was introduced for inkjet printer named Siemens which was the first successful application of microfluidic devices [38].

Toward analytical applications, microfluidics techniques evolve as important platforms in the field of chemistry and pharmaceutical research. Furthermore, for advanced analysis of chemicals or molecules, the more precise manipulation of fluid in microfluidic is indispensable which can facilitate by the development of micropumps [39] and microvalves [40]. After a decade, the idea of miniaturized micro total analysis systems (μ TAS) was familiarized by Manz et al., where pretreatment of sample, separation, control, and detection were performed in a chip. At the same time, researchers were interested in developing of a portable device for sensing with good selectivity and storage stability. Although initial focus was improved the performance of the devices by miniaturization, after that, it became in interesting of analysis small volumes of samples with short analysis time. Toward POCT, microfluidics and lab-on-a-chip technologies have been particularly highlighted and widely studied because of consumption of minute volume of sample and reagent, high capability of integration, and fast reaction from the miniaturize platforms [34,41-43]. Also, the development of the POCT tools is advancing from the massive potential of microfluidics to detect specific biomarkers of proteins, cells, nucleic acids, metabolites, etc. Various steps are usually involved in a microdevice for specific analysis and detection of the analytes.

1.3.1 On-chip sample preparation

Sample preparation on-chip is the critical requirement for POCT devices. In the clinical diagnostic test, samples used for the analysis usually contain very low concentrations of the target analytes. Thus, concentration steps as well as cell separation steps are inevitable to carry out a reliable and reproducible detection [44]. Numerous techniques in microfluidics platforms are being used for the target cell concentration and separation. Unlike centrifugation and filtration [45], the technique of the obstacle structure in microfluidic channel [46], porous polytetrafluoroethylene (PTFE/TeflonTM) membrane [47], deformation (contraction and expansion) of channel [48], dielectrophoresis (DEP) [49] have been reported to enrich and separate of the cell with high efficiency. Effective technique based on the immunoaffinity was reported [50]. For these purposes, aptamers and antibodies are commonly used. Lin and colleagues demonstrated an aptamer-based “sandwich” assay on a microfluidic chip for the capture and detection of rare cells, and the capture efficiency of the target was more than 70% with the purity of 90% [51]. A standard strategy such as antibody-conjugated magnetic bead-based cell separation has been investigated in microfluidic platforms for rapid detection of dengue virus [52], influenza virus [53], and *S. aureus*

[54]. For cell separation and concentration, different approaches in microfluidic devices are used for the detection of biomolecules (Fig.1.3).

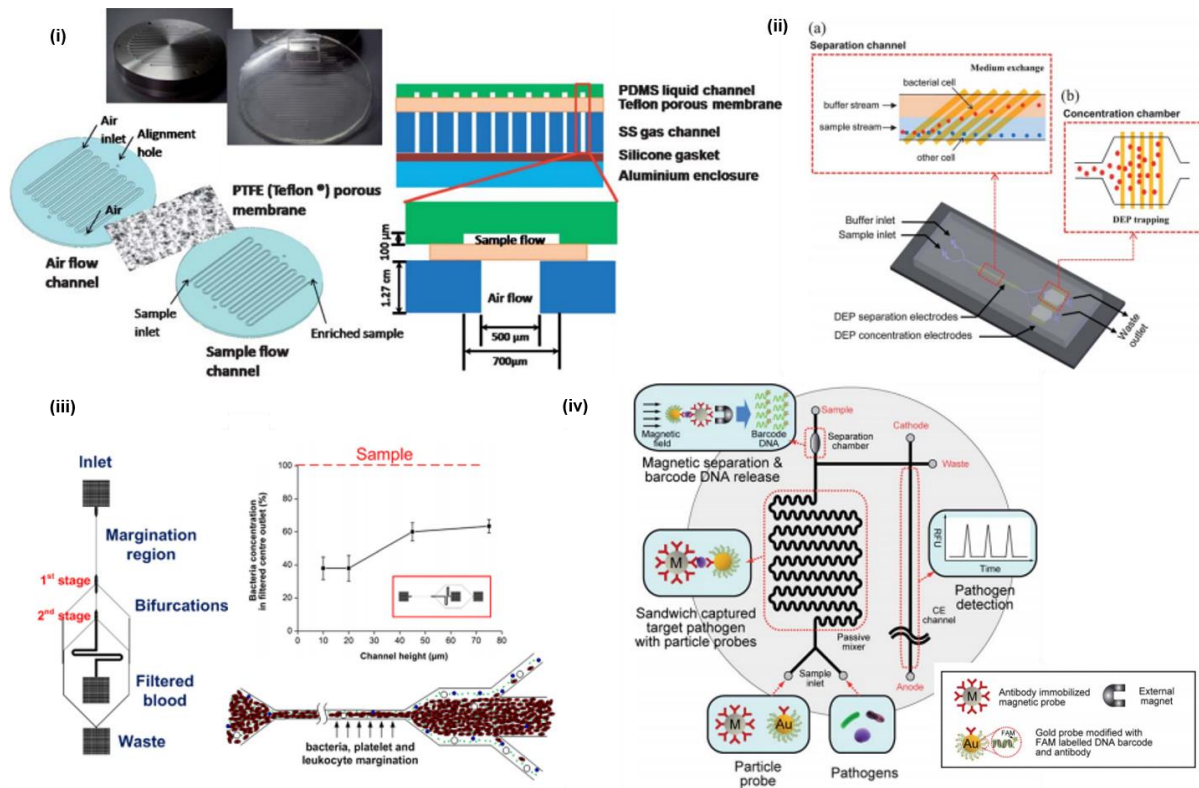


Figure 1.3. Cell separation and concentration in microfluidic devices. (i) Filtration of *Escherichia coli* (*E. coli*) using porous PTFE (TeflonTM) membrane. (ii) Microfluidic device for continuous cell separation and concentration with dielectrophoresis (DEP) approaches. (iii) High-throughput inertial microfluidic device for *S. cerevisiae* removal from blood with higher proficiency. (iv) Representation of integrated PMMS-CE microdevice for isolating and purifying the target *S. aureus*. After that, using microfluidic capillary electrophoresis, nucleic acids of *S. aureus* are analyzed. Fig. i-iv adapted from the ref. [48], [55], [49], [54], respectively.

1.3.2 Microfluidic immunoassays

As the wide range of infectious diseases are identified by a change in protein concentrations in a patient's physiological fluid, proteins have been represented as an important POCT biomarker for the diagnosis of diseases [56]. In clinical testing and diagnosis, immunoassays have routinely been used to detect and quantify protein biomarkers. The use of antigen-antibody interactions facilitates the analysis of proteins with high specificity and sensitivity. Currently, immunoassay on microfluidic platform has been extensively researched [57- 59]. However, the assay results on microdevices are largely affected by the performance of the liquid driving system. To perform the microfluidic-based miniaturized immunoassay, several types of fluidic transportation systems have been reported using the pressure forces, electrical forces, and centrifugal forces. Pressure-driven fluid control can be realized using a micro pneumatic pump in the multilayer microfluidic device. The pump consists of a liquid flow

microchannel, flexible PDMS membranes, and air chambers. The pump is operated by the deformation of the PDMS diaphragm in sequence pneumatically via compressed air [60] and the pump is an appropriate to deliver the reagent sequentially for immunoassay purpose. With the micro pneumatic pumps along with microvalves, Lee and his coworkers detected dengue virus [61], hepatitis C virus, and syphilis [62] from serum samples. Additionally, Lafleur et al. developed a disposable multiplexed sample-to-result microfluidic device to detect the malaria antigen and immunoglobulin M (IgM) (Fig. 1.4 i) [63].

On the other hand, the electrokinetic flow control based on electric forces generated by electroosmosis can facilitate the automatic fluid flow [64]. The flow control depend on electric forces is produced by electroosmosis. As the electric field is applied, the solvated ions and their hydration sheath are driven to the oppositely charged electrode while dragging the bulk fluid via viscous forces to create a constant plug-like flow [13, 60]. As a result, the step of flow switching, sequencing, and stops can easily be attained by applying an electric field in a controlled manner. Based on this principle, Gao et al. detected multiple microbial antigens simultaneously [64]. Additionally, to drive the fluid flow in microfluidic devices, centrifugal force is usually used. To drive fluid flow using centrifugal force, the device was constructed with the flow channel and microchamber [65]. This platform was

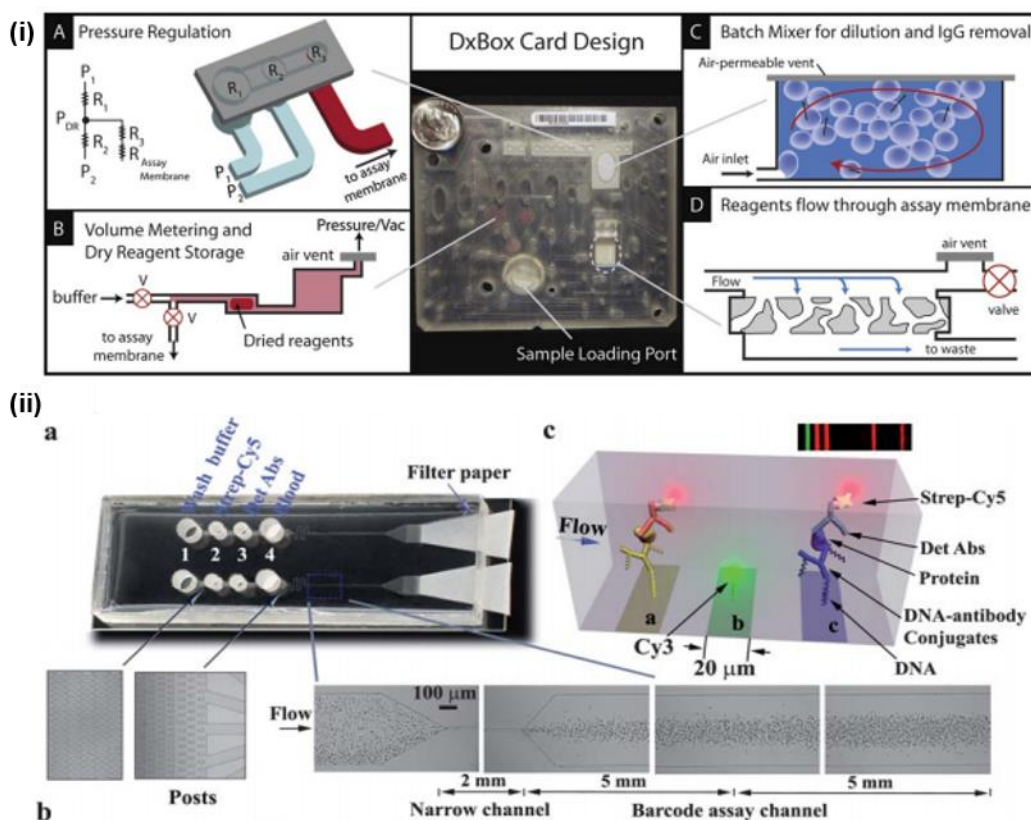


Figure 1.4. Microfluidic immunoassay-based diagnosis toward POCT. (i) Multiplex immunoassay for parallel detection of disease-specific antigen and IgM. The pneumatically-controlled cards used hydrophobic membranes as air-permeable vents to perform some key functions. (ii) Self-powered chip for multiple protein detection from whole blood. Fig. (i) and (ii) adapted from ref. [63], [71], respectively.

incorporated into the existing optical detectors to perform multiple assays. Several studies have been reported of CD-based immunoassaying in either bead- or surface-based heterogeneous formats [66, 67]. Using the pioneering approach, Lee et al. developed a fully automated immunoassay for the detection of hepatitis B virus [65].

To fabricate inexpensive, portable POCT devices, simplification of the device structure and function is of specific interest. Thus, the use of the passive capillary forces to drive the fluid flow could be promising compared to that of pump based on the external component to operate. The Alere Triage® system [68] is one of the effective commercial immunoassay for POCT. Like the lateral-flow assays, the labeled detection antibodies were conjugated first with the target antigens in a sample, followed by introducing the solution mixture into the detection zone where capture antibodies are pre-immobilized. Regarding the higher reproducibility, the improvement in the Triage cartridge is achieved by replacing the nitrocellulose membrane from the lateral-flow assays with the polymer microfluidic channels. The passive capillary flow was used for this system. The fluid flow in the lateral-flow assay is controlled using a spatial hydrophobic area termed “Timegate” which is enabled to regulate flow rate and the incubation time of the labeled detection antibodies in a controllable way. Instead of gold colloids, fluorophore was used in the Triage cartridge as a labeling reagent. All these collective features enabled the Triage cartridge to detect cTnI, CK-MB, myoglobin, from whole blood with high sensitivity and high reproducibility for revealing acute myocardial infarction [69]. Toward POCT, the Triage cartridge has met the POCT requirements by (i) eliminating an active pumps and valves by autonomous passive flow with a manageable flow rate, (ii) using low cost materials, (iii) minimizing the user interventions such as sample processing, fluidic control, and injection of reagents, (iv) providing fast test results (within 30 min) and comparable to bench-top systems, and (v) easy analysis with simplified analyzers. Following the success of the Triage cartridge, Gervais and Delamarche were followed the same principle to detect CRP from human serum in which automatic fluid flow was achieved using the capillary forces [70]. To detect multiple target proteins from 7 μ L of whole blood, Wang et al. presented an automatic fluid flow in microfluidic device using passive pump along with micro-pillars and an absorbent paper [71]. As an alternative device for high-throughput multiplex detection of pathogen, paper-based microfluidic devices have used for the detection of hepatitis B [72], HIV-1 [73], malaria protein Pf HRP2 [74]. Fig.1.4 shows immunoassay on microfluidic- LOC for POCT.

1.3.3 Nucleic acid analysis on microfluidic platforms

Nucleic acid analysis can give evidence for pathogen detection to supplement the protein analysis of antigens and antibodies. Thus, detecting of nucleic acids provides high sensitivity and specificity in diagnosing specific diseases, because of its amplification ability and specific base pairing of complementary nucleotides, respectively. For the diagnosis of the nucleic acid in POCT configuration, microfluidic technology is auspicious to the miniaturization by integrating various complex functional components such as sample lysis, nucleic acid purification, amplification, and detection of amplified targets in a single cartridge [75].

Easley et al. demonstrated an integrated microfluidic genetic analysis system comprising of nucleic acid extraction, PCR, and electrophoresis regions [76]. The flow control was demonstrated using a single syringe pump and five elastomeric normally closed on-chip valves. By solving the PCR inhibition factor, they detected of 15–45 ng of murine DNA anthrax in whole blood, in which assay time was 30 min. Lee and his coworker developed integrated nucleic acid analysis device based on on-chip peristaltic micropumps, suction-type micropumps, and microvalves (Fig. 1.5 (i)) [75]. For mitochondrial DNA mutation and HIV-1 detection, DNA-conjugate magnetic beads were used to capture target DNAs. In contrast to the bench-top PCR machine, the device presented identical band intensities in detecting 100 cells/ μL from the HIV-infected T cell line. Zhou et al. also presented nucleic acid-based diagnostic approach [77] (Fig. 1.5(ii)). By incorporating on-chip pumps and valves, the low-cost, disposable plastic device presented to detect of the sexually transmitted infectious agent, *Neisseria gonorrhoeae*. All assay steps such as cell lysis, nucleic acid purification, multiplex PCR were performed within the device, and end-point analysis was carried out in an automatic fashion.

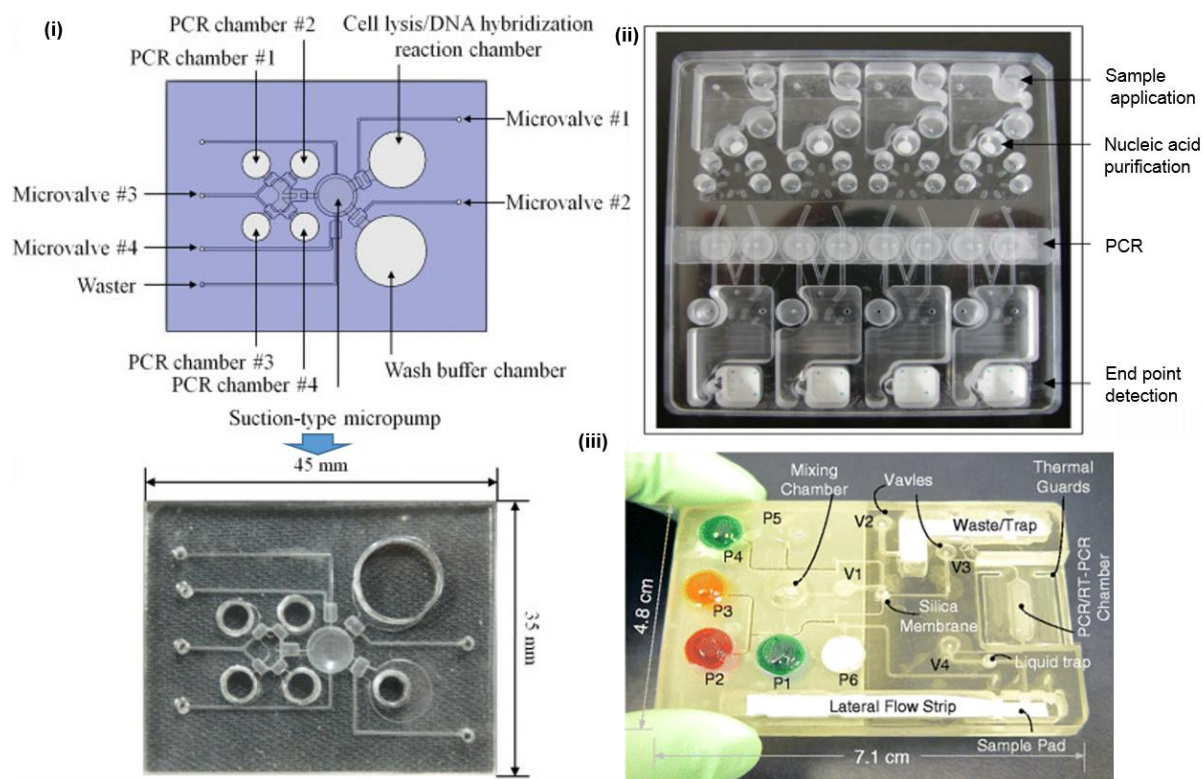


Figure 1.5. Microfluidic-LOC devices for POCT nucleic acid analysis. (i) Integrated nucleic acid analysis device with on-chip sample processing, sample pretreatment and PCR process for HIV-1 detection. (ii) A Rheonix Quad CARD with integrated pumps and valves that is enabled of performing up to four real-time molecular assays.(iii) A fully integrated sample- to-answer disposable plastic lab-on-a-chip for detecting viral HIV RNA in saliva. Fig. (i-iii) are adapted from ref. [75], [77], [78], respectively.

“Sample- to-answer” disposable plastic lab-on-a-chip was developed by Chen et al. for the detection of pathogen RNA as a POCT system [78]. The chip was comprised with a silica membrane, pouches, and valves for

fluidic control, and PCR chamber for performing on-chip sample lysis, nucleic acid purification, PCR (RT-PCR), amplicon labeling, and detection by integrating lateral flow strip (Fig. 1.5(iii)). This lab-on-a-chip can meet the major criterion of the nucleic acid POCT diagnostic systems and the system could detect viral HIV RNA in saliva.

However, the development of POCT nucleic acid diagnostic systems involve more complex procedures, long analysis time, more different reagents, a wide range of technologies and research than that of protein analysis. Additionally, the bulky nature of the subsystems such as, high-voltage and high-power systems have not been successfully made the system in realizing portable. For POCT, instead of PCR system for DNA amplification sequence-specific isothermal amplification methods [79], which disregard the necessity for thermal cycling process, can be suitable.

1.3.4 Fully integrated microfluidic systems in POCT

An integrated LOC system is referred that all the analytical steps for clinical samples diagnosis such as, sample pretreatment and pre-concentration, flow actuation and control, removal of PCR inhibitors, PCR amplification (nucleic acid analysis), detection of the amplified targets and analysis are performed on a single monolithic device by the incorporation of the components. During the last decade, many studies have been reported in realizing of the integrated chip-based analysis of various clinical samples, such as whole blood [63], oral fluids [80], urine [81], and serum [23]. These processes are based on nucleic acid amplification. To detect the H1N1 virus from a throat swab sample, the microfluidics based fully integrated, disposable, portable device was realized and all the necessary analytical steps including immunomagnetic target capture, pre-concentration and purification, PCR amplification, and sequence-specific electrochemical detection steps were carried out in a single chip [82]. Furthermore, numerous bacterial pathogens from oral fluids have been detected using integrated LOC systems in which lateral flow assay strip was incorporated [78] for the detection of *Bacillus cereus* and HIV. The whole process of the assay (from sample preparation to detection) was completed within 1 h. Fig. 1.6(i) shows the LOC systems for on-chip DNA analysis in a remote area with poor resources [83].

For the detection of pathogens of infectious diseases, an immunoassay on the microfluidic device is a promising technique. Therefore, to understand the antigen-antibody interaction in microfluidic immunoassaying, transducers such as, fluorescence, SPR imaging, SERS spectroscopy, and electrochemical (amperometry and potentiometry) have also been used [84]. For instance, a disposable multiplexed sample-to-result microfluidic device has been demonstrated to detect *S. typhi* with a LOD of 10 ng mL^{-1} [63]. Otherwise, a remarkable POCT microchip has been developed to detect HIV and syphilis at high sensitivity and specificity, in which the test result can be provided within 20 min (Fig. 1.6 (ii)) [73].

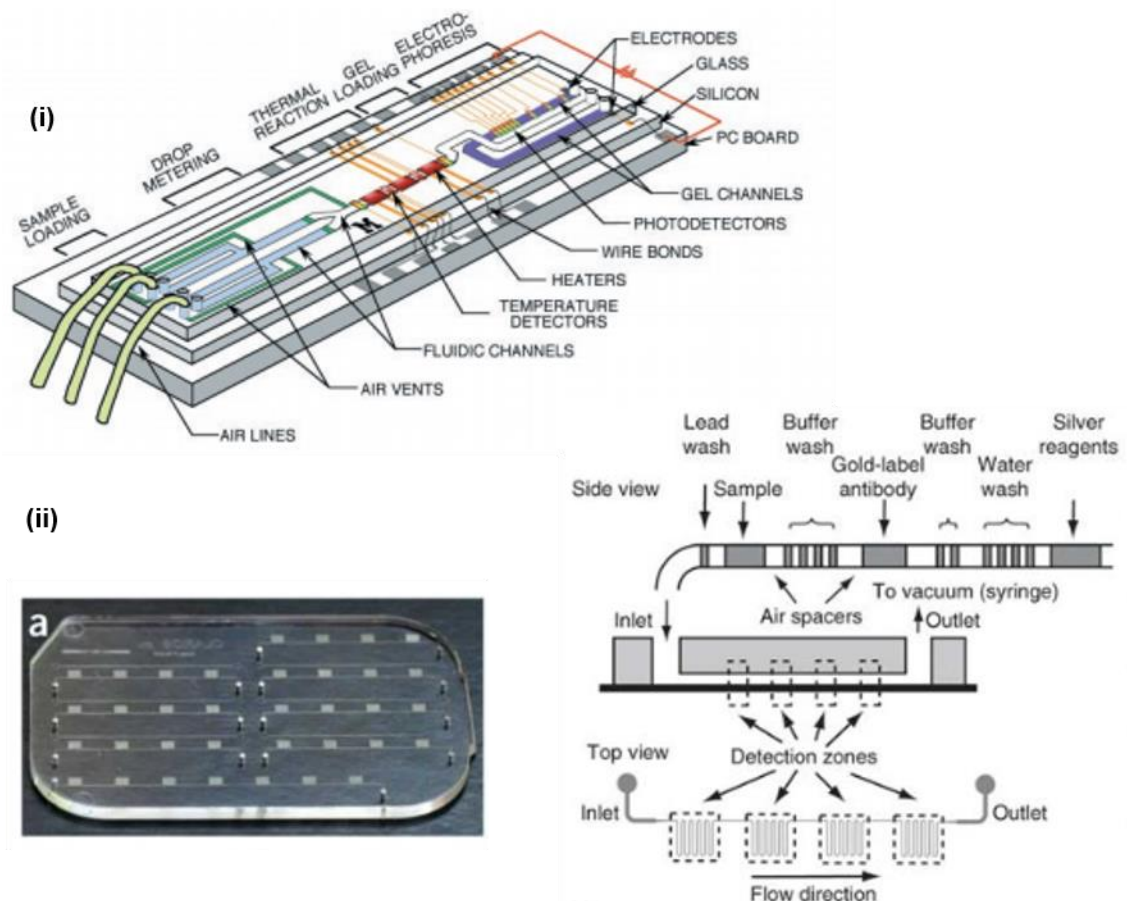


Figure 1.6. Integrated microfluidic-LOC system for diagnosis of infectious diseases in developing countries. (i) DNA analysis using LOC methods in which necessary components are incorporated in the device. (ii) Multiplexed detection of HIV and syphilis based on immunoassay using integrated microfluidic-LOC device in which passive fluid delivery of preloaded reagents was demonstrated over four detection zones by the vacuum generation using a disposable syringe. Fig (i) and (ii) adapted from ref. [83], [73].

Table 1. Commercially available POC infectious diseases diagnostic systems using microfluidic platforms (adapted from ref. [84])

Pathogens	Analytes	Technical features	Company	Website
Bacterial and viral	Primer	Disposable cards with benchtop analyzer, on-card sample processing	Cepheid	cepheid.com
Influenza, Bacterial	Primer	Portable detector, discs with on-extraction	Focus Dx (Quest)	focusdx.com
Bacterial	Primer	Disposable cards with integrated heating, detection, sample processing in a portable instrument	HandyLab (BD)	bd-world.com
Viral	Primer	Automated analysis on Film	Idaho Technologies	BioFireDx.com
Bacterial, HIV/AIDS	Primer	Array™ instrument	IQuum	iquum.com
Bacterial	Primer		LabNow	labnow.com

		Lab-in-a-tube platform for automated analysis Compact tabletop analyzer utilizing membrane-based quantum dot detection		
Viral	Primer or Antibody	Disposable plastic discs (spinit®); label-free, portable SPR analyzer	Biosurfit	biosurfit.com
HIV/AIDS, hepatitis, flu	Primer or Antibody	Integrated fluidic cartridge and low-cost, low-power fluorescence imaging using planar waveguides	Mbio Diagnostics	mbiodx.com
Malaria	Primer or Antibody	Disposable cartridges composed of thin-film laminates and injection-molding	Micronics (Sony)	micronics.net
Bacterial, HIV/AIDS	Antibody	Portable analyzer, injection-molded plastic cassette, low cost optical detection of silver films	Claros Diagnostics	opko.com
Bacterial, HIV/AIDS	Antibody	Compact tabletop fluorescence instruments with disposable cards	LeukoDx	leukodx.com

1.4 Microfluidic components for flow control

Microfluidics is the arena of handling insignificant amounts of fluids (nL to μ L) in sub-millimeter size channels. Fluids exhibit distinctive characteristics inside flow channels. Additionally, for effective μ TAS or LOC systems, microfluidics is one of the remarkable sophisticated emerging science in the field of biochemical analysis. In LOC devices, the integrated fluidic operations are accomplished with a number of components including microchannels, microvalves and micropumps, micromixers, and cell separators. Among these components, microvalves and micropumps have been used solely or collectively to control fluid flow in many analytical devices. In this section, I briefly describe the flow control elements such as microchannels and its resistances, microvalves and pumps for the proper functioning of microfluidic devices toward biochemical analysis.

1.4.1 Flow channels and its resistance

Various components in microfluidic system are connected through the flow channels. The flow channels are characterized by its fluidic resistance. Typically, the flow regime in a macroscale tube is turbulent and the flow regime in a microchannel is laminar. The dimensionless numbers Reynolds number, Re , is given insight of the flow regime, and is defined as the ratio of kinetic energy (ρv^2) and viscous energy ($\eta v/d$).

$$Re = \frac{\rho v d}{\eta}$$

Where, d is the hydraulic diameter of the flow channel, v the average velocity, ρ the mass density of the fluid, η the viscosity of the fluid. For rectangular flow channel $d = 2wh / (h + w)$, where w and h represents the flow channel width and height, respectively. At low Reynolds number, typically less than 1000, the flow in the flow channel is laminar, and at $Re \ll 1$ the flow is moving slowly, i.e. viscous forces govern completely, and inertial forces become insignificant [85]. In laminar flow, layers of liquid flow side by side without crossing streaming line. In microchannel, laminar flow created by pressure typically exhibits a parabolic velocity profile (the fluid has the highest velocity at the center of the channel and velocity along the channel walls has close to zero).

The fluidic resistance, R , of a channel can be considered to be a ratio of the pressure differences across the inlet and outlet of the flow channel, ΔP , and the volumetric flow rate, Q , in the flow channel: $R = \frac{\Delta P}{Q}$. At laminar flow environments, R is influenced by the channel geometry and the fluid viscosity η . For example, as $w > h$ for rectangular flow channel, the R is according to,

$$R = \frac{12\mu L}{wh^3(1 - 0.63h/w)}$$

Where, L , w , and h refers the flow channel length, width and height, respectively.

1.4.2 Microvalves

Valves are the indispensable elements for governing the movement of fluid in microfluidic channels by opening or closing the flow path. Numerous types of valves are involved in the microfluidic system to control the fluid flow in a microchannel based on the changes of the certain macroscopic parameter using a proper actuation method. Valve actuation can be active or passive which are included of mechanical, pneumatical, phase change, or by introducing external force [40]. Active valves which are actuated using an energy input often coming from a peripheral to the device. On the other hand, the actuation process for passive valves accompanied by exploiting energy potential in the device or the sample.

1.4.2.1 Active valves

Numerous actuation methods including electrical, magnetic, piezoelectric, thermal or optical are associated to operate most of the active mechanical valves in which a flexible membrane coupled to an actuator. Active valves can exhibit a reversible function by switching it between an open and closed state. These valves have fast switching times and low leakage and frequently utilized to repetitively dose liquid and manipulate liquid at high pressure. The most widely used PDMS valves were developed by Quake and colleagues and the valves can easily be fabricated and integrated massively [86]. The valve was fabricated by forming an elastomeric membrane at the

intersection of two perpendicular crossing channels. Upon the application of pressure through the control channel, the PDMS membrane is deflected and closes the flow channel (Fig 1.7 (i)). The normally closed valves are functioned using vacuum filled control channels. In immunoassays [87] and nucleic acid analysis [88], the PDMS valves on microfluidic chips have been investigated. These devices are powerful analytical tools in laboratories, however, the necessity of pneumatic tubes and external pumps have been made peripheral equipment large, and the minimization of the complexity of peripheral has been considered a major bottleneck to their use in POCT.

As a solution to minimize the peripheral equipment, solenoids or manual mechanical actuation have been utilized to develop a valve that can be opened and closed of PDMS channels[89]. The open and closed state of the valve was realized by tuning the screws embedded in a layer of polyurethane to collapse PDMS microchannels [90]. Another approach, the valving function is allowed using a magnetic inductor that can generate a force to pull up a silicon membrane electroplated with NiFe permalloy (Fig. 1.7 (ii)) [91].

Besides these actuation process, electrochemically driving method, and the phase transition phenomenon have been used to characterize the valves by the simple structure and made it suitable for disposable devices in POCT applications. The idea of an electrochemical type valve was reported by Suzuki and Yoneyama in 2003, in which electrochemical generation of the hydrogen bubble facilitates to deflect the membrane resulting in very rapid sequential opening and closing of the active check valve (Fig. 1.8 (i)) [92]. By applying 1.6 V, the valve area was deflected of about 30 ~ 70 μm . Some phase change materials have been used to develop the valves. For example, Kaigala et al. were developed a valve that was comprised with resistive heaters of Pt/Ti and PEG [93]. The PEG was changed its phase, by heating through the heaters, from solid to liquid with a large change in volume actuating a PDMS membrane microvalve (Fig. 1.8 (ii)). Valves fabricated from poly(N-isopropylacrylamide) polymer can be functioned using heat from a halogen lamp [94] or a magnetic field heating Fe₃O₄ nanoparticles in the polymer [95].

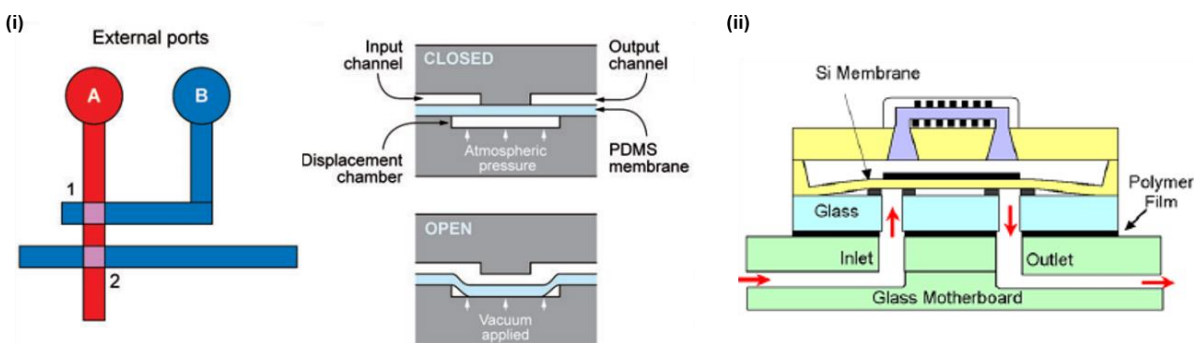


Figure 1.7. Active mechanical microvalves for realizing on and off flow control in microchannel. (i) Pneumatic latches and valves in PDMS. (ii) The normally closed magnetic microvalves coupled with magnetic inductor. Fig. (i) and (ii) are adapted from ref. [86] and [91], respectively.

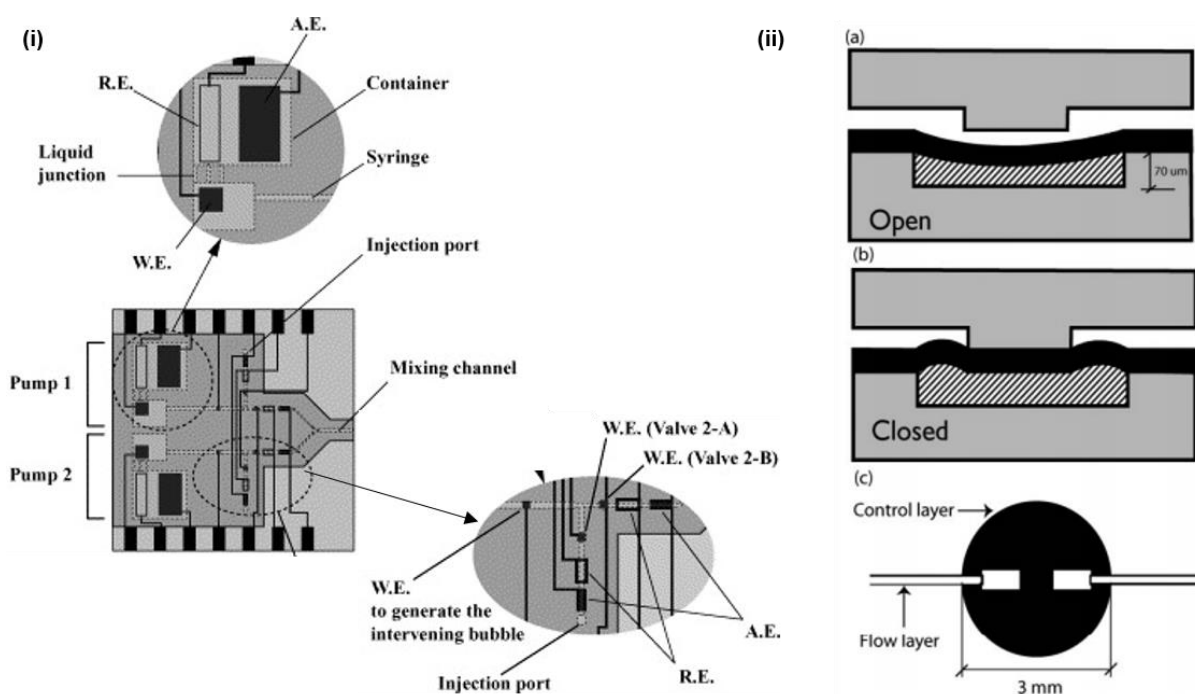


Figure 1.8. Active non-mechanical valves. (i) Electrochemical actuated check valve and pump.(ii) PEG based phase change valve. The phase change of the PEG is accompanied to the volumetric expansion that is used to actuate a flexible PDMS membrane to open or close a path between two discontinuous channels. Fig. (i) and (ii) are adapted from ref. [92], [93], respectively.

1.4.2.2 Passive valves

Passive valves stop the fluid in the area of the valve and valves function as one directional switch utilized to retard the flow of fluid or to stop the flow of fluid till the coming of one more. To carry out incubation steps and sequential steps, the passive valve could often be ideal in POCT devices. As for instance, a passive valve is a capillary valve that can be fabricated using an abrupt opening in a silicon microchannel Fig. (1.9 (i)) [96].The valve function is associated with a sudden expansion of the curvature of the filling front flattens the meniscus and stops the fluid flow. The valve can be initiated its function while a fluid flow forward via the parallel flow channel to the stopped meniscus when a second parallel channel brings the liquid to the stopped meniscus and combines with flow ongoing in a central flow channel. These valves are simple to fabricate and integrate, however, they can be untrustworthy as they rely on the chemical uniformity of the surface. Another promising capillary valve is the electrowetting valve in which the interfacial tension between the liquid and solid can be reduced by regulating the potential between the electrodes and the electrolyte solution. Based on the principle, Satoh et al. fabricated a gold electrode on the narrow flow channel in PDMS to act as a valve. By applying -0.9 V to the electrode, the valve

became wetted with the electrolyte solution and the solution moves to forward [97]. After that, the valve was used to realize the solution exchange sequentially for immunoassay purpose [98].

The appropriate valves for integration in micro-analytical devices are the hydrophobic valve, in which hydrophobic patch formed on the substrate surface in a flow channel. For example, Biosite et al presented a hydrophobic valve by constructing the hydrophobic barrier with hydrophobic particles of latex or hydrophobic polymers of 10 nm and 10 μ m in diameter. [99]. The hydrophobic barrier is transformed to a hydrophilic by the bound components (proteins, polypeptides, polymers, and detergents) from the reaction mixture and the reaction mixture started moving over the valve. Furthermore, SAM (self-assembly monolayer) based hydrophobic valve presented by Biswas et al. in which SAM-layer onto platinum-electrode formed into a microchannel (Fig. 1.9 (ii)). By applying -1V to the electrode, the SAM layer desorbed from the electrode, and the solution moves forward [100]. Another approach of an autonomous valve is the pH-responsive valve that was fabricated by photopolymerization of pH-sensitive hydrogel onto micropillars in the middle of a channel [101]. The access of the fluid in the flow channel can be hindered by swelling of the hydrogel as the solution of pH 11 flows in the adjacent channel (Fig.1.9 (iii)).

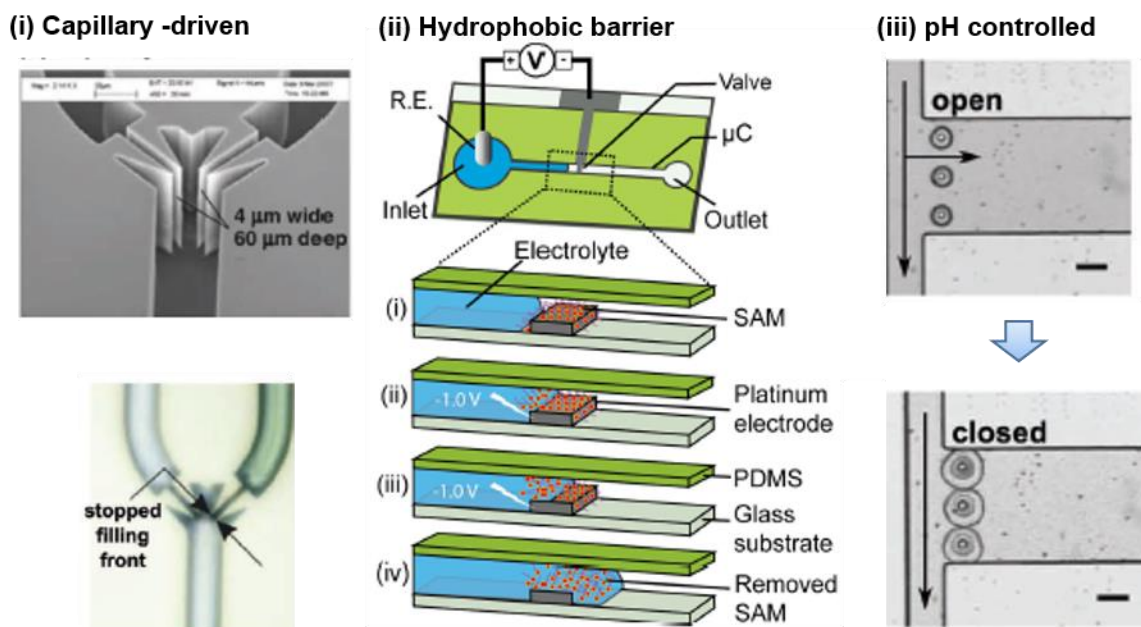


Figure 1.9. Passive valves. (i) SEM image of capillary valve system in which an abrupt change in the curvature of a filling front in a capillary channel. (ii) Illustrates the principle of operation of single SAM valve in microchannel.(iii) pH responsive polymer on the posts that block the channel in presence of a solution of pH 11. Fig. (i-iii) are adapted from ref. [96],[100],[101], respectively.

1.4.3 Micropumps

To understand the proper functioning of the devices, precise flow regulate in microfluidic is significant and the flow control is given using a combination of valves, pumps, and resistances. Among these, pumps govern the overall flow rate and drive of the small volume of fluids by using certain pressure unit. The fluids flow in microfluidic in a controlled manner can be attained using active or passive pumps. Many micropumps have been presented based on their actuation mechanism and can be classified as illustrated in Fig. 1.10.

1.4.3.1 Active pumping

For active pumping system, the external power sources are used mostly to control the flow rate. And the driving forces including of mechanical displacement, electrical fields, magnetic fields or centripetal force can be used to actuate the pump. A huge diversity of microfabricated active pumps have been presented that are typically using membrane valves moving back and forth [25]. The control microliter volumes of liquids in a broad range of flow rates, pressures, viscosities, molecular weights, and compositions can be achieved using such pumps. However, pumps considering inexpensive and effective for POCT applications, it is remaining ambiguous to develop an active micropumps.

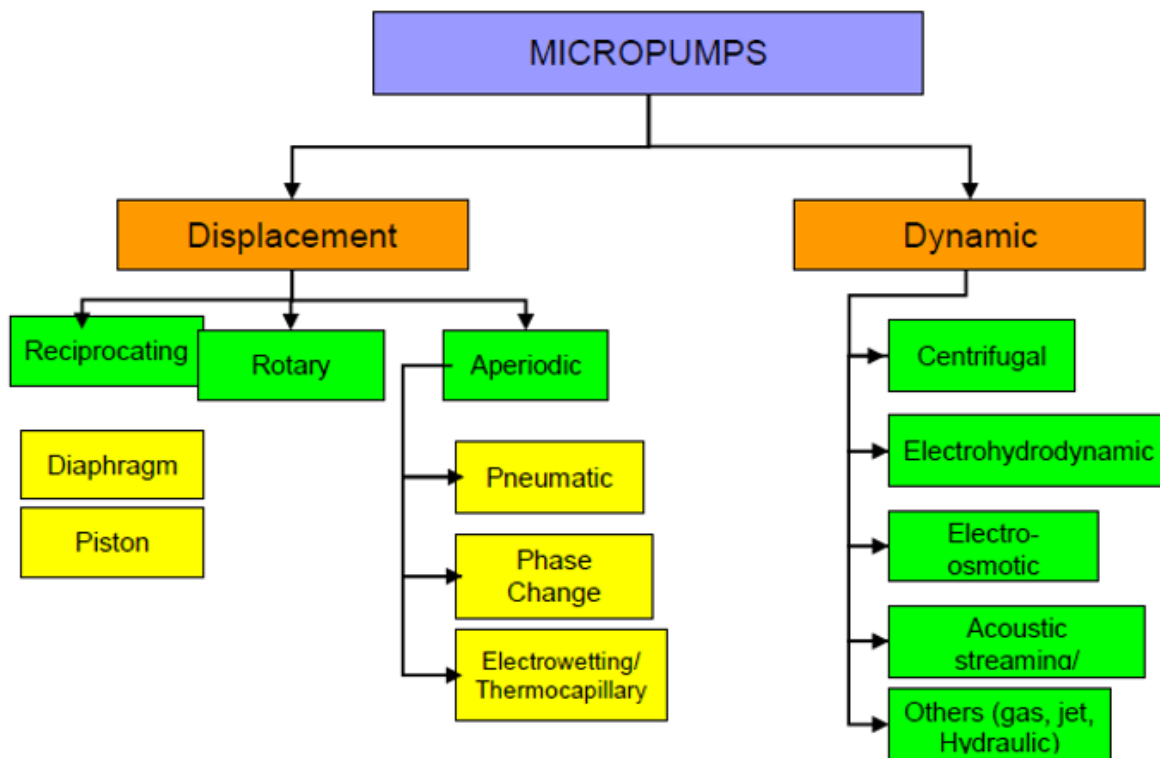


Figure 1.10. Micropumps classification adapted from Laser & Santiago (2004) [25].

One of the simplest microfluidic pumps is the syringe pump that has been used usually in microfluidics laboratories for a wide range of volumes and flow rates. The expected flow rate using such pumps can be attained by the movement of the plunger in a syringe at a constant speed using a stepper motor. Microfabricated mechanical displacement pumps trigger with a membrane valve in a countering movement. One such pump utilizes a piezoelectric (PZT) disc to actuate a diaphragm for generating a stroke volume which creates the pressure needed to generate the suction and discharge fluid flow consecutively (Fig. 1.11 (i)) [102]. Another attractive approach is to use the air bubble for the mechanical displacement to flow control. Such type of pump can be fabricated using air bubble creators triggered in succession to move a blood sample via the flow channel [103]. Electro-osmotic pumping based on a chemical equilibrium established at the boundary between solid and liquid and as results there are charged surface and counterions. When the electric field applied, the counter ions in a liquid move forward with electric current (Fig. 1.11 (ii)) [104].

A digital microfluidics device has been developed for POCT immunoassay in which manipulate droplets of reagents and sample on an array of electrodes insulated by a hydrophobic dielectric layer. The temporarily changes of the wetting properties of the surface from hydrophobic to hydrophilic were associated with the electrostatic and dielectrophoresis forces that were produced upon the application of electrical potentials between ground and actuation electrodes (Fig. 1.11 (iii)). With this system, the blood droplets dispense from a reservoir, mixes the droplets with reagents and performs the optical detection [105].

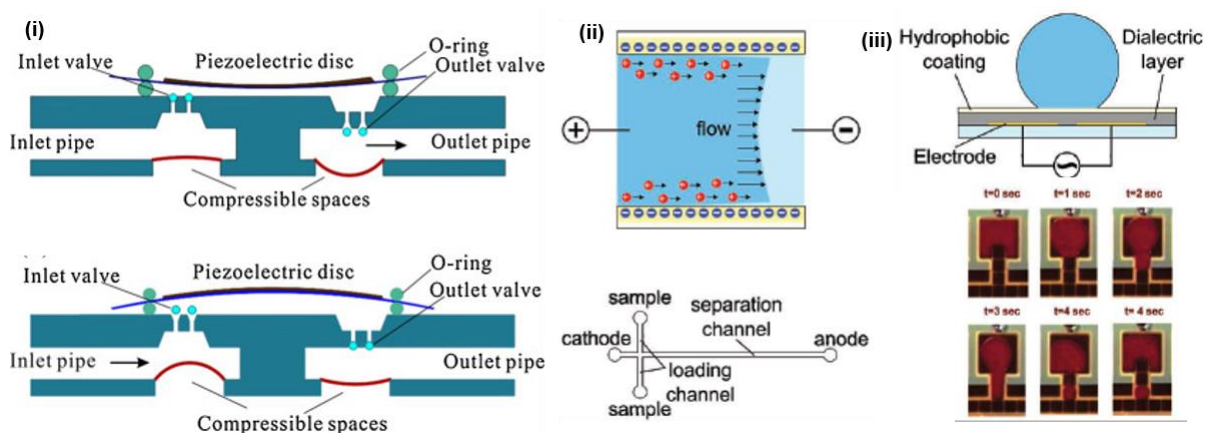


Figure 1.11. Active microfluidics pump. (i) Structure of PZT type micropump and pumps function by dispensing mode and absorbing mode. (ii) Electro-osmotic pumping for capillary electrophoresis. (iii) Electrowetting based pump for driving the liquid droplets. Fig. (i-iii) are adapted from ref. [102], [104], [105], respectively.

1.4.3.1 Passive pumping

In passive microfluidic, representative driving forces for driving fluids are chemical gradients on surfaces, osmotic pressure, permeation in PDMS or capillary forces, and the flow rates in passive pumping are determined in the design as well as passive valves. Because of such microfluidics fill spontaneously without used external

power, and their portability, low dead volume, and zero power consumption are making the passive system attractive in POCT applications. Although these devices are given several benefits, the flow rate can only be tuned to a limited degree as it set in the design.

An immunoassay strip test known as the Clearblue pregnancy test was presented, in which porous capillary membranes (filter membrane, a nitrocellulose membrane) for perceiving antibodies and a wicking membrane for pumping are squeezed in [106]. A substitute to this approach, the devices containing microchannels in plastic was given reproducible flow rate [99] and a number of POC immunoassays like for drug testing, cardiovascular disease, and infectious disease were carried out using it. Furthermore, capillary driven microfluidic system using capillary pumps have been demonstrated using micropillars arrays (Fig. 1.12 (i)) [107]. With the change of the dimension and wettability of the surface, the flow rate and filling fronts can be accurately regulated. Additionally, flow rates and the expected volume can be adjusted by governing the evaporation rate of liquid in the capillary pump [108]. Although Capillary microfluidic system offers several benefits like portability, inexpensive, it does not always scale favorably.

Micropumps based on the controlled evaporation of liquid through a membrane into a gas space containing a sorption agent has been developed by Zhang et al (Fig. 1.12 (ii)) [109]. The device was fabricated by bonding two PDMS layer, viz. PDMS-1 (containing a sampling pool, a simple sampling microchannel, and a microgroove) and PDMS-2 (containing an array of 10 independent microchambers and a waste pool). Using an evaporation temperature of 20–45 °C, environmental humidity conditions (RH=65%), and evaporation areas with a size of 40 mm², the fluid velocity could be tuned in the range of 20–120 μm/s. The integrated devices containing a

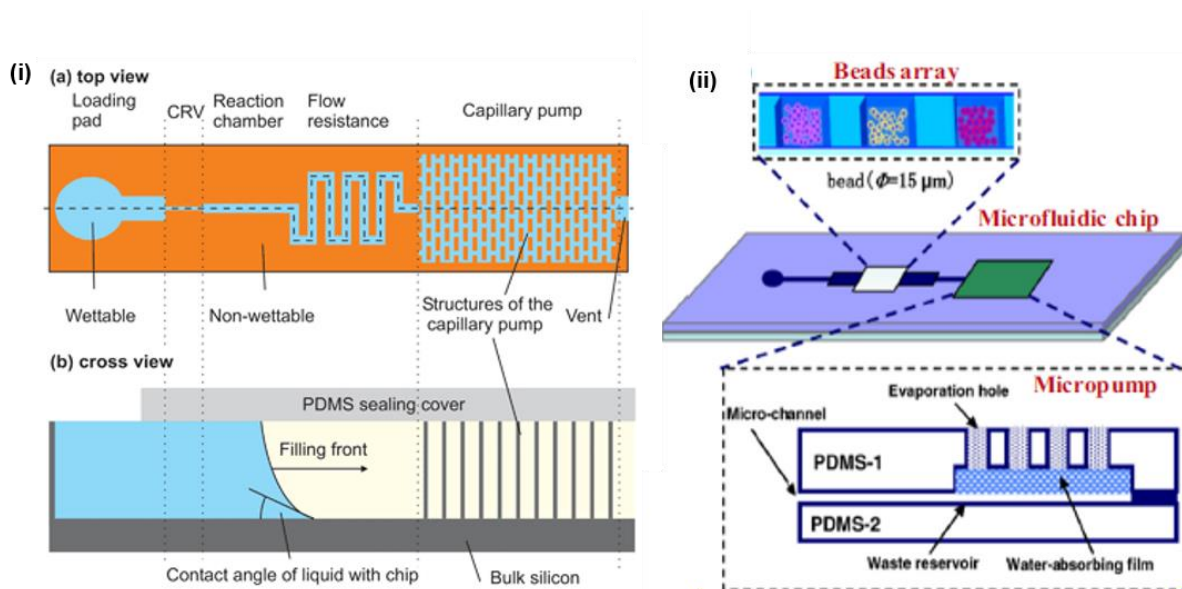


Figure 1.12. Passive pumping system for autonomous microfluidic (i) Micro- fabricated capillary pump Encoded flow rates of a liquid in a capillary system. (ii) Micropump operated by evaporation of and capillary forces. Fig. (i-ii) are adapted from ref. [107], [109], respectively.

micropump-integrated microfluidic microbead array chip was used to detect single – nucleotide. Improve passive pumping can also be realized using gravity vacuum or compressed air. DiagnoSwiss developed A gravity fed immunoassay system was presented by DiagnoSwiss, and the rates can be controlled from 10 to 1000 nL min⁻¹ [110]. Another passive pumping was demonstrated by Ahn et al.in 2004, in which pressurized gas kept in a chamber and separated from a microchannel using a thin membrane [111]. The liquid introduces into microchannel while the pressurized gas escapes from the chamber upon heating and melting the membrane.

1.5 Scope and aim of this thesis

Till to dates, peoples are relying mostly on centralized laboratories for diagnostic tests. As early detection of diseases causing biomarkers could improve the survival rates of the diseases, thus, inexpensive and effective biomarker examines is an urgent requirement. Microfluidic- technologies are encouraging to understand such type of diagnosis. To realize an effective on-chip measurement, ideally, a controllable assay condition is desired, for example, reagent concentrations, sample volume, washing flow conditions, etc. Moreover, automated and rapid analysis on-chip systems can bring of great advantage for portable diagnostic testing. Many devices have been utilized to process the fluids in μ TAS using valves and pumps that can be operated by a different principle. However, the simple, effective and on-device operated microfluidic components should be chosen for highly sensitive detection of biomarkers in microfluidic immunoassay platform. Therefore, the current study is aimed to develop on-chip immunoassay using a microfluidic platform that can facilitate the on-chip exchange of multiple solutions automatically in a controlled manner for the point-of-care diagnostics. For this purpose, the microfluidic channels and detection chamber, flow control elements like valves and pumps are incorporated on a single chip. To achieve the goal, the specific objectives are outlined as follows:

- To fabricate and optimize a valve-less microfluidic device for sequential exchange of solutions.
- To detect the protein (IL-2) using the device.
- To realize the exchange of solutions by the push-pull movement more practically.
- To develop a superabsorbent polymer-based new micropump for understanding on-chip exchange of solutions properly.
- To develop a new conducting polymer-based valve to control the fluid in microfluidic devices
- To integrate the developed microvalve into the integrated device for the exchange of solutions with minimal user intervention.
- To develop an integrated system for protein sensing.

1.6 Structure of this dissertation

Chapter 1 provides the introduction to POCT for infectious diseases diagnosis and their necessity toward early diagnosis of the diseases. We explained the current constraints of the POCT tools in the application and the state of art of the present solutions of POCT tools were focused for the developing countries. The advances of microfluidic components to control the flow in microfluidic flow channel has also been discussed. The aims of this study has been mentioned regarding to the development of inexpensive and effective microfluidic immunoassay platform for POCT.

Chapter 2 describes the microfluidic devices comprising with eight flow channels and a reaction chamber at the center. The exchange of multiple solutions in the reaction chamber has been done efficiently by using a positive and negative pressure with a plastic syringe. Furthermore, the device utility has been shown by detecting protein (IL-2) by sandwich fluorescence immunoassay.

Chapter 3 introduces a superabsorbent polymer-based new micropump for facilitating the on-chip exchange of solutions efficiently. Based on the swelling properties of the polymer, the sample has been flowed from the inlet to the reaction chamber and based on its superabsorbent properties, the sample solution again withdrawn from the reaction chamber. The pump has been characterized by several sample solutions to be exchanged.

Chapter 4 describes the development of the conducting polymer-based hydrophobic microvalves to control the capillary flow in the microfluidic flow channels. The valve consisted of a platinum electrode covered with a hydrophobic sodium dodecylbenzenesulfonate-doped polypyrrole (NaDBS-doped PPy) film. The valve has been characterized in accordance with switching time, dopant concentration, pH effect, and storage stability. The applications of the valve have been also investigated by integrating the valve in a complex microfluidic system and in the hydrodynamic flow focusing devices. Furthermore, the application of the valve have been investigated by the integration of the valves into the integrated device for the exchange of solution with minimal user intervention.

Chapter 5 the study has been summarized.

References

1. Atkinson Jr, A. J., Colburn, W. A., DeGruttola, V. G., DeMets, D. L., Downing, G. J., & Spilker, B. A., *Clinical Pharmacology & Therapeutics*, **2001**, 69(3), 89-95
2. Hung, L. Y., Wu, H. W., Hsieh, K., & Lee, G. B., *Microfluidics and nanofluidics*, **2014**, 16(5), 941-963.
3. Baylin, S. B., & Jones, P. A., *Nature Reviews Cancer*, **2011**, 11(10), 726-734.
4. Luo, X., & Davis, J. J., *Chemical Society Reviews*, **2013**, 42(13), 5944-5962.
5. Lozano, R., Naghavi, M., Foreman, K., Lim, S., Shibuya, K., Aboyans, V., & AlMazroa, M. A., *The lancet*, **2012**, 380(9859), 2095-2128.
6. Nelson, K. E., & Williams, C. M. (Eds.). *Infectious disease epidemiology*. Jones & Bartlett Publishers, **2013**.
7. Yager, P., Domingo, G. J., & Gerdes, J., *Annual review of biomedical engineering*, **2008**, 10, 107-144.
8. Harris, M., and Reza, J., *World Health Organization*, **2012**.
9. United Nations. *United Nations General Assembly 68th Session*, **2013**.
10. Dye, C., *Philosophical Transactions of the Royal Society B: Biological Sciences*, **2014**, 369(1645), 20130426.
11. Nii-Trebi, N. I., *BioMed research international*, **2017**, 2017, 245021.
12. Wild, D. (Ed.), *The immunoassay handbook: theory and applications of ligand binding, ELISA and related techniques*. **2013**, Newnes.
13. Jaye, D. L., Bray, R. A., Gebel, H. M., Harris, W. A., & Waller, E. K. *The Journal of Immunology*, **2012**, 188(10), 4715-4719.
14. Gubala, V., Harris, L. F., Ricco, A. J., Tan, M. X., & Williams, D. E., *Analytical chemistry*, **2011**, 84(2), 487-515.
15. Urdea, M., Penny, L. A., Olmsted, S. S., Giovanni, M. Y., Kaspar, P., Shepherd, A. & Burgess, D. C. H., *Nature*, **2006**, 444, Suppl 1:73-79.
16. Jung, W., Han, J., Choi, J. W., & Ahn, C. H., *Microelectronic Engineering*, **2015**, 132, 46-57.
17. El-Ali, J., Sorger, P. K., & Jensen, K. F., *Nature*, **2006**, 442(7101), 403-411.
18. Wu, L., Ma, C., Ge, L., Kong, Q., Yan, M., Ge, S., & Yu, J., *Biosensors and Bioelectronics*, **2015**, 63, 450-457.
19. Wu, Y., Xue, P., Hui, K. M., & Kang, Y., *Biosensors and Bioelectronics*, **2014**, 52, 180-187.
20. Wang, S., Ge, L., Yan, M., Yu, J., Song, X., Ge, S., & Huang, J., *Sensors and Actuators B: Chemical*, **2013**, 176, 1-8.
21. Zhou, X., Wong, T. I., Song, H. Y., Wu, L., Wang, Y., Bai, P., & Knoll, W., *Plasmonics*, **2014**, 9(4), 835-844.
22. Jokerst, J. C., Adkins, J. A., Bisha, B., Mentele, M. M., Goodridge, L. D., & Henry, C. S., *Analytical chemistry*, **2012**, 84(6), 2900-2907.
23. Lee, Y. F., Lien, K. Y., Lei, H. Y., & Lee, G. B., *Biosensors and Bioelectronics*, **2009**, 25(4), 745-752.

24. Wang, J., *Biosensors and Bioelectronics*, **2006**, 21(10), 1887-1892.
25. Laser, D. J., & Santiago, J. G. *Journal of micromechanics and microengineering*, **2004**, 14(6), R35.
26. Woias, P., *Sensors and Actuators B: Chemical*, **2005**, 105(1), 28-38.
27. Zarei, M., *Biosensors and Bioelectronics*, **2018**, 106, 193-203.
28. Chin, C. D., Linder, V., & Sia, S. K., *Lab on a Chip*, **2007**, 7(1), 41-57.
29. Shevkoplyas, S. S., Yoshida, T., Munn, L. L., & Bitensky, M. W., *Analytical chemistry*, **2005**, 77(3), 933-937.
30. Sia, S. K., Linder, V., Parviz, B. A., Siegel, A., & Whitesides, G. M., *Angewandte Chemie International Edition*, **2004**, 43(4), 498-502.
31. Linder, V., Sia, S. K., & Whitesides, G. M., *Analytical chemistry*, **2005**, 77(1), 64-71.
32. Park, S. J., Taton, T. A., & Mirkin, C. A., *Science*, **2002**, 295(5559), 1503-1506.
33. Hannan, M. A., Mutashar, S., Samad, S. A., & Hussain, A., *Biomedical engineering online*, **2014**, 13(1), 79.
34. Whitesides, G. M., *Nature*, **2006**, 442(7101), 368.
35. Daw, R., & Finkelstein, J., *Nature*, **2006**, 442(7101), 367.
36. Martin, A. J. P., & Syngé, R. M., *Biochemical Journal*, **1941**, 35(12), 1358.
37. Kunkel, H. G., & Tiselius, A., *The Journal of general physiology*, **1951**, 35(1), 89-118.
38. Le, H. P., *Journal of Imaging Science and Technology*, **1998**, 42(1), 49-62.
39. Woias, P., *Sensors and Actuators B: Chemical*, **2005**, 105(1), 28-38.
40. Oh, K. W., & Ahn, C. H., *Journal of micromechanics and microengineering*, **2006**, 16(5), R13.
41. Harink, B., Le Gac, S., Truckenmüller, R., van Blitterswijk, C., & Habibovic, P., *Lab on a Chip*, **2013**, 13(18), 3512-3528.
42. Beebe, D. J., Mensing, G. A., & Walker, G. M., *Annual review of biomedical engineering*, **2002**, 4(1), 261-286.
43. Zhang, Z., & Nagrath, S., *Biomedical microdevices*, **2013**, 15(4), 595-609.
44. Lee, W. G., Kim, Y. G., Chung, B. G., Demirci, U., & Khademhosseini, A., *Advanced drug delivery reviews*, **2010**, 62(4-5), 449-457.
45. Gorkin, R., Park, J., Siegrist, J., Amasia, M., Lee, B. S., Park, J. M., & Cho, Y. K., *Lab on a Chip*, **2010**, 10(14), 1758-1773.
46. Liu, C., Geva, E., Mauk, M., Qiu, X., Abrams, W. R., Malamud, D., & Bau, H. H., *Analyst*, **2011**, 136(10), 2069-2076.
47. Zhang, J. Y., Do, J., Premasiri, W. R., Ziegler, L. D., & Klapperich, C. M., *Lab on a Chip*, **2010**, 10(23), 3265-3270.
48. Wu, Z., Willing, B., Bjerketorp, J., Jansson, J. K., & Hjort, K., *Lab on a Chip*, **2009**, 9(9), 1193-1199.
49. Park, S., Zhang, Y., Wang, T. H., & Yang, S., *Lab on a Chip*, **2011**, 11(17), 2893-2900.
50. Beyor, N., Seo, T. S., Liu, P., & Mathies, R. A., *Biomedical microdevices*, **2008**, 10(6), 909.

51. Liu, W., Wei, H., Lin, Z., Mao, S., & Lin, J. M., *Biosensors and Bioelectronics*, **2011**, 28(1), 438-442.
52. Lien, K. Y., Lee, W. C., Lei, H. Y., & Lee, G. B., *Biosensors and Bioelectronics*, **2007**, 22(8), 1739-1748.
53. Lien, K. Y., Hung, L. Y., Huang, T. B., Tsai, Y. C., Lei, H. Y., & Lee, G. B., *Biosensors and Bioelectronics*, **2011**, 26(9), 3900-3907.
54. Jung, J. H., Kim, G. Y., & Seo, T. S., *Lab on a Chip*, **2011**, 11(20), 3465-3470.
55. Wei Hou, H., Gan, H. Y., Bhagat, A. A. S., Li, L. D., Lim, C. T., & Han, J., *Biomicrofluidics*, **2012**, 6(2), 024115.
56. Rusling, J. F., Kumar, C. V., Gutkind, J. S., & Patel, V., *Analyst*, **2010**, 135(10), 2496-2511.
57. Gervais, L., De Rooij, N., & Delamarche, E., *Advanced materials*, **2011**, 23(24), H151-H176.
58. Han, K. N., Li, C. A., & Seong, G. H., *Annual review of analytical chemistry*, **2013**, 6, 119-141.
59. Ng, A. H., Uddayasankar, U., & Wheeler, A. R., *Analytical and bioanalytical chemistry*, **2010**, 397(3), 991-1007.
60. Sia, S. K., & Whitesides, G. M., *Electrophoresis*, **2003**, 24(21), 3563-3576.
61. Yang, S. Y., Lien, K. Y., Huang, K. J., Lei, H. Y., & Lee, G. B., *Biosensors and Bioelectronics*, **2008**, 24(4), 855-862.
62. Wang, C. H., & Lee, G. B., *Biosensors and Bioelectronics*, **2005**, 21(3), 419-425.
63. Lafleur, L., Stevens, D., McKenzie, K., Ramachandran, S., Spicar-Mihalic, P., Singhal, M. & Lutz, B., *Lab on a Chip*, **2012**, 12(6), 1119-1127.
64. Gao, Y., Hu, G., Lin, F. Y., Sherman, P. M., & Li, D., *Biomedical microdevices*, **2005**, 7(4), 301.
65. Lee, L. J., Yang, S. T., Lai, S., Bai, Y., Huang, W. C., & Juang, Y. J., *Advances in clinical chemistry*, **2006**, 42, 255-295.
66. Lee, B. S., Lee, J. N., Park, J. M., Lee, J. G., Kim, S., Cho, Y. K., & Ko, C., *Lab on a Chip*, **2009**, 9(11), 1548-1555.
67. Nagai, H., Narita, Y., Ohtaki, M., Saito, K., & Wakida, S. I., *Analytical Sciences*, **2007**, 23(8), 975-979.
68. Apple, F. S., Christenson, R. H., Valdes, R., Andriak, A. J., Berg, A., Duh, S. H., & Mascotti, K., *Clinical chemistry*, **1999**, 45(2), 199-205.
69. Clark, T. J., McPherson, P. H., & Buechler, K. F., *Point of Care*, **2002**, 1(1), 42-46.
70. Gervais, L., & Delamarche, E., *Lab on a Chip*, **2009**, 9(23), 3330-3337.
71. Wang, J., Ahmad, H., Ma, C., Shi, Q., Vermesh, O., Vermesh, U., & Heath, J., *Lab on a Chip*, **2010**, 10(22), 3157-3162.
72. X. Liu, C. Cheng, A. Martinez, K. Mirica, X. Li, S. Phillips, M. Mascarenas, G. Whitesides, *IEEE 24th International Conference on Micro Electro Mechanical Systems*, **2011**, 75-78.
73. Chin, C. D., Laksanasopin, T., Cheung, Y. K., Steinmiller, D., Linder, V., Parsa, H., & Karita, E., *Nature medicine*, **2011**, 17(8), 1015.

74. Toley, B. J., McKenzie, B., Liang, T., Buser, J. R., Yager, P., & Fu, E., *Analytical chemistry*, **2013**, 85(23), 11545-11552.
75. Wang, J. H., Cheng, L., Wang, C. H., Ling, W. S., Wang, S. W., & Lee, G. B., *Biosensors and Bioelectronics*, **2013**, 41, 484-491.
76. Easley, C. J., Karlinsey, J. M., Bienvenue, J. M., Legendre, L. A., Roper, M. G., Feldman, S. H., ... & Landers, J. P., *Proceedings of the National Academy of Sciences*, **2006**, 103(51), 19272-19277.
77. Spizz, G., Young, L., Yasmin, R., Chen, Z., Lee, T., Mahoney, D. Roswech, T., and Zhou, p., *Point of care*, **2012**, 11(1), 42.
78. Chen, D., Mauk, M., Qiu, X., Liu, C., Kim, J., Ramprasad, S. & Bau, H. H., *Biomedical microdevices*, **2010**, 12(4), 705-719
79. Chang, C. M., Chang, W. H., Wang, C. H., Wang, J. H., Mai, J. D., & Lee, G. B., *Lab on a Chip*, **2013**, 13(7), 1225-1242.
80. Gao, Y., Lam, A. W., & Chan, W. C., *ACS applied materials & interfaces*, **2013**, 5(8), 2853-2860.
81. Kaigala, G. V., Huskins, R. J., Preiksaitis, J., Pang, X. L., Pilarski, L. M., & Backhouse, C. J. *Electrophoresis*, **2006** 27(19), 3753-3763.
82. Ferguson, B. S., Buchsbaum, S. F., Wu, T. T., Hsieh, K., Xiao, Y., Sun, R., & Soh, H. T., *Journal of the American Chemical Society*, **2011**, 133(23), 9129-9135.
83. Burns, M. A., Johnson, B. N., Brahmasandra, S. N., Handique, K., Webster, J. R., Krishnan, M., & Mastrangelo, C. H., *Science*, **1998**, 282(5388), 484-487.
84. Su, W., Gao, X., Jiang, L., & Qin, J., *Journal of Chromatography A*, **2015**, 1377, 13-26.
85. Gravesen, P., Branebjerg, J., & Jensen, O. S., *Journal of micromechanics and microengineering*, 1993, 3(4), 168-182.
86. Melin, J., & Quake, S. R., *Annu. Rev. Biophys. Biomol. Struct.*, **2007**, 36, 213-231.
87. Kartalov, E. P., Zhong, J. F., Scherer, A., Quake, S. R., Taylor, C. R., & French Anderson, W., *BioTechniques*, **2006**, 40(1), 85-90.
88. Ottesen, E. A., Hong, J. W., Quake, S. R., & Leadbetter, J. R., *Science*, **2006**, 314(5804), 1464-1467.
89. Vestad, T., Marr, D. W. M., & Oakey, J., *Journal of Micromechanics and Microengineering*, **2004**, 14(11), 1503.
90. Weibel, D. B., Kruithof, M., Potenta, S., Sia, S. K., Lee, A., & Whitesides, G. M., *Analytical chemistry*, **2005**, 77(15), 4726-4733.
91. Oh, K. W., Han, A., Bhansali, S., & Ahn, C. H., *Journal of Micromechanics and Microengineering*, **2002**, 12(2), 187-191.
92. Suzuki, H., & Yoneyama, R., *Sensors and Actuators B: Chemical*, **2003**, 96(1-2), 38-45.
93. Kaigala, G. V., Hoang, V. N., & Backhouse, C. J., *Lab on a Chip*, **2008**, 8(7), 1071-1078.
94. Chen, G., Svec, F., & Knapp, D. R., *Lab on a Chip*, **2008**, 8(7), 1198-1204.

95. Satarkar, N. S., Zhang, W., Eitel, R. E., & Hilt, J. Z., *Lab on a Chip*, **2009**, 9(12), 1773-1779.
96. Zimmermann, M., Hunziker, P., & Delamarche, E., *Microfluidics and Nanofluidics*, **2008**, 5(3), 395-402.
97. Satoh, W., Hosono, H., & Suzuki, H., *Analytical chemistry*, **2005**, 77(21), 6857-6863.
98. Nashida, N., Satoh, W., Fukuda, J., & Suzuki, H., *Biosensors and Bioelectronics*, **2007**, 22(12), 3167-3173.
99. Buechler, K. F., U.S. Patent No. 5,458,852., **1995**, Washington, DC: U.S. Patent and Trademark Office.
100. Biswas, G. C., Watanabe, T., Carlen, E. T., Yokokawa, M., & Suzuki, H., *ChemPhysChem*, **2016**, 17(6), 817-821.
101. Beebe, D. J., Moore, J. S., Bauer, J. M., Yu, Q., Liu, R. H., Devadoss, C., & Jo, B. H., *Nature*, **2000**, 404(6778), 588-590.
102. Ren, Y. J., Ma, Y. T., Huang, D., Chen, J., & Feng, Z. H., *Sensors and Actuators A: Physical*, **2004**, 244, 126-132.
103. Chiu, S. H., & Liu, C. H., *Lab on a Chip*, **2009**, 9(11), 1524-1533.
104. Ramsey, R. S., & Ramsey, J. M., *Analytical Chemistry*, **1997**, 69(6), 1174-1178.
105. Sista, R., Hua, Z., Thwar, P., Sudarsan, A., Srinivasan, V., Eckhardt, A., & Pamula, V., *Lab on a Chip*, **2008**, 8(12), 2091-2104.
106. Clearblue Pregnancy Test–Easy To Use and Accurate Tool!,” can be found under <http://www.clearblue.com/uk/clearblue-pregnancytest-with-colour-change-tip.php>, 2010 .
107. Zimmermann, M., Schmid, H., Hunziker, P., Delamarche, E., *Lab on Chip*, **2007**, 7 (1), 119 – 125.
108. Zimmermann, M., Bentley, S., Schmid, H. , Hunziker, P. , Delamarche, E. , *Lab on Chip*, **2005** , 5(12) , 1355 – 1359
109. Zhang, H., Fu, X., Zhu, Z., *Chin. J. Analytical Chemistry*, **2013**, 41(4), 473–480.
110. Rossier, J. , Baranek, S. , Morier, P. , Vollet, C., Vulliet, F., Dechastonay, Y. , Reymond, F. , J. Assoc. *Journal of the Association for Laboratory Automation*, **2008** , 13(6) , 322 – 329 .
111. Ahn, C.H., Choi, J.W. , Beaucage, G. , Nevin, J., Lee, J.B., Puntambekar, A., Lee. R. J. Y., *Proc. IEEE*, **2004**, 92 , 154 – 173 .
112. Murray, C. K., Gasser, R. A., Magill, A. J., & Miller, R. S. (2008). Update on rapid diagnostic testing for malaria. *Clinical microbiology reviews*, 21(1), 97-110.

Chapter 2: Valve-less microfluidic device with push-pull sequential solution exchange function for fluorescence immunoassay

2.1 Introduction

Point-of-care testing (POCT) is essential for prompt treatment of acute diseases and for homecare diagnostics [1]. In POCT, diagnostic results are given quickly even by non-trained personnel, which allow patients to take follow-up treatment [2].

The analysis of protein is becoming increasingly important in clinical diagnosis to understand cellular behavior, as mainly the proteins regulate cellular phenomena. The quantitative detection of proteins in biological fluid is critical for the evaluation of biomarker or the study of complex cellular processes, such as inflammation, cancer, infectious diseases, drug toxicity and autoimmune diseases [3-5]. In the proteomic research, chemical methods (electrophoresis and staining) as well as physical methods (spectroscopy) have been developed to detect proteins [6]. However, all of these methods are unsuitable in terms of sensitivity and precise quantitative determinations, rely on expensive and bulky instrument, and the time-consuming process. Regarding to sensitivity, reproducibility and variability, immunological methods have been extensively used as a useful tool for the detection of protein in physiological fluid [7-10].

To detect proteins, enzyme-linked immunosorbent assay (ELISA) has been the most widely used technique [11]. However, their applications are limiting in clinical diagnosis in a point of care setup as the process is labor intensive, need substantial volumes of costly reagents and sample, and take longer time to complete, and the system is not portable. In this respect, immunoassays in microfluidics platforms could be an attractive solution [12-18]. Microfluidics system has a distinctive characteristic of high surface-to-volume ratio resulting in fast analysis [19]. Also, microfluidic platforms offers decreasing the consumption of sample volume, a miniaturized format with portability, complex sample manipulations that are well-suited of the microfabrication designs and methods [20]. These microfluidic platforms will have a substantial potential to upgrade the global health care system, mostly for medical care and emergency situations at the poor resource conditions in underdeveloped and developing countries. On the other hand, the poor device performance (reproducibility and stability), complicated device structure and function, the incorporation of multiple functional units into a single chip with a complete automation have presented a challenge to the accessibility to the non-professional end user. Consequently, we believe that microfluidic devices with the simplified of structure and function would be a useful tools for POCT.

2.2 Solution handling for on-chip sandwich immunoassay

In conducting the sandwich heterogeneous immunoassays in microfluidics, solution management comprises several steps, with multiple sequential reagents injection and thorough washings between reagents incubation. For realizing sensitive protein detection in microfluidic immunoassays, the control transportation of the solutions are important for the step by step reactions. Typically, external pressure driven flow such as syringe pump has been extensively used for processing of solutions in microfluidic immunoassay. However, the external power source is required to operate the pump. Additionally, manual pipetting is practiced to load solution into the inlets, then the solution introduced into the target location by creating vacuum or using different kinds of on-device pumps and valves (piezoelectric, thermal, electro-hydrodynamic, electrostatic, rotary, and acoustic micro pumps etc.) [21]. For sandwich immunoassay, the preloaded reagents in the separate zones are flowed into reaction chamber in a sequent manner by the computer control microvalve and pump [22], by capillary valves [23], by the pneumatically-driven valve and pump [24, 25]. Conclusively, the necessity to integrate the microvalves with these micropumps along with complicated device structures and function has rarely been successful in realizing the simple pumping function.

To make the functions simpler, valveless microfluidic systems have been used to drive a sequence of reagents using capillary forces [26, 27], but the complicated microchip design has limited its application to practical settings. As a solution to this problem, Linder et al., reported automated technique for delivering a sequence of reagents [28]. However, to make a cartridge, the technical and human resources are needed to operate syringe for sequentially injecting plugs of reagents separated by air spacers in a tube. To make the process automatic, a simple technique for handling multiple reagents within a microchip is needed. Previous methods include sequential injection of solutions into a reaction chamber and flushing [29], shifting of solutions in the form of continuous liquid [30] or plug [31]. Also, an electrowetting-based microfluidic device for sequential injection and flushing of solutions for the detection of proteins has been presented [29]. Moreover, in realizing devices for POCT, a critical point is how to make the structure and procedure as simple as possible to exchange multiple solutions.

In this report, we demonstrate a novel method and device to realize efficient solution exchange for biochemical analyses. Fig. 2.1 illustrates the procedure of the solution is introduced from the inlet reservoir to the reaction chamber and the solution is thrown out. In typical devices, a solution is injected into a sensing region and is moved to a waste reservoir after completing the necessary function (Fig. 2.1A). To realize the function, pumps and valves are needed. In contrast, in our device, the solution is returned to the inlet reservoir after it is used (Fig. 2.1B). When multiple solutions are handled, the mechanism shown in Fig. 2.1A needs pumps and valves to control the movement of solutions and also necessary waste reservoir to manage large volume of waste. On the other hand, only push-pull movement is sufficient in the case of the mechanism shown in Fig. 1B. Using the mechanism, the performance of the exchange of multiple solutions were investigated. Furthermore, the usefulness of the device was demonstrated by conducting heterogenous immunoassay to detect human Interleukin 2 (IL-2).

2.3 Experimental

2.3.1 Reagents and materials

For fabrication and characterization of the devices, the reagents and materials were obtained from the following commercial sources : Glass wafers (No. 7740, 3 inch, 500 μm thick) from Corning Japan (Tokyo, Japan); a thick-film photoresist SU-8 25 from the Micro Chem (Newton, MA, USA); negative photoresist (OMR 83 from Tokyo Ohka Kogyo (Kawasaki, Japan); a prepolymer solution of PDMS (KE-1300T), its curing agent CAT-1300, and (3-aminopropyl)triethoxysilane (APTES) from Shin-Etsu Chemical (Tokyo, Japan); phosphate-buffered saline (PBS, pH 7.4), bovine serum albumin (BSA), fluorescein and a dye, sunset yellow FCF, from Wako Pure Chemical Industries (Osaka, Japan). Dyes, Orange G and methyl violet, were obtained from MERCK (Darmstadt, Germany). A fluorescein isothiocyanate (FITC) antibody labeling kit was obtained from (Thermo Scientific, Rockford, IL, USA). Food dyes were bought from Kyoritsu Foods (Tokyo, Japan). A standard ELISA kit for human IL-2 (Human IL-2 ELISA MAX Deluxe) was bought from Bio Legend (San Diego, CA, USA). In the kit, the concentration of the reagents was not revealed. The PBS solution containing 0.5% BSA was utilized to dilute the Human IL-2. The cAb was diluted (200-fold) using the coating buffer. The detection antibody was also diluted by 200-fold. Instead of these, all of the other reagents were purchased from Wako Pure Chemical Industries (Osaka, Japan). All of the solutions were prepared using ultrapure water produced by a water purification system (Direct-Q UV 3, Merck, Darmstadt, Germany).

2.3.2 Fabrication of the microfluidic device

The microfluidic device was fabricated by bonding a poly(dimethylsiloxane) (PDMS) substrate with pattern with glass. The pattern containing a reaction chamber, eight flow channels, solution reservoirs, and air vents were made by replica molding using a template that was formed with a thick-film photoresist SU-8 25 (Fig. 2.2). The overall procedures of the template formation are described briefly in the appendix. After forming the PDMS with the patterns, it was cut into chips of desire dimensions. To form solution inlets at the solution reservoirs, the PDMS substrate was gently punched using a small needle. The height of the flow channels and reaction chamber was 100 μm for all devices, and the diameter of the reaction chamber was 2 mm (volume: 310 nL). To optimize the flow channel structure, devices were constructed with flow channel of different widths (200- μm and 250- μm), and the entrance of the 200 μm flow channels to the reaction chamber was constricted to 50 μm to avoid entering of an injected solution into the other flow channels. The air vents (30- μm wide) were also formed at the reaction chamber to inject the solution efficiently.

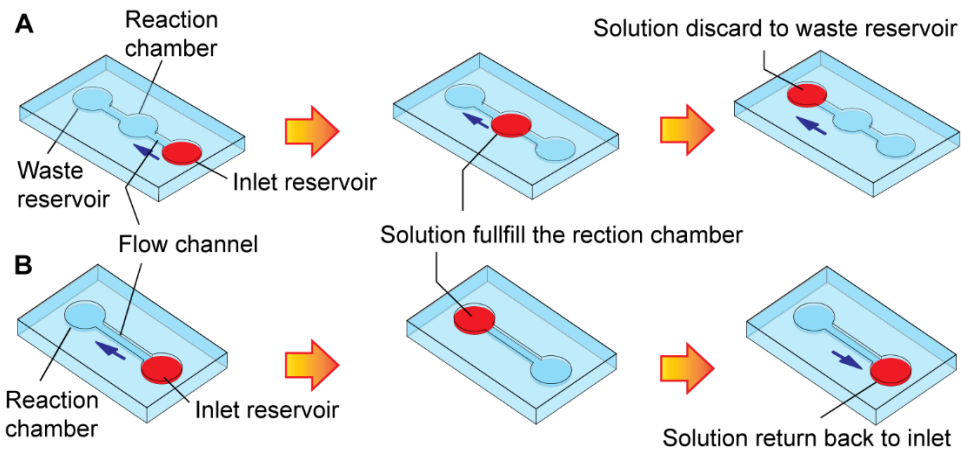


Figure 2. 1. Schematic illustration of the exchange of solutions for biochemical analyses. (A) Exchange of solutions using conventional devices: Firstly, solution is loaded into the inlet reservoir; secondly, reaction chamber is filled by injecting the solution; finally, the solution is flushed-out to the waste reservoir after it is used. (B) Exchange of solution in our fabricated device: firstly, solution is loaded into the inlet reservoir; secondly, the solution is moved to reaction chamber and is filled completely; finally, solution is withdrawn via the same flow channel to the inlet reservoir, and inlet reservoir is hold the used solution.

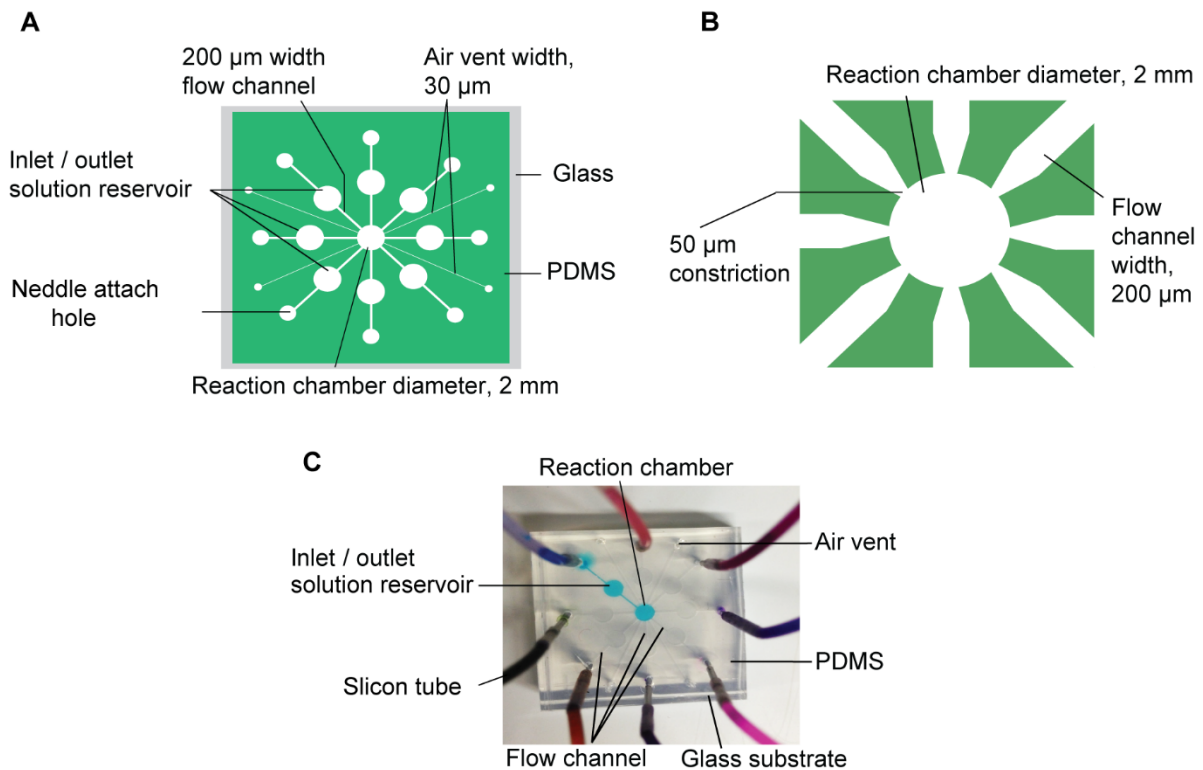


Figure 2.2. Microfluidic device for exchange of multiple solutions. (A) Top view. (B) Enlarge view of the device in which 50 μm constriction formed in the 200 μm flow channel at the entrance of the reaction chamber. (C) Photograph of the device with silicone tubes for injection of solutions and application of pressure.

To bond PDMS and glass substrates, the PDMS surface was plunged in a solution prepared by mixing 37% HCl, 30% H₂O₂, and water with a volume ratio 1:1:5 for 5 min. After rinsing the substrate with water for 10 min and with ethanol for 5 min, oxygen plasma treatment was carried out for 15 s at 20 W and 25 Pa oxygen pressure. After proper alignment, the PMDS and glass substrates were bonded by applying gentle pressure to the PDMS surface by hand.

2.3.3 Solution exchange procedure

To visualize the movement of solutions in microfluidic device, dye solutions of different colors were used. Disposable syringes (Terumo syringe 1mL SS-01T, Terumo Medical Corporation, Tokyo, Japan) were connected to one end of silicon tubes and were loaded with the dye solutions. The other end of the tubes was connected to the inlets through a shortened syringe needle. To inject the solution into the reaction chamber, the air pressure was applied gently by hand using the syringe. After the reaction chamber was entirely occupied with a solution, negative pressure was applied via the same syringe to extract the solution into the corresponding solution reservoir. The solution exchange method is shown in Fig. 2.3. The same methods were used repeatedly for the solution exchange sequentially through eight flow channels.

2.3.4 Tagging of detection antibodies with FITC

To label the detection antibodies (anti-IL-2 antibodies) with FITC, the standard procedure was followed as stated by the manufacturer's. Briefly, the solution of the IL-2 detection antibodies was prepared by dissolving 1 mg of IL-2 detection antibodies in 500 μ L of 50 mM borate buffer. After that the desired concentration 2 mg/mL of IL-2 detection antibodies were obtained by adding 40 μ L of borate buffer (0.67 M) to 500 μ L of the IL-2 detection antibody solution. The FITC solution in the vial was mixed with the 500 μ L of the prepared detection antibody (anti-IL-2) solution by pipetting and brief vortexing. Then the solution was incubated for 60 min. The labeled antibodies were purified using spin column packed with a purification resin that were provided by manufacturer within the kit. For this purpose, 250 μ L of the incubated solution having FITC-labelled and unlabeled detection antibodies were added to spin column, and was mixed with the resin by brief vortexing. Then the labeled antibodies were eluted from the column by centrifuging the spin column at $1,000 \times g$ for 30 - 45 s and the purified products were collected in a collection tube. According to manufacturer's guideline, the FITC-to-protein ratio was estimated and an average number of FITC fluorophore per FITC-labeled antibody was approximately 4.

2.3.5 Procedure for on-chip fluorescence immunoassay

The principle of detection of IL-2 is illustrated in Fig. 2.4. To immobilize the cAb, initially, the surface of the reaction chamber was functionalized with APTES and the APTES-functionalized surface can facilitate the effective immobilization of cAb by electrostatic interaction between amino groups of APTES and carboxylic

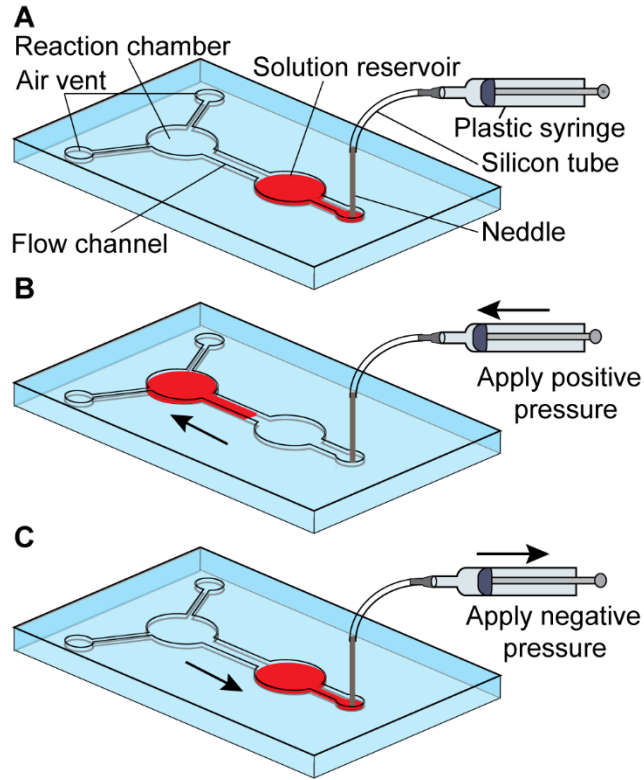


Figure 2.3. Schematic illustration of the solution exchange method: (A) Solution is loaded into the solution reservoir. (B) Solution is introduced into the reaction chamber by the application of positive pressure, (C) By the application of negative pressure, the solution is flashed out from the reaction chamber into the solution reservoir via the same flow channel.

groups of the cAb. APTES tends to self-polymerize in an aqueous solution and the moderately polymerized network allows to increase the effective sites for the immobilization of the cAb [32, 33].

The immobilization procedure starts by injecting 1 μL of solution containing cAb, APTES (1% v/v), and coating buffer into the reaction chamber, followed by incubation for 30 min at 4°C. After withdrawal of the incubated solution, the functionalized reaction surface was passivated with 1 μL of PBS containing 0.5% BSA and Tween 20 following incubation for 30 min at room temperature. To detect IL-2, a series of IL-2 standard solutions were prepared by the dilution of an IL-2 solution with PBS, and a solution having FITC-labeled detection antibodies (0.02 mg L⁻¹). *(I have corrected it)* It should be noted that, the same volume of FITC-labeled detection antibody was used for the case of the preparation of IL-2 standard solutions. After that, the prepared standard solutions were introduced instantly into the reaction chamber and incubated for 25 min at 4 °C. In conventional fluorescence immunoassays, the target antigens and FITC-labeled detection antibodies are injected sequentially and immunological -reactions are carried out step by step. However, in our experiment, a solution was prepared off-chip by the mixing of solutions of IL-2 and FITC-labeled detection antibodies and was injected immediately into the reaction chamber [34].

After withdrawing the solution, the washing solution containing PBS and Tween 20 [35, 36] was injected into and withdrawn from the reaction chamber to remove the unbound conjugate of IL-2 and FITC-labeled dAb. The washing step was repeated 3 times. Then the antigen-antibody complexes were detected by measuring fluorescence using a fluorescence microscope (IX-73; Olympus, Japan) with a filter unit (U-FBNA, Olympus) and CMOS camera (ORCA-Flash 4.0; Hamamatsu Photonics, Japan). During the measurement, UV light (wave length: 494 nm) was projected for 3 s. Finally, the intensity of fluorescence was plotted as a function of IL-2 concentrations.

2.4. Results and Discussion

2.4.1 Optimization of the structure of flow channel

Regarding the efficient solution exchange in a microfluidic device, an attempt is to inject the solution into the reaction chamber only without introduce into other flow channels and to withdraw the solution completely to the corresponding inlet reservoirs. For this purpose, exchange of solutions was performed using devices that were comprised with 250- μm and 200- μm wide flow channel structures without constriction at the entrance of the reaction chamber. When the 250- μm wide flow channels were used, the solution was not confined in the reaction chamber only, otherwise parts of the solutions permeated into the other flow channels (Fig. 2.5A), although all solution reservoirs were occupied with solutions and the flow channels were closed. The small volume of solutions introduced into the others flow channels could not be withdrawn completely after extracting the solutions from the reaction chamber to the corresponding inlet reservoir (Fig. 2.5C). The small volume of solution inside the flow

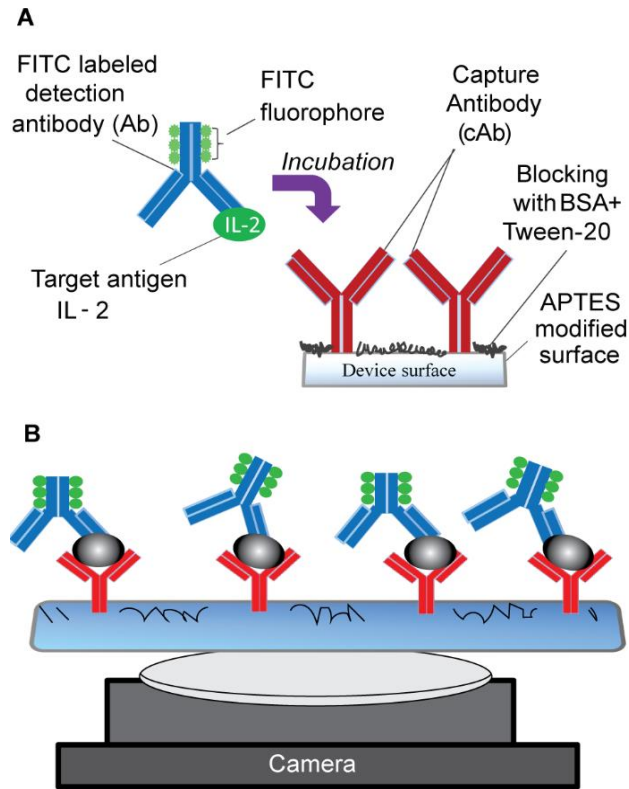


Figure 2.4. Schematic illustration of one-step sandwich fluorescence immunoassay to detect the target antigen IL-2. (A) Solution containing target antigen IL-2 and FITC label detection antibodies is injected into the reaction chamber and incubated 25 min at 4 °C for the formation of protein complex with the immobilized cAb (B) After removal of unbound target Ag, fluorescence is measured from protein complex (cAb-Ag-dAb-FITC) using fluorescence microscope.

channels was then interrupted in the precise solution exchange and can also impede the series of solution injection into reaction chamber. Furthermore, it would be the sources of the contamination during the process of immunoassay by merging with the next injected solution from the other solution reservoir (Fig. 2.5D). The penetration of the small amount of solution into the other flow channels decreased with the device of 200- μm wide flow channels (Fig. 2.5B). Although better results are anticipated by making the flow channels narrower, it affects the length of time for solution exchange.

The issue could effectively be addressed by forming constrictions in the flow channel at the entrance of the reaction chamber (Fig. 2.2B). When device with 200- μm wide flow channels and 50- μm constrictions was used for the exchange of solution, the solutions did not permeate into unrelated flow channels from the reaction chamber spontaneously. With this structure, the most reproducible exchange of solutions was attained. Additionally, this distinctive microfluidic design was effective to keep the solution only in the reaction chamber for more than 30 min.

2.4.2 Exchange of multiple solutions

The multiple solutions were exchanged sequentially using the device with the 200- μm wide flow channels with the constrictions. Fig. 2.6 indicates how solutions were introduced into the reaction chamber from different reservoirs and came back to each reservoir one after another. When the dye solutions were injected from the inlet reservoir into the reaction chamber, the solutions did not permeate into the other flow channels. Furthermore, by applying a negative pressure, subsequent effective withdrawing of the solution through the same flow channel was achieved very efficiently. During the process, we observed that solutions did not split and all solutions were completely withdrawn from the reaction chamber without remaining any residues.

In the process of immunoassay, the reaction surface become hydrophobic by the non-specific adsorption of biomolecules such as antibodies, antigens. This hydrophobicity may interrupt the smooth solution injection into and flush out from the reaction chamber, may impede the solution confined only reaction chamber, or sometimes hydrophobicity may be the reason of air trapping inside reaction chamber. Thus, to evaluate the effect of hydrophobicity on solution exchange, the bottom of the reaction surface was made hydrophobic by patterning a hydrophobic negative photo-resist OMR-83 and SU-8 and the water contact angle was measured. The contact angle was 86 degrees for OMR-83 pattern and 72 degrees for SU-8 pattern and it can be clearly shown that pattern of OMR-83 photoresist was made more hydrophobic surface than SU-8 (Fig. 2.7A). Therefore, OMR-83 was used in the following experiments. There was no unfavorable influence of the hydrophobic surface in solution exchange (Fig. 2.7C).

For quantitative immunosensing in a confined microfluidic environment, surface passivation is indispensable to reduce non-specific adsorption of biomolecules. Additionally, it should be noted that untreated bare PDMS

surface as well as incompletely cured monomers could be one of the crucial factor for the increasing of background noise for bio-sensing as it may contain the dangling molecular structures for the non-specific binding of proteins. Therefore, bovine serum albumin (BSA) is frequently used to passivate the reaction surface for reducing non-specific adsorption of biomolecules in immunoassay [37]. However, the concentration of BSA is needed to be optimized to introduce the BSA solution into the reaction chamber consistently without forming bubbles. The solution could be injected into the reaction chamber without any difficulties for the cases of the BSA solutions of concentration up to 0.5%. With a 1% BSA solution, however, air bubbles were sometimes formed in the reaction chamber due to its viscosity. Therefore, 0.5% BSA solution was applied for blocking the surface in this study. The effectiveness of blocking was validated by fluorescence measurement and the low fluorescence intensity from the zero-protein controls determines that there was no unfavorable effect in immunoassay (Fig. 2.10).

2.4.3 Device application to immunoassay

In order to validate the usefulness of the device, fluorescence immunoassay was performed to detect human IL-2. For this purpose, we used one flow channel for injecting and extracting of the solution mixture containing coating buffer, 1 % (v/v) APTES, and capture antibodies (cAb). The second and third flow channels were applied to introduce and withdraw a blocking reagent solution (0.5% BSA+ Tween 20) and a mixture of solution containing a conjugate of FITC labeled detection antibody and target antigen (IL-2), respectively. For washing purpose, the rest of the flow channels were used. It should be noted that the fluorescence was detected from the reaction chamber as the protein complexes (cAb-Ag-FITC labeled dAb) were formed in the reaction chamber.

For detecting IL-2, a mixture of cAb and APTES was injected into the reaction chamber and followed by incubation for 30 min to immobilize cAb onto the reaction surface. After removing the solution, the blocking solution was then introduced and the solution was removed after 30 min incubation. To make the calibration curve, a series of IL-2 standard solutions were injected into the reaction chamber, followed by incubation for 25 min to form protein complexes. After that the reaction surface were washed 3-4 times to remove the unbound conjugates of Ag-FITC labeled dAb, the extent of complex formation (cAb-Ag- dAb-FITC) in the reaction chamber was measured using a fluorescence microscopy.

The fluorescence from the reaction chamber indicates the binding of the antigen (IL-2) with capture antibody which is shown in Fig. 2.8A. The number of protein complexes (cAb-Ag-FITC labeled dAb) could be influenced the intensity of fluorescence which itself is directly proportional to the number of target antigen IL-2 bound to the immobilized capture antibody. Fig. 2.8B illustrates the dependence of fluorescence intensity on IL-2 concentration. It can be clearly shown that fluorescence intensity increased with the increase in IL-2 concentration in a range of concentration between 125 pg/mL and 2.0 ng/mL. For zero concentration of IL-2, weak fluorescence was supposed from the reaction chamber, demonstrating the background signal due to the non-specific binding of

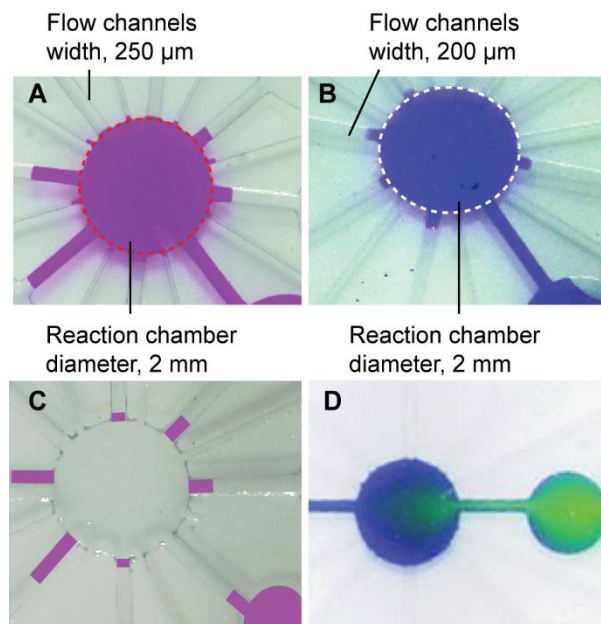


Figure 2.5. (A) & (B) The solution penetrate into the other flow channels using the device with 250- μm and 200- μm width flow channels, respectively. (C) After removing the solution from reaction chamber to the corresponding inlet reservoir, the previous solution is left. (D) The next solution is contaminated by the previous remaining solution.

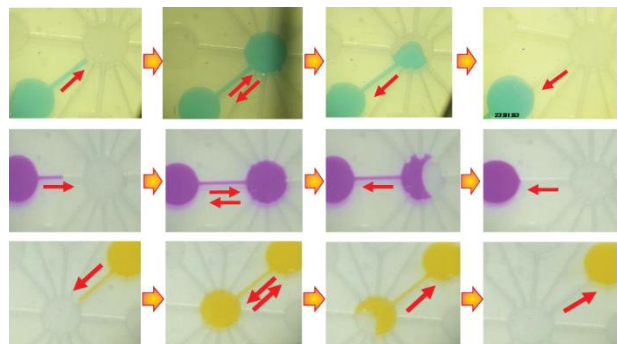


Figure 2.6. Images demonstrating sequential exchange of solutions in the microfluidic device comprised with 200 μm width flow channels and 50 μm constriction.

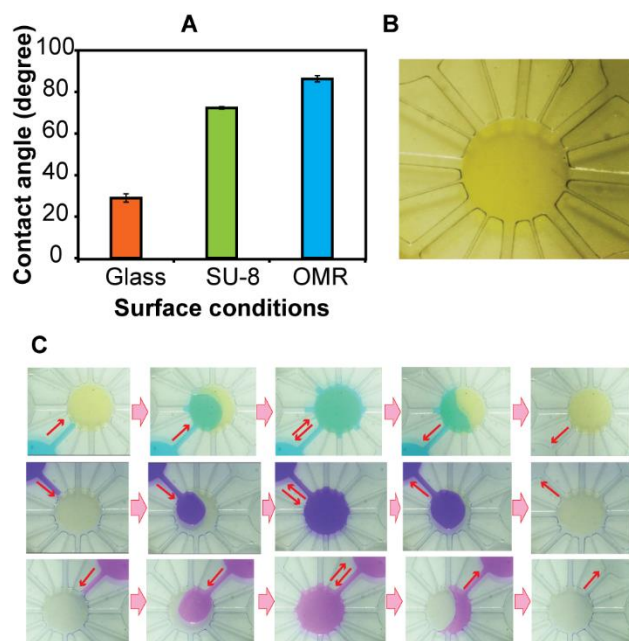


Figure 2.7. (A) Dependence of water contact angle on different reaction chamber surface. (B) Image of the hydrophobic (pattern with negative photoresist OMR-83) bottom surface of the reaction chamber. (C) Images that show sequential exchange of solutions in the microfluidic device with hydrophobic reaction chamber.

dAb-FITC onto the surface. At concentrations higher than 4 ng/mL, fluorescence intensity tended to saturate. The calculated limit of detection (LOD) of IL-2 was 105.4 pg/mL or 9.0 pM (average response of the blank plus three times the standard deviation) and relative standard deviation was 5.0%, indicating the reproducibility of the assay.

For detection of IL-2, the performance of the assay also depends on the effective immobilization of the capture antibodies. Prior to this work, our group also reported that APTES based immobilization of capture antibodies was more effective than physical adsorption, which was the almost factor two, and 1 % APTES was the best choice for the immobilization of cAb [34]. The effectiveness of the APTES-based cAb immobilization process was also investigated by measuring the amount of cAb immobilized on the bottom of the reaction chamber. For this purpose, the immobilization of cAb onto the reaction surface was performed using two immobilization processes. In one method, cAb and APTES were mixed gently in a tube, then the solution mixture was injected into the reaction chamber, followed by incubation for 30 min. In the another method, the immobilization was started by the functionalization of the surface of the reaction chamber with APTES prior to capture antibodies immobilization, then cAb injected into the APTES functionalized surface followed by incubation for 30 min. The efficiency of cAb immobilization using these methods are compared in Fig. 2.9. For both cases, the obtained fluorescence intensities from the reaction chambers were similar if the concentration was same. Therefore, the results indicate that both immobilization processes are effective to immobilize the capture antibodies onto surface.

2.4.4 Reducing the non-specific binding of proteins

To reduce the nonspecific adsorption of FITC-labeled detection antibodies, we performed the immunoassay on the different surface conditions of the reaction chamber: (i) no blocking with BSA (ii) blocking with 0.5% BSA and (iii) blocking with 0.5% BSA+ 0.01% Tween 20. In case of (i) and (ii), ethanol and water were used to rinse the surface of the reaction chamber. After that, the cAb were immobilized on the APTES modified surface by injecting the solution containing cAb and APTES (1% v/v) into the reaction chamber, followed by incubation. For the case of (ii), the BSA solution was injected in the subsequent step to block the surface additionally. In case (iii), an oxidative solution ($\text{H}_2\text{O}:\text{H}_2\text{O}_2:\text{HCl}$; volume ratio 5:1:1) was injected into the reaction chamber for 5 min to activate the internal surface, followed by rinsing with water and ethanol. After that, cAb was immobilized on the APTES functionalized surface while a solution containing cAb, APTES (1% v/v) was introduced into the reaction chamber followed by incubation. The subsequent surface blocking step was carried out by injecting a solution containing 0.5% BSA, 0.01% Tween 20 into the reaction chamber and incubated it to block the surface. The amount of non-specifically bound proteins on the differently treated surfaces is shown in Fig 2.10. In the case of (i), significant non-specific binding of FITC-labeled detection antibodies was noticed. On the other hand, in the cases of (ii) and (iii), the non-specific binding were decreased by 28% and 47% compared with the case of (i), correspondingly. The significant decline of non-specific adsorption of protein for case (iii) indicates that hydrophobic PDMS turn into hydrophilic by introducing hydroxyl groups as the surface treated with an oxidative

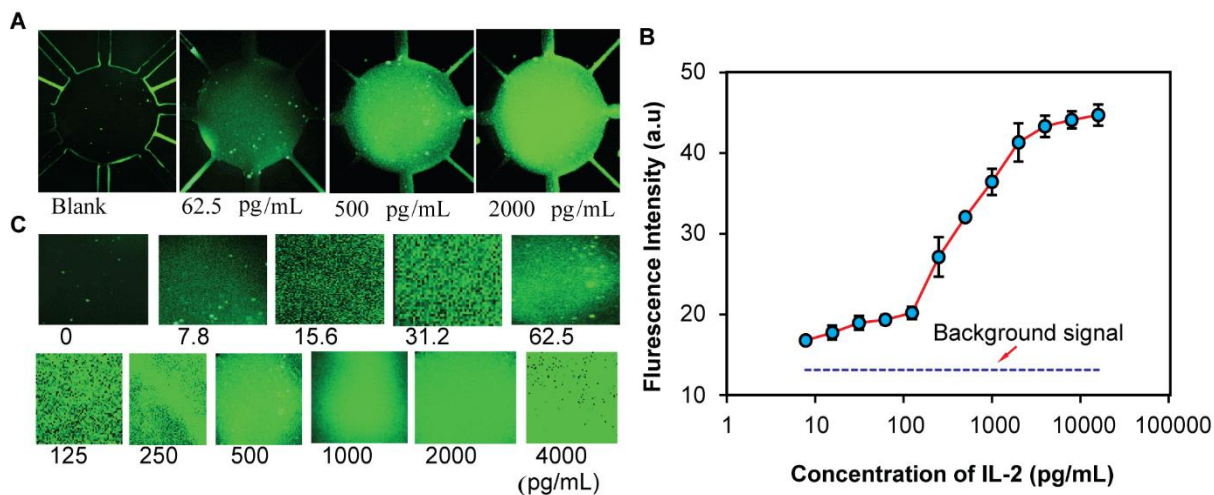


Figure 2.8. Detection of IL-2 by sandwich fluorescence immunoassay. (A) Optical microscope images of fluorescence from the reaction chamber. (B) Dependence of fluorescence intensity on IL-2 concentration. Three measurements were carried out for each data point, and the averages and standard deviations are shown. (C) Images of fluorescence from the reaction chamber (dimension: approximately 1.6×1.6 mm) of different concentrations IL-2.

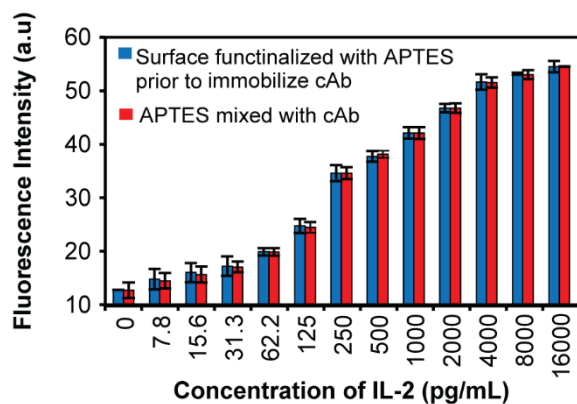


Figure 2.9. Efficiency of APTES-based immobilization of capture antibodies (cAb) by two methods. Three measurements were carried out for each data point, and the averages and standard deviations are shown.

solution, and the resulting surface can diminish the hydrophobic interactions between protein and surface in the non-specific adsorption [38].

2.4.5 Towards incorporating micropumps

To manipulate the solutions by the push-pull movement more practically, different approaches have been demonstrated that are operated by different actuation strategy including the volume change of gas bubbles [39, 40], gels [41, 42], and the deformation of a shape-memory alloy [43, 44]. They can be incorporated with the device by deforming an elastic water-impermeable membrane sandwich between the inlet reservoir and the actuator. Fig.2.11 shows that the initial experiment was carried out using a device consisting of a reaction chamber connected with eight flow channels. The performance of the device was realized by placing a 50 μm -thick silicone rubber sheet on the solution reservoirs after solutions were loaded into the solution reservoirs and the sealed chamber were formed by fixing it. The diaphragm undergoes deformation with the small rod, the solutions in the reservoirs can be transported into the reaction chamber one after another as in the case of using the syringe. When the rod was removed, the elastic diaphragm returned to its original state and the solutions were withdrawn completely from the reaction chamber to the solution reservoir. The exchange of multiple solutions was performed sequentially by rotating the device in a clockwise direction and by pushing and discharging the diaphragm using the static rod. The experimental set-up is shown in Fig. 2.12A. Fig. 2.12B also shows that how multiple solutions were exchanged efficiently in microfluidic device with the simple push-pull procedure.

2.4. Conclusions

The exchange of solutions in a microfluidic system can be performed efficiently using a device consisting of a reaction chamber connected to eight flow channels. Without using additional space and elaborate mechanisms, multiple solutions can be exchanged effectively by properly designing the flow channel structures and the surface in the reaction chamber, where the injected solutions can be confined only into the reaction chamber without entering the solutions to unrelated flow channels and the solution in the reaction chamber can be withdrawn completely into the inlet reservoir. Thus, the unique microfluidic design can be aided to eliminate the contamination between solutions during the exchange of multiple solutions. IL-2 could actually be detected within 25 min by consuming minimal (nL) volume sample or reagents. The limit of detection was 105 pg/mL. The mechanism of push-pull movement enables the integrating of the device with micropumps. Solution movement can easily be attained by applying pressure to the solutions thorough a diaphragm placed on the solution reservoirs. Finally we anticipate that this simple and rapid approach could be guided a great potential to fabricate an economical and sensitive lab-on-system for POCT.

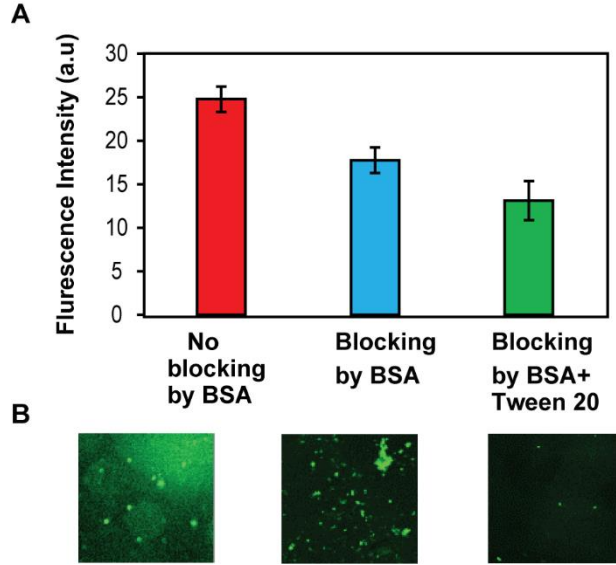


Figure 2.10. Non-specific adsorption of FITC-dAb on the reaction surface. (A) Dependence of fluorescence intensity on differently treated surfaces of the reaction chamber: no blocking the reaction surface; no treatment of reaction surface, blocking with 0.5% BSA; reaction surface treated with oxidative solution ($\text{H}_2\text{O}:\text{H}_2\text{O}_2:\text{HCl}$; volume ratio 5:1:1), surface blocked with a solution containing 0.5% BSA+ 0.01% Tween 20. Error bars represent means \pm standard deviation over 3 replicates. (B) Optical microscopy images of fluorescence from the reaction chamber of zero-protein (IL-2) concentration.

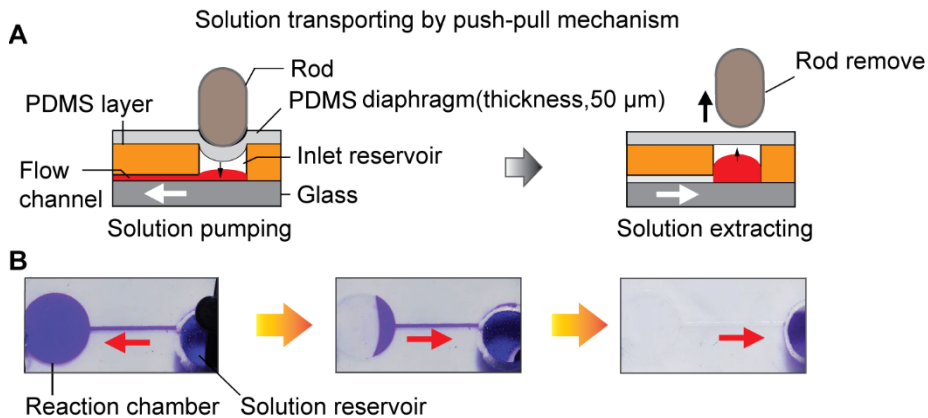


Figure 2.11. (A) Schematic illustration of push-pull mechanism for injection and extraction of a solution in the reaction chamber by using elastic diaphragm and a small rod. (B) Photographs showing the movement of solution. The arrows indicate the direction of movement.

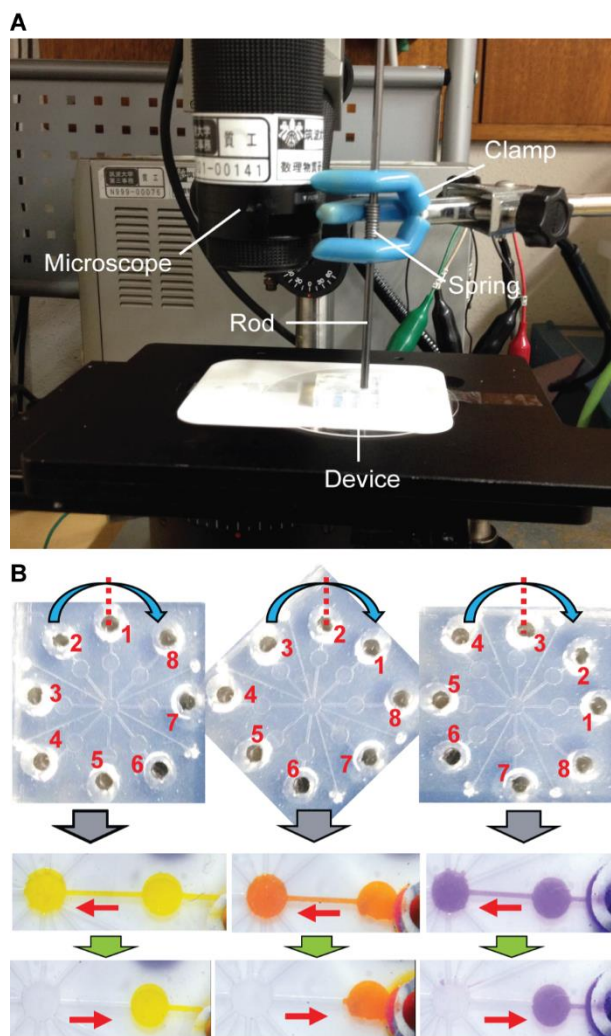


Figure 2.12. Exchange of multiple solutions by push-pull of the diaphragm using rod. (A) Photograph of the experimental set-up. Solutions were exchanged one by one by rotating the device and push and release the diaphragm using a fixed rod. The rod is fixed with the clamp using spring for the flexible up and down movement of the rod. (B) Images shows that the exchange of multiple solutions sequential in microfluidic device by push-pull mechanism.

References

1. Huckle, D., *Expert review of molecular diagnostics*, **2008**, 8(6), 679-688.
2. Gubala, V., Harris, L. F., Ricco, A. J., Tan, M. X., & Williams, D. E., *Analytical chemistry*, **2011**, 84(2), 487-515.
3. Mauck, C. K., Lai, J. J., Weiner, D. H., Chandra, N., Fichorova, R. N., Dezzutti, C. S., & Callahan, M. M., *AIDS research and human retroviruses*, **2013**, 29(11), 1475-1486.
4. Visintin, I., Feng, Z., Longton, G., Ward, D. C., Alvero, A. B., Lai, Y., & Azori, M., *Clinical Cancer Research*, **2008**, 14(4), 1065-1072.
5. Chandra, P. E., Sokolove, J., Hipp, B. G., Lindstrom, T. M., Elder, J. T., Reveille, J. D., & Robinson, W. H., *Arthritis research & therapy*, **2011**, 13(3), R102.
6. Westermeier, R., & Marouga, R., *Bioscience reports*, **2005**, 25(1-2), 19-32.
7. Ellington, A. A., Kullo, I. J., Bailey, K. R., & Klee, G. G., *Clinical chemistry*, **2009**, 55(6), 1092-1099.
8. Ellington, A. A., Kullo, I. J., Bailey, K. R., & Klee, G. G., *Clinical chemistry*, **2010**, 56(2), 186-193.
9. Brown, E. N., McDermott, T. J., Bloch, K. J., & McCollom, A. D., *Clinical chemistry*, **1996**, 42(6), 893-903.
10. Hatch, A., Kamholz, A. E., Hawkins, K. R., Munson, M. S., Schilling, E. A., Weigl, B. H., & Yager, P., *Nature biotechnology*, **2001**, 19(5), 461-465.
11. Findlay, J. W. A., Smith, W. C., Lee, J. W., Nordblom, G. D., Das, I., DeSilva, B. S., & Bowsher, R. R., *Journal of pharmaceutical and biomedical analysis*, **2000**, 21(6), 1249-1273.
12. Sackmann, E. K., Fulton, A. L., & Beebe, D. J., *Nature*, **2014**, 507(7491), 181-189.
13. Chikkaveeraiah, B. V., Mani, V., Patel, V., Gutkind, J. S., & Rusling, J. F., *Biosensors and Bioelectronics*, **2011**, 26(11), 4477-4483.
14. Liu, Y., Wang, H., Huang, J., Yang, J., Liu, B., & Yang, P., *Analytica chimica acta*, **2009**, 650(1), 77-82.
15. Hu, W., Lu, Z., Liu, Y., Chen, T., Zhou, X., & Li, C. M., *Lab on a Chip*, **2013**, 13(9), 1797-1802.
16. Wang, J., Ibáñez, A., Chatrathi, M. P., & Escarpa, A., *Analytical chemistry*, **2001**, 73(21), 5323-5327.
17. Linder, V., Verpoorte, E., de Rooij, N. F., Sigrist, H., & Thormann, W., *Electrophoresis*, **2002**, 23(5), 740-749.
18. Lin, F. Y., Sabri, M., Erickson, D., Alirezaie, J., Li, D., & Sherman, P. M., *Analyst*, **2004**, 129(9), 823-828.
19. Han, S. W., & Koh, W. G., *Analytical chemistry*, **2016**, 88, 6247-6253.
20. Zimmermann, M., Delamar, E., Wolf, M., & Hunziker, P., *Biomedical microdevices*, **2005**, 7(2), 99-110.
21. Iverson, B. D.; Garimella, S. V., *Microfluid. Nanofluid.*, **2008**, 5, 145 - 174.
22. Im, S. B., Uddin, M. J., Jin, G. J., & Shim, J. S., *Lab on a Chip*, **2018**, 18(9), 1310-1319.
23. He, H.; Yuan, Y.; Wang, W.; Chiou, N.-R.; Epstein, A. J.; Lee, L. J., *Biomicrofluidics*, **2009**, 3, 022401.
24. Li, J., Chang, K. W., Wang, C. H., Yang, C. H., Shiesh, S. C., & Lee, G. B., *Biosensors and Bioelectronics*, **2016**, 79, 887-893.

25. Weng, C.-H.; Huang, T.-B.; Huang, C.-C.; Yeh, C.-S.; Lei, H.-Y.; Lee, G.-B., *Biomedical Microdevices*, **2011**, 13, 585 - 595.
26. Juncker, D., Schmid, H., Drechsler, U., Wolf, H., Wolf, M., Michel, B., & Delamarche, E., *Analytical chemistry*, **2002**, 74(24), 6139-6144.
27. Novo, P., Volpetti, F., Chu, V., & Conde, J. P., *Lab on a Chip*, **2013**, 13(4), 641-645.
28. Linder, V., Sia, S. K., & Whitesides, G. M., *Analytical chemistry*, **2005**, 77(1), 64-71.
29. Nashida, N.; Satoh, W.; Fukuda, J.; Suzuki, H., *Biosensor & Bioelectronics*, **2007**, 22 (12), 3167-3173.
30. Satoh, W., Takahashi, S., Sassa, F., Fukuda, J., Suzuki, H., *Lab on Chip*, **2009**, 9, 35-37.
31. Shimizu, Y., Takashima, A., Satoh, W., Sassa, F., Fukuda, J., Suzuki, H., *Sensors Actuators B*, **2009**, 140, 649-655.
32. Vandenberg, E. T., Bertilsson, L., Liedberg, B., Uvdal, K., Erlandsson, R., Elwing, H., & Lundström, I., *Journal of Colloid and Interface Science*, **1991**, 147(1), 103-118.
33. Acres, R. G., Ellis, A. V., Alvino, J., Lenahan, C. E., Khodakov, D. A., Metha, G. F., & Andersson, G. G., *The Journal of Physical Chemistry C*, **2012**, 116(10), 6289-6297.
34. Usuba, R., Yokokawa, M., Ackermann, T. N., Llobera, A., Fukunaga, K., Murata, S., & Suzuki, H., *ACS Sensors*, **2016**, 1(8), 979-986.
35. Hua, B., Han, K. Y., Zhou, R., Kim, H., Shi, X., Abeyirigunawardena, S. C., & Ha, T., *Nature methods*, **2014**, 11(12), 1233.
36. Yu, Z. T. F., Guan, H., Cheung, M. K., McHugh, W. M., Cornell, T. T., Shanley, T. P., & Fu, J., *Scientific reports*, **2015**, 5, 11339.
37. Ren, K., Dai, W., Zhou, J., Su, J., & Wu, H., *Proceedings of the National Academy of Sciences*, **2011**, 108(20), 8162-8166.
38. Yu, L., Li, C. M., Zhou, Q., & Luong, J. H., *Bioconjugate chemistry*, **2007**, 18(2), 281-284.
39. Obata, H., Kuji, T., Kojima, K., Sassa, F., Yokokawa, M., Takekoshi, K., & Suzuki, H., *ACS Sensors*, **2015**, 1(2), 190-196.
40. Suzuki, H., & Yoneyama, R., *Sensors and Actuators B: Chemical*, **2003**, 96(1-2), 38-45.
41. Suzuki, H., Tokuda, T., & Kobayashi, K., *Sensors and Actuators B: Chemical*, **2002**, 83(1-3), 53-59.
42. Richter, A., Klatt, S., Paschew, G., & Klenke, C., *Lab on a Chip*, **2009**, 9(4), 613-618.
43. Benard, W. L., Kahn, H., Heuer, A. H., & Huff, M. A., *Journal of Microelectromechanical systems*, **1998**, 7(2), 245-251.
44. Sassa, F., Al-Zain, Y., Ginoza, T., Miyazaki, S., & Suzuki, H., *Sensors and Actuators B: Chemical*, **2012**, 165(1), 157-163.

Chapter 3: Polymer-based on-chip micro-pump for the exchange of solutions in valve-less microfluidic device

3.1. Introduction

The development of simple methods to transport of a small volume solution or reagent in a typical microfluidic platform is one of the key challenges for the successful miniaturization and integration of a variety of analytical and bioanalytical reactions in a portable Micro Total Analysis Systems or a lab-on-a-chip (LOC) as well as embedded medical devices [1]. Precise displacement of the small volume of solutions in microfluidics can be realized by either actuated or passive microfluidics. Flow is manipulated in actuated microfluidics using an external power source or pump which is driven mostly by displacement, centrifugal, electric-field or magnetic-field pumping mechanisms [2]. On the other hand, passive microfluidics have been employed the typical driving forces such as chemical gradients on surfaces, osmotic pressure, degassed PDMS [3], permeation in PDMS [4] or capillary forces [5] for propelling liquids. Actuated microfluidics is the most powerful in pumping on demand milliliters and microlitres of liquids for a long time and with a high flow rate.

Till to now, numerous on-device micropumps with different designs and principles have been proposed to drive a fluid to the target location in the microfluidic chip [6-8]. However, mostly they rely on bulky instruments to operate, and their fabrication complexity, unreliable fluid manipulation have made slow progress to the integration of pumps into miniaturization for point-of-care testing (POCT). To address this problem, an attempts have been initiated to integrate the micropumps on a single chip that can be operated without troubling hands of users [9]. Additionally, an approaches of on-chip microfluidic transport based on volume change of gas bubbles have been demonstrated to transport a solution [10-12]. However, the arrangement of a large number of electrodes and flow channels into the device was difficult as the number of pumps and valves increases. Additionally, direct electrolysis of the transported solution may have an adverse influence. In this respect, we suppose that simplifying structures, fabrication, and functions of micropumps is an emergency demand.

To substitute the active pumping, numerous passive pumping approaches that depend only on the microchannel geometry have been demonstrated for realizing simple pumping and facilitating portability of the devices [13-16]. Thus, passive liquid transport using the change of the microchannel geometry along with the capillary interfaces could provide the effective, rapid and suitable means for numerous bioanalysis platforms. However, the additional fabrication step and difficulties to adjust the flow rate may be a major concern for the failure to construct highly integrated microfluidic systems. Therefore, the chapter aims to develop a micropump that can be integrated into the microfluidic device for the efficient exchange of multiple solutions on-device. Specifically, the simple

micropumps operated without external instruments will be used to realize automatic solution exchange in the developed immunoassay device.

3.2. Objective of the propose study

For biochemical analyses or experiments, sequential exchange of solutions is often necessary for carrying out reactions step by step and cleaning of the reaction surface. The exchange of multiple solutions has been carried out effectively using a micropump that can be operated by electrochemically producing gas bubbles [10-12]. Also, the exchange of solutions as plugs can perform with a micropump as reported by Shimizu et al [17]. However, these systems have not necessarily been successful applied in the management of significant volume of solutions during analysis. Therefore, a more efficient pump with its simple structure and function is required that can enable efficiently to transport solutions to the reaction chamber as well as extracts completely from the reaction space to the waste reservoir.

In this study, we present a superabsorbent polymer (SAP), sodium polyacrylate (SP)-based micropump for solution injection into and the extraction from the reaction chamber. SP is a representative SAP and is used widely for commercial products such as disposable diaper [18]. Dry SP takes the form of random coils and cross-links between polymer chains to form a three-dimensional network (Fig. 3.1A). When it is in contact with water, the dissociation of hydrophilic groups create osmotic pressure imbalance between the internal network and external solution, which acts as a driving force for the penetration of water molecules and forms a hydrogen bond. On the one hand, the polymer network is expanded by electrostatic repulsion of charged groups ($-\text{COO}^-$) that are produced by dissociation of sodium ions from functional groups in the polymer gel (Fig. 3.1B). Based on the swelling properties of the polymer, we designed SP polymer actuated diaphragm micropump for solution injection from the inlet to the reaction chamber. On the other hand, for the extraction of solution from the reaction chamber, we designed an extraction pump based on the superabsorbent properties of the polymer. To realize a compact pump with this material, a cylindrical disc was made by freeze-drying.

Micropumps operated by the displacement of a flexible diaphragm has been demonstrated. In this respect, various actuation methods such as, electrostatic [19], shape memory alloy [20], liquid-vapor phase change [21] P(VDF-TrFE) –based electroactive polymer actuation [22] are being used. The pump is functined based on the movement of the elastomeric thin membrane. When the diaphragm undergoes deformation, it creates a positive pressure to pump the fluid from the inlet to the desired location. Like the mechanism , we propose a micropump to inject solution from the solution reservoir into reaction chamber. When a small volume of deionized water (DI) water is added to the polymer disc, the volume change of the polymer disc deflects the flexible polydimethylsiloxane (PDMS) diaphragm to downward, which then can change the volume of a sealed pump chamber with the diaphragm and thus generates positive pressure to transport the solution. After completely full-

filling the reaction chamber, the polymer disc is inserted into the extraction chamber. And, once the solution is in contact with the disc, the solution was started withdrawal from the reaction chamber. Therefore, in this study, we propose a micropump, which is comprised of a sealed pump chamber with a diaphragm, extraction chamber and actuation chamber containing SP disc for the exchange of multiple solutions on-device for immunoassay. The exchange of solutions has previously been performed by injecting and extracting solutions using microsyringe pumps or other conventional mechanisms.

3.3. Experimental section

3.3.1 Reagents and materials

All of the materials and reagents were obtained from the commercial sources which are as follow: Glass wafers (No. 7740, 3 inch diameter, 500 μm thick) from Corning Japan (Tokyo, Japan); a thick-film photoresist SU-8 25 from MicroChem (Newton, MA, USA); prepolymer solution of PDMS (KE-1300T) and its curing reagent (CAT-1300) from Shin-Etsu Chemical (Tokyo, Japan); potassium chloride (KCl), cellulose acetate (CA), glycerol, and a dye, sunset yellow FCF, from Wako Pure Chemical Industries (Osaka, Japan). Absorbing polymer, cross-linked sodium polyacrylate (SP) was obtained from Sigma-Aldrich (St. Louis, USA). Dyes, Orange G and methyl violet, were obtained from Merck (Darmstadt, Germany). Standard procedure was followed to prepare phosphate-buffered saline (PBS, pH 7.4). Other reagents were obtained from Wako Pure Chemical Industries (Osaka, Japan). All the solutions were prepared using ultra-pure water.

3.3.2 Preparation of the freeze-dried polymer disc

To develop a pump, superabsorbent cylindrical polymer discs were prepared by mixing SP, CA and DI water at an appropriate ratio. Briefly, the thick gel of the sodium polyacrylate polymer was made by mixing approximately 600 μL of DI water and 100 mg of SP in a centrifuge tube and stirred vigorously with a stick. Then, 100 mg of CA was added to the gel and stirred to mix CA with the gel. Once more, 200 μL of water and 50 mg of CA were added into the gel, and the mixture was stirred for properly distribute of the CA into the gel. After that, a thick semi-solid gel of the polymer containing inert supporting material (CA) was obtained. To make small cylindrical compact discs, the semi-solid gel was put into the PDMS template containing circular holes (diameter: 3.5 μm) that was formed by punching. Then, semi-solid gel in the template was kept at $-80\text{ }^{\circ}\text{C}$ for 2 h, followed by freeze-drying at $-50\text{ }^{\circ}\text{C}$ for 3.5 h. The polymer disc with very porous structure was formed by the freeze-drying, which facilitate the efficient absorption of the solution as well as volume changes of the polymer disc. After freeze-drying, the polymer discs were stored in air tight container to avoid the contact of humid air. Fig. 3.2 illustrates the preparation steps of the cylindrical polymer disc.

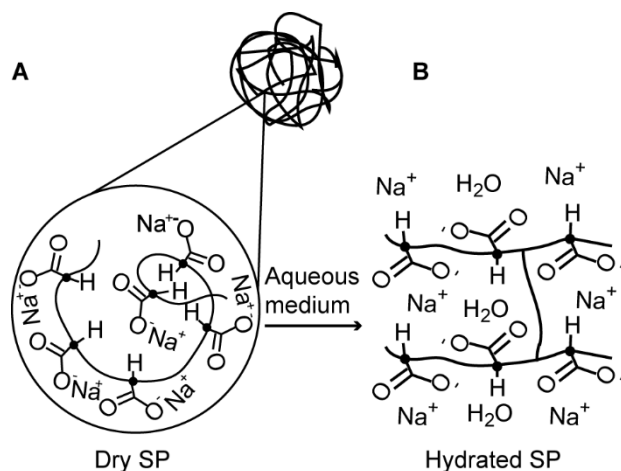


Figure 3.1. Mechanism of swelling behavior of SP by absorbing of an aqueous solution. (A) Polymer chain collapsed in a dry state. (B) Polymer chain expanded in a wet state.

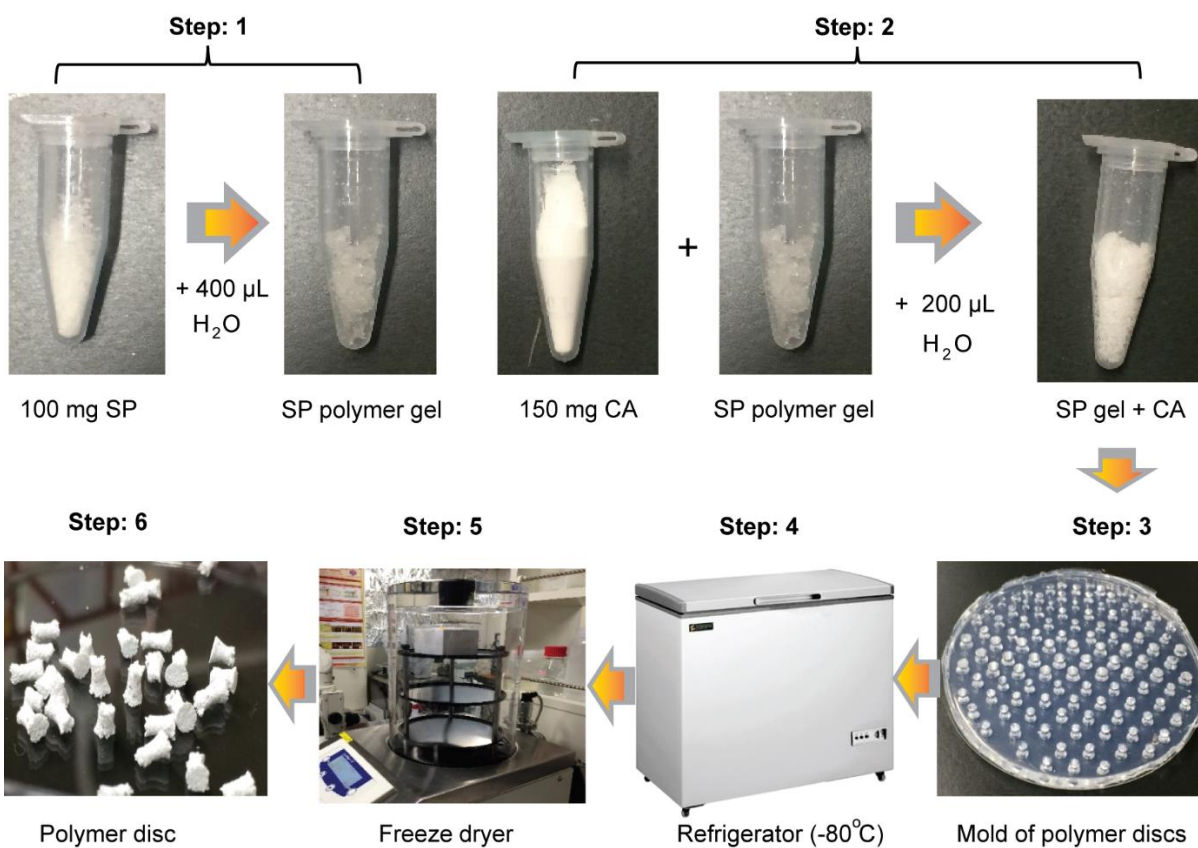


Figure 3.2. Schematic illustration of the preparation of cylindrical polymer discs: (Step 1 and 2) Preparation of the polymer gel; (Step 3) Gel put into the PDMS mold; (Step 4 and 5) Freeze drying of polymer gel; (Steps 6) Collect the discs for preserving in air tight container.

3.3.3 Design and fabrication of micropumps

The main structure and design of the device is illustrated in Fig. 3.3A. The device was constructed with the bonding of glass substrate and four individual PDMS layers which are bottom PDMS layer, diaphragm layer, PDMS actuation layer, and PDMS top layer. Structures including flow channels, reaction chamber (diameter: 2 mm), inlet solution reservoirs (diameter: 2 mm), pump chambers were formed on the bottom PDMS layer by replica molding using a template made from the thick-film photoresist. The fabrication procedures are explained in the appendix. Similarly, the PDMS actuation layer and PDMS top layer with specific pattern were formed. To fabricate 50- μm thick silicone rubber diaphragm (without any pattern), the PDMS prepolymer solution containing curing agent was spin-coated on the glass substrate at 1500 rpm for 10 min (3 times), and then cured at 80 °C for 30 min. The height of the completed flow channel, reaction chamber, and an inlet reservoir was 100 μm for all devices. The length of the flow channels from solution reservoir to the reaction chamber was 4.25 mm and width was 200- μm . The compartment of the circular shaped pump chamber with the diameter of 4.5 mm (for solution injection) was formed to the one end of the main flow channel by punching holes (punch no. 1256, Takashiba Gimune Seisakujo, Hyogo, Japan) in the PDMS bottom layer. In the same manner, another circular shape compartment with the diameter of 4 mm (for solution extraction) was formed in-between the reaction chamber and solution reservoir, and it was connected to the main flow channel through the connecting flow channel with the 45 degrees angle. The structure of the connecting flow channel and the design of the compartment for solution extraction is shown in Fig 3.3C. In the PDMS actuation layer (PDMS 3rd layer), circular shape through hole (4 mm) was formed for placing the cylindrical polymer disc. In the top PDMS layer has a circular shape pattern (diameter: 4.5 mm) connected to inlet through 1 mm long flow channel that is designed to add priming solution to polymer disc for actuating the pump. To transport solutions smoothly, 30- μm wide air vents were also formed at the reaction chamber. A small through hole was formed by punching the PDMS using a small needle at the solution reservoir to fill the solution in its reservoir.

In fabricating the final device, the glass substrate and four individual PDMS layers were rinsed with ethanol and water and the device was assembled by layer by layer bonding of each layer. Each layer of PDMS present different functions and characteristics. Fig 3.3A shows that different structures were formed on each layer of the final device. Firstly, the bottom layer of the PDMS including pump chambers (both for solution injection and extraction), solution reservoir, and the flow channel and reaction chamber was aligned and bonded with the glass substrate. Then, 50 μm -thick silicone rubber diaphragm was placed on the bottom PDMS layer and was sandwiched between the bottom PDMS layer and the PDMS actuation layer which is placed exactly above the bottom layer. The pump chamber (for solution injection) was then sealed with the diaphragm and the volume of the pump chamber was ca. 32 μL ($r = 2.25$ mm, $h = 2$ mm, surface area: 60 mm^2). It is important to note that the actuation cavity (polymer disc holding cavity) in the PDMS actuation layer should be properly aligned with the pump chamber cavity in the bottom PDMS layer which is just below the diaphragm layer. A cylindrical polymer

disc was then inserted into the actuation cavity of the third PDMS layer and the volume changes of this disc by absorbing priming solution can provide a driving force to actuate the pump to transport the solution from the solution reservoir to the reaction chamber. The top PDMS layer containing a flow channel with a solution reservoir was aligned and similarly bonded with the actuation layer. Finally, the device presented in Fig. 3.3C was obtained with the dimensions of 24 mm length, 24 mm width, and height approximately 7 mm.

To exchange of multiple solutions in a microfluidic device, the device was constructed by integrating four flow channels along with solution reservoirs in the bottom layer and each flow channel was extended from the reaction chamber. The injection and extraction pumps were integrated into the flow channels for injecting into and withdrawing solution from the reaction chamber, respectively. The design and structure of the pumps are the same as we explained in previous for single flow channel device.

To make the irreversible bonding each layer, oxygen plasma treatment was performed for 15 s at 20 W and 25 Pa oxygen pressure. After that, the glass and layers of PDMS substrates were aligned one by one and slight pressure was applied by hand to the PDMS surface to bond these substrates.

3.3.4 Working principle and characterizing the pump

Fig. 3.4 illustrates the working principle of the micropump for solution injection into and extraction from the reaction chamber. The pump is designed based on superabsorbent material named SP (crosslinked polymer) along with silicone rubber diaphragm. For solution injection, the pump is actuated by the deformation of the diaphragm upon the volume change of the polymer disc. The volume change of the polymer disc is accompanied with the swelling of the polymer disc by the absorbing of priming solution (adding DI water) Fig. 5A [23, 24]. The cylindrical cavity in the bottom PDMS structure working as a pump chamber for solution injection is surrounded by silicone rubber diaphragm, and a cylindrical shape polymer disc is placed exactly above the pump chamber cavity. The pump chamber is connected to the solution reservoir through the flow channel (flow channel: 1 mm long) and the solution reservoir is connected to the reaction chamber via flow channels (200 μm width and 4.25 mm long). Initially, the solution was loaded into the solution reservoir via a narrow hole using a pipette and the hole was sealed with adhesive tape after loading the solution. To initiate pumping, a small volume of priming solution is added to polymer disc via through hole, the pressurizing of the polymer disc with the volume change deforms the diaphragm to the downward which is resulting in decreasing the volume of the pump chamber (cavity), and pump generates a positive pressure to transport the loaded solution from reservoir to the reaction chamber (Fig. 3.4 (ii))

Based on the superabsorbent property of the polymer disc (Fig. 3.5B), the extraction of the solution from the reaction chamber is performed by generating a negative pressure with the polymer disc, and the solution is extracted from the reaction chamber through the same flow channel. For this case, the extraction chamber (in the

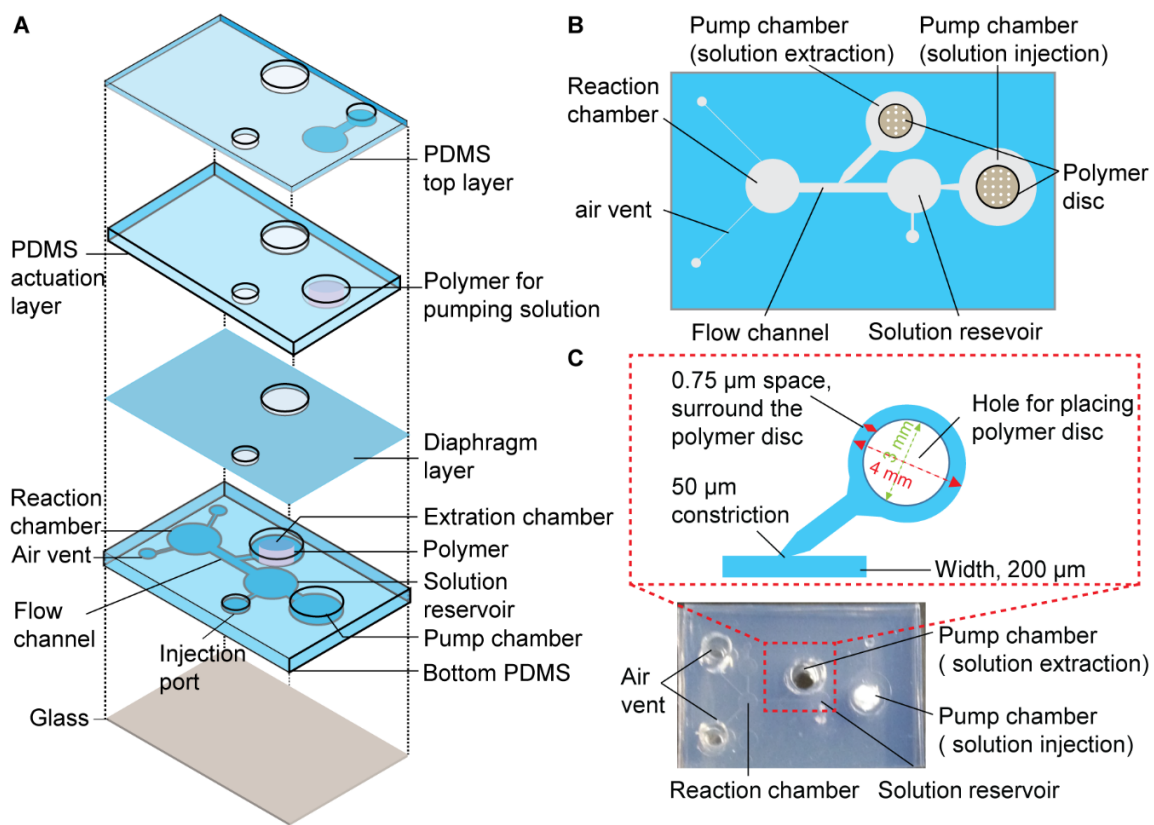


Figure 3.3. (A) Structure and design of the device with a single flow channel for solution injection and extraction using the SP polymer discs. (B) Top view of the device. (C) Photo of the device and structure of the extraction chamber along with its flow channel.

bottom PDMS layer) is connected to the main flow channel through a flow channel. When the solution was injected into the reaction chamber from the solution reservoir, the solution was also introduced at the entrance of the extraction chamber through the connection flow channel (Fig. 3.4 (ii)). After inserting the polymer disc into a circular extraction chamber via through-hole, the edge of the polymer disc makes contact with the introduced solution and initiates to absorb solution. As a result, the solution from the reaction chamber starts to move to the extraction chamber smoothly (Fig. 3.4 (iii)). Finally, the solution is completely withdrawn from the reaction chamber within a short time (Fig. 3.4 (iv)). The pump operation was video recorded using a microscope (Multiviewer system VB-S20, Keyence, Osaka, Japan).

To achieve exchange of multiple solutions using these integrated pumps, aqueous dye solutions of different colors were used to observe the movement of solutions. Initially, all solution reservoirs were loaded with the aqueous dye solutions. The solutions were injected into the reaction chamber by generating a positive pressure with the polymer discs as mentioned above. After the reaction chamber was completely filled with a solution, it was withdrawn into the corresponding extraction reservoir by a negative pressure through the polymer disc. The same steps were repeated one-by-one for the four flow channels. Fig. 3.6 illustrates the procedure of the multiple solutions exchange step-by-step in the microfluidic device.

3.3.5 Calculation of the flow rate

The performance of the pumps was evaluated by measuring the injection and extraction flow rate as well as the capability of the efficient exchange of solution in the device. The injection flow rate, Q , the length of time is required to full-fill the reaction chamber with the injected solution which is defined as, $Q = C/t$, where, C = storage capacity of the solution in the reaction chamber, and t = time is needed to full-fill the reaction chamber. Similarly, the extraction flow rate Q , the length of time is needed to withdraw the solution completely from the reaction chamber which is defined as, $Q = C/t$, where, C = amount of solution, t = time is needed to extract the solution completely.

3.4. Results and discussion

3.4.1 Optimizing the structure of the pump chambers

In order to optimize the structure of the pump chamber (for solution injection), five devices with a single flow channel that correspond to their cylindrical pump chambers with cross-sectional areas of 7.06, 9.62, 12.56, 15.90 and 19.63 mm² and height of 2 mm were considered for the measurement of the injection flow rates. Additionally, the SP polymer discs containing SP and CA at a ratio 1: 1.5 and the dimension of the actuation chambers (diameter 4 mm, height 3 mm) was similar for the all characterization experiments.

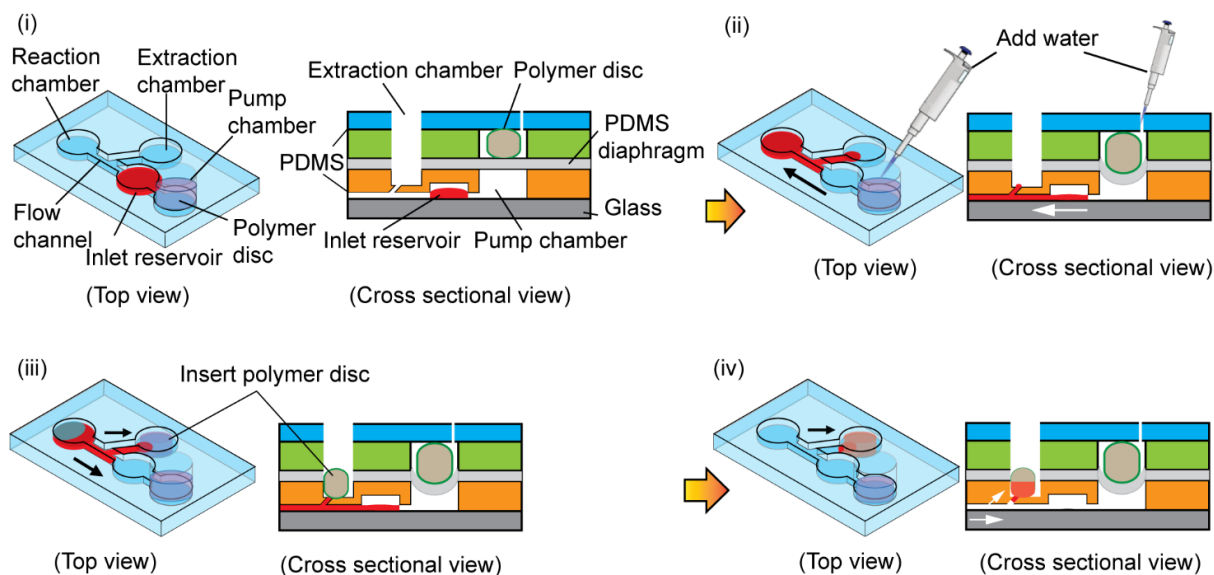


Figure 3.4. Working principle of the SP polymer actuated micropumps for on- device solution exchange: (i) solution is loaded in the inlet reservoir; (ii) After adding water to the polymer disc, solution is moved to the reaction chamber and is filled completely; (iii) After inserting the disc into the extraction compartment, solution is started to extract; (iv) The solution is flushed-out completely from the chamber. The flushed solution permeates into the polymer disc.

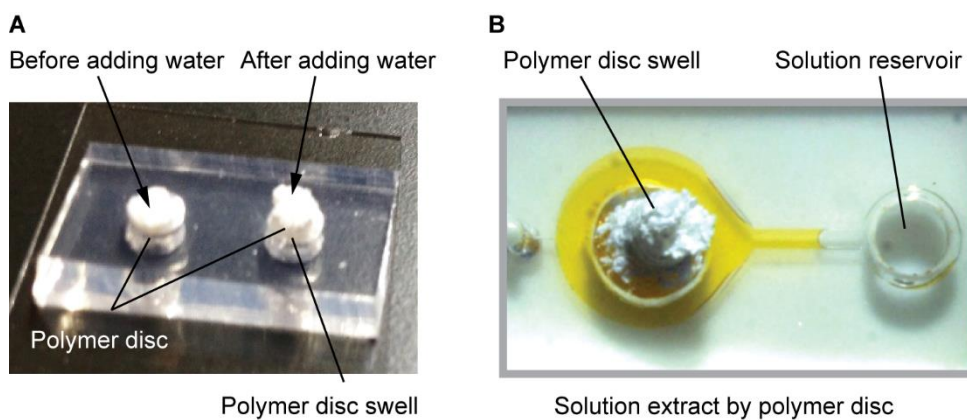


Figure 3.5. (A) Volume change of the polymer discs after absorbing water. (B) Superabsorbing capability of the polymer disc.

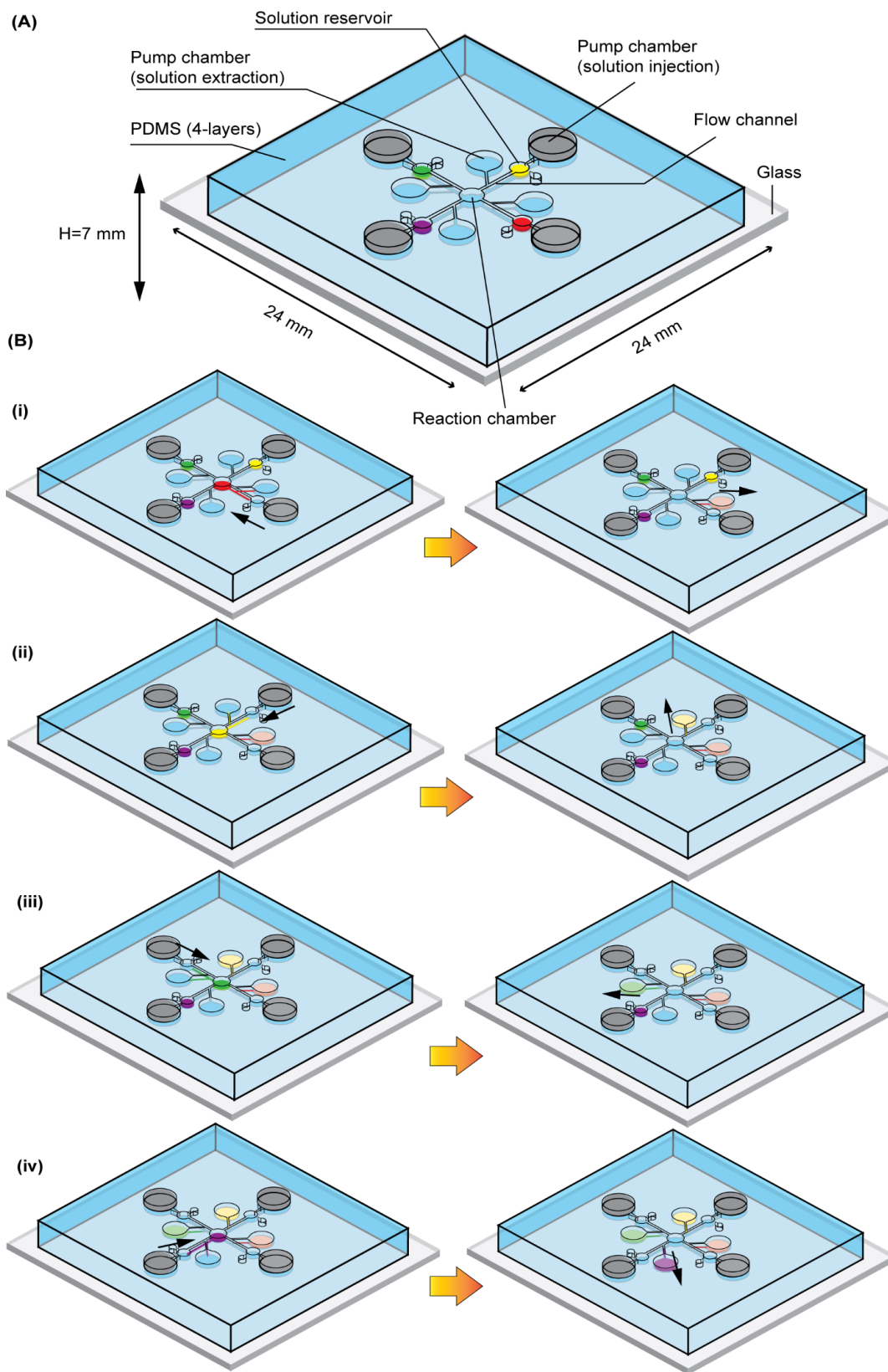


Figure 3.6. Procedures showing the exchange of multiple solutions using the SP polymer actuated pumps.

For characterization, distilled water containing food dye was used to measure the flow rate Q . The pumping was initiated by adding priming solution (DI water) onto to the polymer disc via a narrow hole, and the polymer disc was swelled by absorbing DI water. The volume change of the disc deflect the diaphragm and it was generated a positive pressure to transport the solution from solution reservoir to the reaction chamber. To correlate the injection flow rate and cross-sectional areas of the pump chamber, the length of time was measured to full-fill the reaction chamber completely with the t solution for individual devices. Fig. 3.7 shows the relationship between the injection flow rates and cross-sectional area of the pump chamber. The flow rate was significantly low for the case of the device using a pump chamber of the cross-sectional area of 7.06 mm^2 , and the flow rate linearly increased with the increase cross-sectional area of the pump chamber. The highest flow rate was $25.8 \text{ }\mu\text{L}/\text{min}$ and $26.2 \text{ }\mu\text{L}/\text{min}$ for the pump chamber of the cross-sectional area of 15.9 mm^2 and 19.6 mm^2 , respectively. The flow rate was almost the same for cross-sectional area of 15.9 and 19.6 mm^2 Therefore, pump chamber of cross-sectional area 15.9 mm^2 was used for further experiments.

To optimize the extraction chamber of the pump, the entire solution extraction capacity from the reaction chamber was evaluated by inserting the polymer disc into the extraction chamber, while the reaction chamber was completely filled with the solution. The solution extraction efficiency of the disc was examined using devices with different design of the extraction chambers; (i) of 4 mm in diameter of a circular chamber with a through hole of 4 mm in diameter and (ii) of 4 mm in diameter of circular chamber with a through hole of 3 mm in diameter. For second cases, the interior of the pumping chamber was 4 mm in diameter and the hole was 3 mm in diameter, leaving a space around the disc (Fig. 3C). When first design was used for the extraction of the solution from the reaction chamber, the polymer disc into the circular chamber was swelled by absorbing solution. As a result, the swelled polymer disc functioned as a valve and closed the flow channel exit, which can then impede the absorption of solution and the extraction of the entire solution from the reaction chamber was interrupted (Fig. 3.8A). On the other hand, the problem can be solved effectively with the second design of the extraction chamber (Fig. 3.8B), and the solution was absorbed by the polymer disc until the reaction chamber became empty.

3.4.2 Pump performance

Exchange of multiple solutions was performed using a device consisting of one reaction chamber and four flow channels connected to the independent injection and extraction pumps. Fig. 3.9 shows how solutions were injected into the reaction chamber from the solution reservoirs by the injection pump and the solution was returned to each extraction chamber by the extraction pump one by one. When the aqueous dye solutions were injected into the reaction chamber, solution was confined in the reaction chamber without intrusion into the other flow channel.

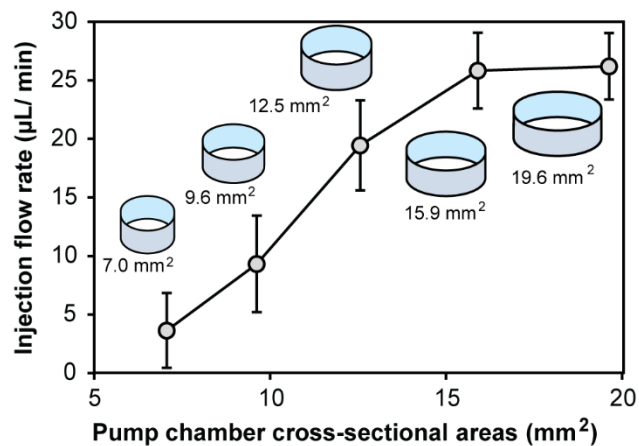


Figure 3.7. Injection flow rate of the SP polymer actuated pump with different pump chamber. Error bars represent the \pm standard deviation over the 3 replicates.

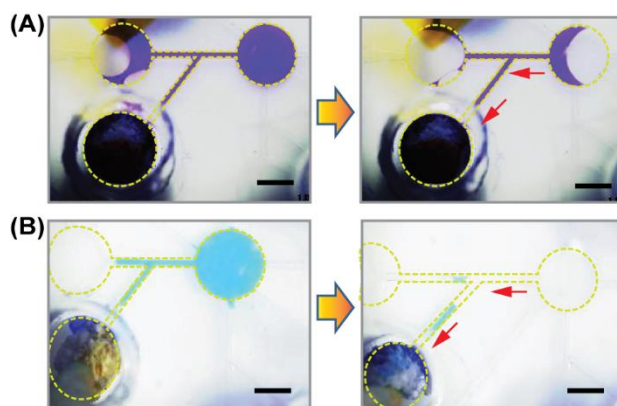


Figure 3.8. Solution extraction efficiency of the polymer disc using device with two design of the extraction chamber. (A) Circular chamber of 4 mm in diameter with a through hole of 4 mm in diameter. (B) Circular chamber of 4 mm in diameter with a through hole of 3 mm in diameter. Scale bar: 1 mm.

In addition, the solution was withdrawn subsequently via the same flow channel by the insertion of the disc into the extraction chamber. The experimental results suggest that solutions did not split during the process and no residues were left in the reaction chamber after extracting the solutions.

Furthermore, the performance of the pumps was characterized by checking the solution exchange capability of the pump. For this purpose, we measured the injection and extraction flow rate of aqueous sample solutions containing DI water, 0.1 M KCl, 0.1% (v/v), 1 M KCl, 0.1% (v/v), Glycerol (2X dilution) and Glycerol (99 %). Fig. 10 shows the average flow rates (both injection and extraction flow rate) of the sample solutions to be exchanged. The injection flow rate was almost same (25.8 $\mu\text{L}/\text{min}$) for DI water, 0.1 M KCl, and 1M KCl. However, the injection flow rate decreased to 17.4 and 2.7 $\mu\text{L}/\text{min}$ for the cases of viscous solutions of glycerol (2X dilution) and glycerol (99 %), respectively, due to the viscosity effect of the solutions. In addition, the extraction flow rate decreased gradually for solutions other than DI water (Fig. 3.10). The DI water was extracted at a constant flow rate (0.73 $\mu\text{L}/\text{min}$). Considering the material and structure, the stable pumping at a constant flow rate is surprising. Also, the sample solutions including 0.1 M KCl, 1 M KCl and glycerol (2x dil.) were extracted entirely from the reaction chamber, the flow rate of the solutions 0.1 M KCl, 1 M KCl and glycerol (2x dil.) decreased to 0.34, 0.12 and 0.06 $\mu\text{L}/\text{min}$, respectively. Though the absorption capacity of the superabsorbent polymer (SP) was the highest with distilled water and the lowest with the electrolyte solution [25], thus, the extraction flow rate was low for the KCl solution. For the KCl solution, the low extraction flow rate is the result of the polyelectrolyte effect. The cations in the solution can bind to the carboxylic groups of the superabsorbent polymer and lead to the neutralization of the polyanions. As the ionic strength of the solution increase, the osmotic pressure is decreased, thus, the absorption as well as flow rate is slows down [18, 25, 26]. The viscosity of solutions can also affect absorption efficiency of the polymer discs. As a result, the extraction flow was observed substantial low for the Glycerol (2x dilution) solution, and for the case of glycerol (99%), solution was not extracted at all from the reaction chamber. The extraction flow rate for all the cases can be increased by increasing temperature. Absorption of water by the superabsorbent polymer (SP) is highest at around 55°C [25].

Furthermore, the extraction efficiency of the polymer disc was checked using the optimized device for the aqueous solution at different pH conditions. Under acidic (< pH 6) or basic (> pH 10) conditions, the SP polymer can absorb a small volume of water. [27]. Fig. 3.11 shows the extraction flow rate of an aqueous solution at different pH conditions. The extraction flow rate reduced significantly for solutions in the pH range between 2 and 5, became almost steady in the pH range between 6 and 9, and decreased again in the pH range between 11 and 13. This results can be attributed by the fact that under acidic conditions, the degree of dissociation of the sodium carboxylate groups in the polymer decreased, thus, affinity of polymer network for water is reduced. On the other hand, in basic media, the number of cations in the polymeric network increased, thus, the expansion of polymer voids is restricted. As a result, the water absorbency could also decreased in basic condition.

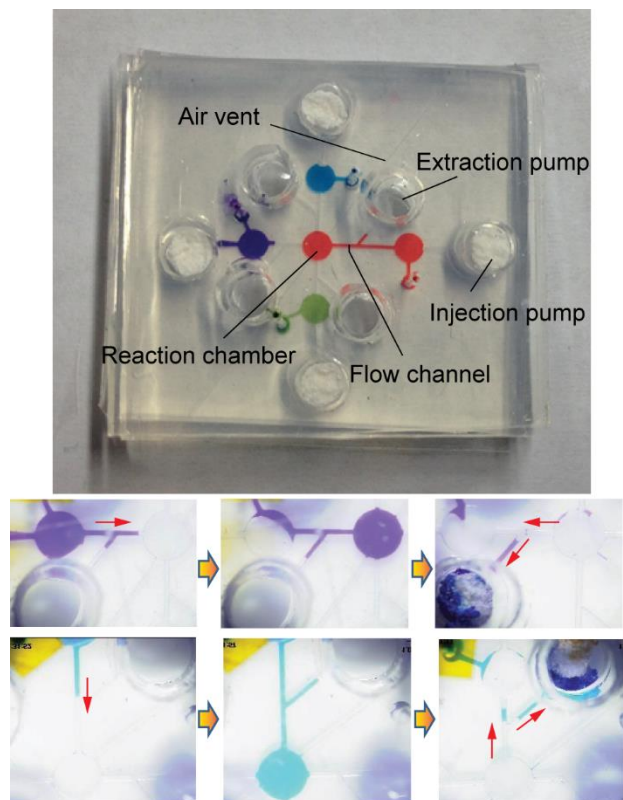


Figure 3.9. Images shows that exchange of multiple solutions using the SP polymer-based injection and extraction pumps.

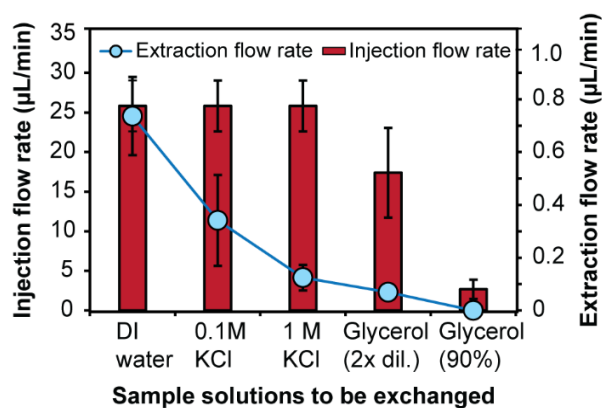


Figure 3.10. Dependence of the injection and extraction flow rate on the sample solutions to be exchanged. Error bars represent the \pm standard deviation over the 6 replicates.

3.4.3 Tuning of the injection and extraction flow rate

The polymer pump-driven flow rate may depend on the several parameters like structure and geometry of the flow channels, nature of substrate surface (i.e. hydrophilic or hydrophobic), properties of solutions (i.e. concentration, viscosity) and materials used for pumping [13, 14, 28]. In this pump system, the injection flow rate depends on the swelling capacity of the polymer disc which generates the pressure to deflect the thin diaphragm to the downward. As the rate of swelling of polymer is decreased with the increasing of concentration of NaCl solution [27], we hypothesized that addition of different concentration of NaCl solutions to the polymer disc would be influenced on the injection flow rate as well as the volume changes of the polymer disc. Our data confirmed this hypothesis. To control the injection flow rate, five concentrations of NaCl solutions (0.5%, 1%, 2.5%, 5% and 10% aq. NaCl solution) and DI water containing no NaCl were used. Fig. 3.12 shows the dependence of the injection flow rate of DI water on DI water and different salt concentrations added to the polymer disc. The highest flow rate was obtained with DI water and the flow rate decreased gradually with the increases the NaCl concentration. For the case of addition of 10% NaCl solution, solution was not flow from the inlet to the reaction chamber. The results indicate that with the increase the salt concentration, osmotic pressure difference between the internal and external of the disc will be smaller and the absorption of the solution as well as the change of volume of the disc is reduced [27]. Additionally, the swelling properties of the polymer are associated with the electrostatic repulsion of $-\text{COO}^-$ groups acting on the charging network of the gel, and $-\text{COO}^-$ groups are produced by the dissociation of sodium ions from functional groups ($-\text{COONa}$) in the polymer gel. At high salt concentrations, the dissociation will be smaller resulted the decreasing the electrostatic repulsion among the $-\text{COO}^-$ groups and volume change. As a result, the diaphragm deflects to a less extent and thus flow rate decreased with the increasing of salt concentration.

To tune the extraction flow rate, the solution extraction performance of the pump was examined by changing the composition and the proportions of SP and CA in the polymer disc: (i) ratio of SP and CA was 1:0.5, and prepared with DI water (ii) ratio of SP and CA was 1:1, and prepared with DI water (iii) ratio of SP and CA was 1:1.5, and prepared with DI water and (iv) ratio of SP and CA was 1:1.5, prepared with saline solution (0.9 % NaCl) or organic solvent (aq. ethanol) [25-27]. Fig. 3.13 illustrates the extraction efficiency of the solution in terms of extraction flow rate with different compositions of polymer disc. The flow rate could be decreased for the case (iv) when polymer disc prepared with 0.9 % NaCl solution or aq. Ethanol. Although, the highest rate was attained for the cases (i) and (ii), but, the solution was split during extraction, thus the complete solution extraction from the reaction chamber was interrupted with theses composition. After extraction, some solution always left in the reaction chamber. On the other hand, the best result with an optimum flow rate was achieved for the case of (iii), in which all the solution was smoothly extracted from the reaction chamber, no such problems were observed as we mentioned for above the cases. Therefore, the flow rate could be tuned in several ways according to the demand, and the pump would be feasible for the devices where a slow flow rate is required.

3.5. Conclusions

A PDMS micropump can be demonstrated using a superabsorbent polymer, “SP” for exchanging of multiple solutions. Solution injection and extraction were realized by using the swelling and super-absorbing properties of the polymer disc, respectively. The superabsorbent polymer used in our pump absorbs solutions whose volumes are much larger than that of the dry SP disc. Despite the simple structure, the micropump can realize a constant flow rate. The injection flow rate can be tuned by optimizing the volume of the (dimensions) of the pump chamber that creates an elastic restoration force and by choosing an appropriate priming solution. Also, the extraction flow rate can be adjusted by modulating the composition of the materials in the polymer disc and choosing an appropriate sample solution to be extracted. The developed micropump was also used of an uncomplicated microfabrication process. The simple micropumps will be useful for user-friendly disposable microfluidic devices with multiple solutions processing function in which miniaturization offers an advantage to acting biological assays. Since the microfluidic operations were accomplished without using any external power or pressure sources, the platform can be extensively applicable for POC analysis.

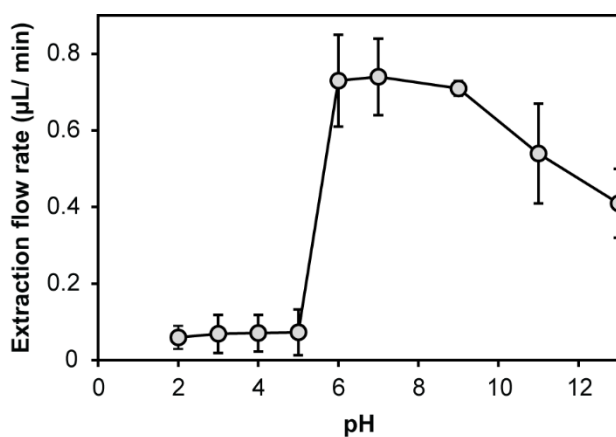


Figure 3.11. Dependence of the extraction efficiency of the polymer actuated extraction pump on pH of the aqueous solution. Each data point shows an average of three measurement ($n = 3$) and error bars represent the \pm standard deviation over 3 replicates.

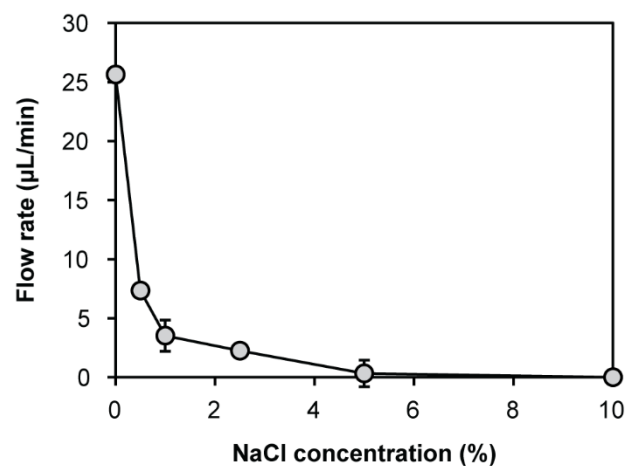


Figure 3.12. Dependence of the injection flow rate of DI water on the DI water and different concentrations of NaCl solutions added to the polymer disc. DI water used as a sample solution to be transported. (n = 3).

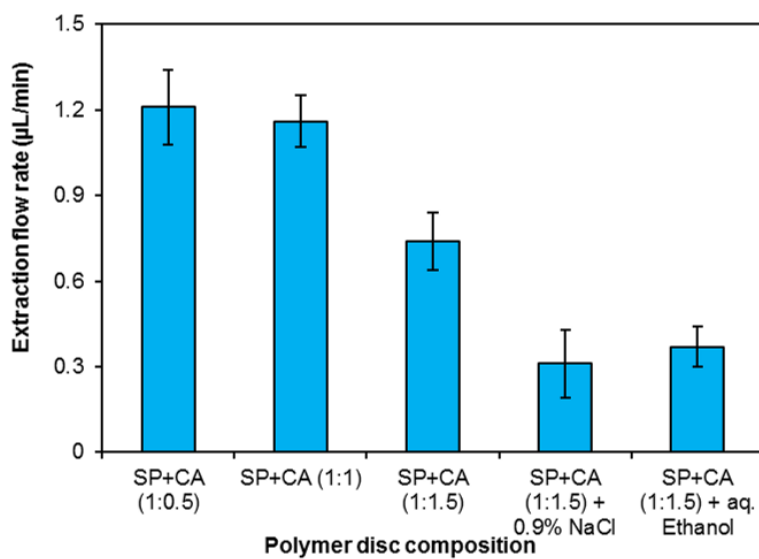


Figure 3.13. Dependence of the extraction pump efficiency on the different composition of SP polymer disc. Each data point shows an average of three measurement (n = 3) and error bars represent the \pm standard deviation over 3 replicates.

References

1. Squires, T. M., & Quake, S. R., *Reviews of modern physics*, **2005**, 77(3), 977.
2. Woias, P., *Sensors and Actuators B: Chemical*, **2005**, 105(1), 28-38.
3. Hosokawa, K., Sato, K., Ichikawa, N., & Maeda, M., *Lab on a Chip*, **2004**, 4(3), 181-185.
4. Randall, G. C., & Doyle, P. S., *Proceedings of the National Academy of Sciences*, **2005**, 102(31), 10813-10818.
5. De Gennes, P. G., Brochard-Wyart, F., & Quéré, D., *In Capillarity and Wetting Phenomena* (pp. 33-67), **2004**. Springer, New York, NY.
6. Laser, D. J., & Santiago, J. G., *Journal of micromechanics and microengineering*, **2004**, 14(6), R35.
7. Wang, Y. N., & Fu, L. M., *Microelectronic Engineering*, **2018**, 195, 121-138.
8. Au, A. K., Lai, H., Utela, B. R., & Folch, A., *Micromachines*, **2011**, 2(2), 179-220.
9. Culbertson, C. T., Mickleburgh, T. G., Stewart-James, S. A., Sellens, K. A., & Pressnall, M., *Analytical chemistry*, **2013**, 86(1), 95-118.
10. Suzuki, H., & Yoneyama, R., *Sensors and Actuators B: chemical*, **2002**, 86(2-3), 242-250.
11. Suzuki, H., & Yoneyama, R., *Sensors and Actuators B: Chemical*, **2003**, 96(1-2), 38-45.
12. Satoh, W., Shimizu, Y., Kaneto, T., & Suzuki, H., *Sensors and Actuators B: Chemical*, **2007**, 123(2), 1153-1160.
13. Walker, G. M., & Beebe, D. J., *Lab on a Chip*, **2002**, 2(3), 131-134.
14. Zimmermann, M., Schmid, H., Hunziker, P., & Delamarche, E., *Lab on a Chip*, **2007**, 7(1), 119-125.
15. Liang, D. Y., Tentori, A. M., Dimov, I. K., & Lee, L. P. *Biomicrofluidics*, **2011**, 5(2), 024108.
16. Dimov, I. K., Basabe-Desmonts, L., Garcia-Cordero, J. L., Ross, B. M., Ricco, A. J., & Lee, L. P., *Lab on a Chip*, **2011**, 11(5), 845-850.
17. Shimizu, Y., Takashima, A., Satoh, W., Sassa, F., Fukuda, J., & Suzuki, H., *Sensors and Actuators B: Chemical*, **2009**, 140(2), 649-655.
18. Hu, Y., Beach, J., Raymer, J., & Gardner, M., *Journal of Exposure Science and Environmental Epidemiology*, **2004**, 14(5), 378.
19. Machauf, A., Nemirovsky, Y., & Dinnar, U., *Journal of Micromechanics and Microengineering*, **2005**, 15(12), 2309.
20. Xu, D., Wang, L., Ding, G., Zhou, Y., Yu, A., & Cai, B., *Sensors and Actuators A: Physical*, **2001**, 93(1), 87-92.
21. Sim, W. Y., Yoon, H. J., Jeong, O. C., & Yang, S. S., *Journal of Micromechanics and Microengineering*, **2003**, 13(2), 286.
22. Xu, T. B., & Su, J., *Sensors and Actuators A: Physical*, **2005**, 121(1), 267-274.
23. Sakohara, S., Muramoto, F., & Asaeda, M., *Journal of Chemical Engineering of Japan*, **1990**, 23(2), 119-124.
24. Flory, P. J., *Principles of polymer chemistry*. *Cornell University Press*, **1953**.

25. Liu, M., & Guo, T. *Journal of Applied Polymer Science*, **2001**, 82(6), 1515-1520.
26. Liu, Z. S., & Rempel, G. L., *Journal of Applied Polymer Science*, **1997**, 64(7), 1345-1353.
27. Ogawa, I., Yamano, H., & Miyagawa, K., *Journal of applied polymer science*, **1993**, 47(2), 217-222.
28. Wang, X., Hagen, J. A., & Papautsky, I., *Biomicrofluidics*, **2013**, 7(1), 014107.

Chapter 4: Control of microfluidic solution transport by switchable hydrophobic microvalves based on conducting polymer

4.1. Introduction

Nowadays, the most widely used microvalves in microfluidics are the Quake valve [1-3]. The valves comprises of a double-layer polymer flow channel structure with an elastomeric membrane separating the two layers. With the deformation of the membrane, the solution in the fluidic channel is transported in a control manner and **many** valves in microchannel networks can control solution transport for multiplexed processing of solutions. However, external instruments for actuation, such as air pump, is required to operate the microvalve, which makes the microsystem complex and limits its further miniaturization. Furthermore, other promising microvalves are ones that are based on the phase transformation of the materials. The volumetric changes of these materials in response to changes in temperature or pH value are allowed to forces the material flowing into the microchannel or actuated the deformation of the adjacent microchannel to control the fluid flow inside the channel [4-8]. However, the valve fabrication process is not uncomplicated and their response was relatively slow. Capillary-burst valves are attractive because it can manipulate fluid flow inside microchannels by changing the capillary forces without moving parts, and the valve can be fabricated easily. For a passive capillary valve, the changes of the capillary forces are accompanied by an abrupt geometry expansion in the microchannel or by the electrocapillary and thermocapillary effects that can control the capillary force [9]. However, the valve function is difficult to reproduce once opened, which limits its further application. For numerous applications, it is expected to have an uncomplicated valve configuration that does not rely on any moving parts, does not involve an external pressure source, regulator and timer, and can be incorporated with numerous diverse forms of substrate materials. In this chapter, we introduce a new valve to control transport of the solutions in a network of flow channels employing the wettability changes of a conducting polymer. After that, the integration of the valves into the previous device (Chapter 3) demonstrate an efficient exchange of solutions with minimal user intervention.

4.2. Toward development of the novel valve

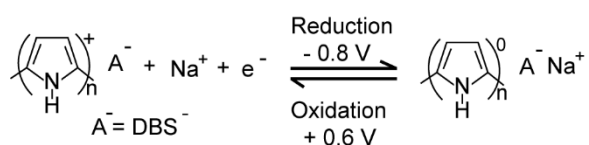
Hydrophobic patch valves with a hydrophobic region on the bottom surface of a microchannel is attractive because they do not have any moving parts and its straightforward fabrication process make it applicable for high-density integration [10]. The hydrophobic valves were used in combination with the application of pressure. A solution stopped at the valve passes through the region by the application of pressure [11]. However, with this method, a pressure source is required. To solve this problem, alternative mechanisms, such as the use of temperature, pH changes, and the application of electric potential have been reported [12- 14]. Previously, Biswas

et al, reported a switchable hydrophobic valve based on the switching of the potential of an electrode that constitutes the valve [14]. However, a problem with this valve was contamination by alkanethiol dissolved after opening the valve. Also, after long time storage, the valves no longer operate.

Here, we report a switchable polypyrrole (PPy)-based hydrophobic valve for controlled transport of solution in microfluidic channels, whose surface wettability may be tuned in situ under the application of a redox potential. A variety of surface-switchable materials which change their wettability in response to optical [15], thermal [16], and electrochemical stimuli [17], have been investigated. Among these approaches, electrically activated materials (wettability changes by applying electric potential) are promising [18]. PPy is an example of such a material. The properties of the PPy can be reversibly tuned by doping or dedoping different ions [19]. Due to its dynamically-controllable properties and excellent chemical stability, PPy has been used to develop valve to control fluid flow in lateral flow device [18] pump to drive fluid flow to the sensing area [20]. However, to understand truly practical valves, improvements are required taking into consideration that the valves can be integrated into complex microchannel architectures and can be operated in an automated fashion with a short response time.

In this study, we developed a valve using a conducting polymer PPy. The valve function is accompanied by changing the wettability of the doped polymer film according to the scheme 1 [17]. Our valves can be functioned with low-power electrical signals that can be interfaced directly to a computer and enables direct control of timing sequences. The simple structure and operation enabled controlled transport of solutions in a network of flow channels for applications such as biochemical analyses or others.

Scheme 1. The cations insertion and expulsion in the polymer film facilitated by the electrochemical reduction and oxidation of the polymer



4.3. Experimental

4.3.1 Reagents and Materials

Reagents and Materials used for fabrication and experiments were purchased from the following Ycommercial sources: Glass wafers (No. 7740, 3 inch diameter, 500- μm thick) from Corning Japan (Tokyo, Japan); positive photoresist (S-1818G) from Dow Chemical (Midland, MI, USA); a thick-film photoresist (SU-8 25) from MicroChem (Newton, MA, USA), prepolymer solution of PDMS (KE-1300T) and its curing reagent (CAT-1300) from Shin-Etsu Chemical (Tokyo, Japan); pyrrole and sodium dodecylbenzenesulfonate (NaDBS) from Sigma-

Aldrich (St. Louis, USA), sodium dodecylsulphate (NaDS) and a dye (sunset yellow) from Wako Pure Chemical Industries (Osaka, Japan). All the other reagents were obtained from Wako Pure Chemical Industries. All the solutions were prepared with ultra-pure water.

4.3.2 Formation of the polypyrrole films

To form the surfactant (NaDS and NaDBS)-doped PPy films, platinum (Pt) layer was deposited on a glass substrate by sputtering (300 nm thick). After that, the substrate was diced into chips of 10 mm × 10 mm. The electrochemical polymerization was carried out using a three-electrode cell consisting of a platinum working electrode, a platinum auxiliary electrode, and a commercial Ag/AgCl as the reference electrode (2060A, Horiba, Kyoto, Japan) (Fig 4.1A). The electrodes were connected to a potentiostat (Autolab PGSTAT12; Eco Chemie, Utrecht, Netherlands). A freshly prepared polymerization solution containing 0.2 M pyrrole dissolved in a 0.2 M sodium dodecylbenzenesulfonate (NaDBS) or 0.2 M sodium dodecylsulphate (NaDS) was degassed by purging it with a nitrogen gas for 5 min. Then, a constant current 1 mA/cm² was applied to the platinum layer for 120 s to deposit PPy. The film thickness of PPy(DBS) or PPy(DS)-doped PPy was accurately controlled by adjusting the amount of applied charge. For instance, a 1 C cm⁻² surface charge produces a 3 μm thick film [21]. Finally, the deposited PPy film was rinsed with ultra-pure water and dried by blowing nitrogen gas.

4.3.3 Measurement of the wettability of the NaDS or NaDBS-doped PPy film

An appropriate dopant was selected and polymerization time was optimized by measuring the changes in the wettability of the NaDS and NaDBS-doped PPy film using an as-deposited film, and electrochemically reduced and oxidized films. The wettability was evaluated by measuring the contact angle of a water droplet (1 μL) placed on the film using a contact angle meter (Model G-1-1000, ERMA INC., Tokyo, Japan) before (as-deposited film) and after the application of -0.8 V (vs. Ag/AgCl) (reduced film) and +0.6 V (vs. Ag/AgCl) (oxidized film) to the platinum electrode. The electrochemical cell used to change the redox state was the same as the one used for the synthesis of the PPy films (Fig. 4.1B). After immersing the NaDBS or NaDS-doped PPy film in a 0.1 M KCl solution, -0.8 V (vs. Ag/AgCl) was applied to the platinum electrode for 90 s to convert the oxidized PPy to neutral PPy. The film was rinsed with ultra-pure water and dried by blowing dry nitrogen gas and contact angle of a water droplet was measured. The film was then immersed in a 0.1 M KCl solution, and +0.6 V (vs. Ag/AgCl) was applied to the electrode for 90 s to re-oxidized PPy. After rinsing the re-oxidized film in ultra-pure water and dried by blowing dry nitrogen gas, the contact angle of a water droplet was measured in the same manner. The wettability switching experiments were carried out twice using the same sample.

4.3.4 Fabrication and operation of the valve

To fabricate the valves, platinum (300-nm-thick) was deposited on a glass substrate by sputtering with a 50-nm-thick chromium intermediate layer. Electrode patterns were formed by lift-off. To form the NaDBS-doped PPy film on the platinum electrode, a solution containing water, 25% NH₃, 30% H₂O₂ in a 4:1:1 volumetric ratio was used to clean the electrode. The cleaned electrode was then dried by blowing dry nitrogen gas. To deposit PPy, the platinum electrode was immersed into a solution containing 0.2 M pyrrole and 0.2 M NaDBS, and a constant current (1 mA/cm²) was applied to the electrode for 120 s. Following the deposition of NaDBS-doped PPy film onto platinum electrode the surface was rinsed with ultra-pure water, and was dried by blowing nitrogen gas.

To demonstrate the applicability of the valve, a microfluidic device was constructed by bonding a poly(dimethylsiloxane) (PDMS) substrate with a flow channel structure and a glass substrate with the valve (Fig. 4.2A). To bond the two substrates, slight pressure was applied to the PDMS surface by hand. The NaDBS-doped PPy was used for the valve. The PDMS flow channel was formed by replica molding using a mold formed with a thick-film photoresist SU-8 25. The height of the flow channel was 80 μm for all devices, and the channel width was varied between 500 and 1000 μm. An inlet and an outlet were formed at the ends of the flow channel by punching a hole of 4 mm diameter (punch no. 1256, Takashiba Gimune Seisakujo, Hyogo, Japan) in the PDMS layer.

To characterize the valve, a 0.1 M KCl solution was first injected into the solution inlet. The solution moved in the flow channel by capillary action, but stopped at the edge of the valve. A commercial Ag/AgCl reference electrode (2080 A-06T, Horiba, Kyoto, Japan) was then inserted into the solution inlet (Fig. 4.2A), and a potential was applied to the valve electrode using a potentiostat (HA-151, Hokuto Denko, Tokyo, Japan) with respect to the Ag/AgCl reference electrode. Fig. 4.2C explains the principle of valve operation. The application of a reductive potential to the platinum electrodes switched the valve from a hydrophobic state to a hydrophilic state via the reorientation of dopant molecules according to $[(PPy^+){}_n DBS^-] + Na^+ + e^- \leftrightarrow [(PPy^0){}_n DBS^- Na^+]$ [22]. Following this, the solution started to pass through the valve region and moved forward in the flow channel.

A dye solution containing 0.1 M KCl was used to visualize the movement of the liquid column in the flow channel under a microscope (Multiviewer system VB-S20, Keyence, Osaka, Japan). All the experiments were carried out at room temperature.

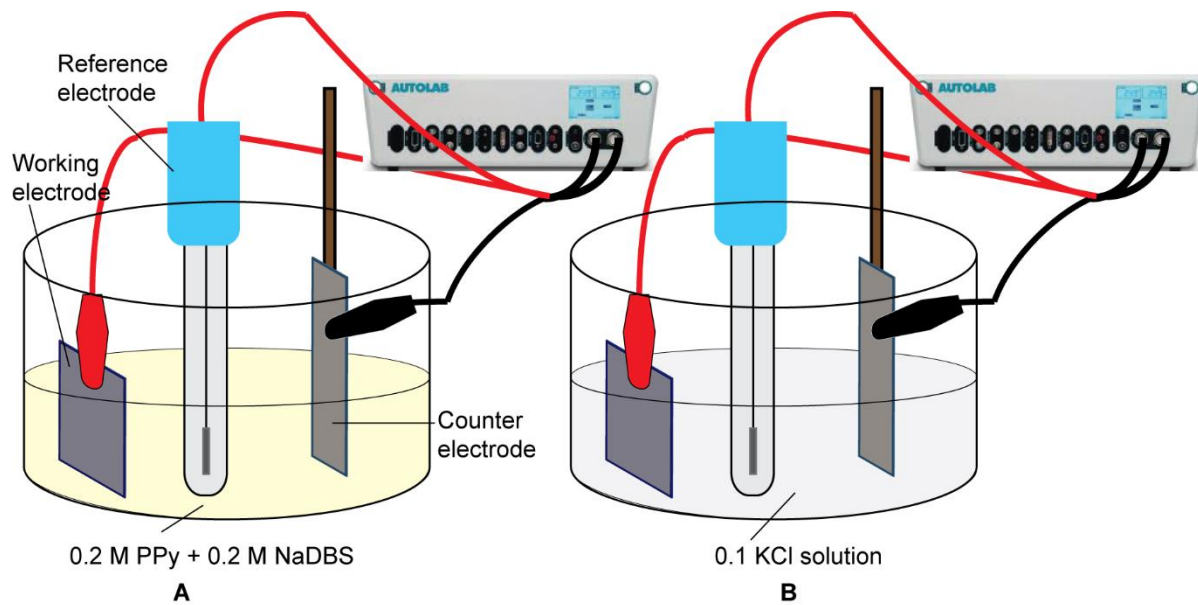


Figure 4.1. Schematic of three-electrode electrochemical cell: (A) Set-up for formation of doped PPy film onto platinum electrode. (B) Set-up for characterization of wettability switching of the doped film.

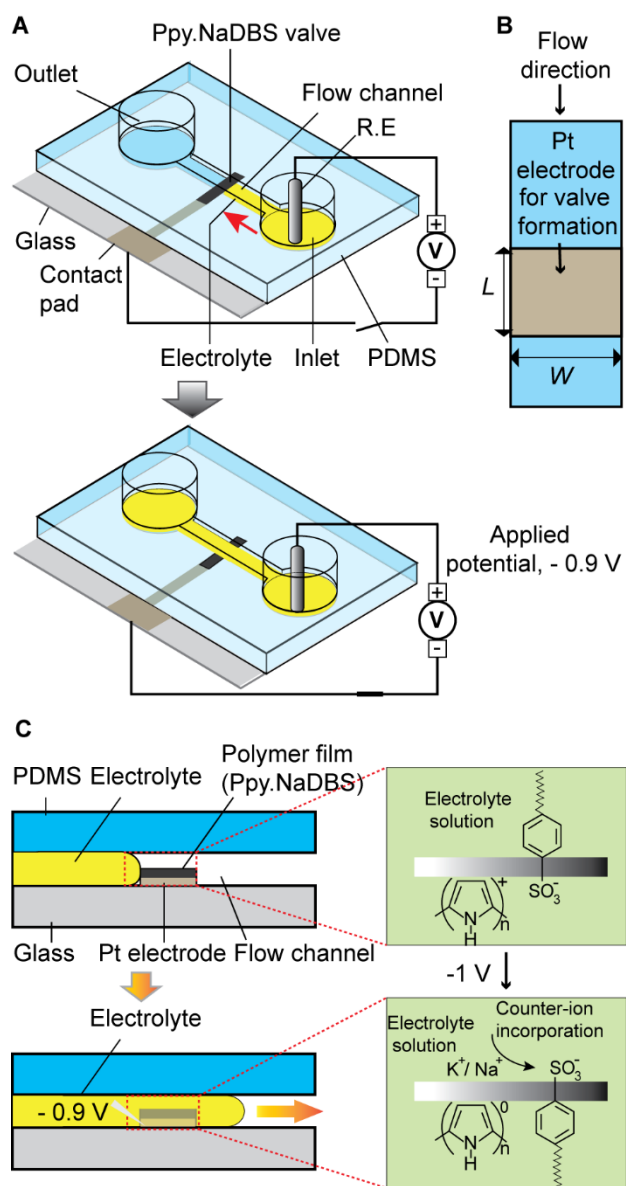


Figure 4.2. (A) Schematic of the microfluidic system with the switchable hydrophobic valve. (B) Platinum electrode dimensions in the microchannel. (C) Principle of valve operation.

4.4. Results and discussion

4.4.1 Characterizing the wetting behavior of the doped PPy film

As polymerization proceeded, the PPy film coated platinum progressively darkened from pale yellow to pitch black, and uniform polymer film was formed. (Fig. 4.3). The color change of the polymer film can be aided as a visual confirmatory test for deposition. The film grow at constant current or constant voltage can led to better in wettability switching [23]. To form an appropriate film, the application of an appropriate potential or current is indispensable. For example an applied potential lower than 0.5 V results in a poor film with nonhomogeneous coverage, and a potential higher than 0.85 V lead to overoxidation and loss of the redox behavior. As a result, the reversible switching behavior of the film is deteriorated [24, 25].

To select an appropriate dopant (surfactant) for the valve, the wetting behavior of doped PPy film was evaluated by measuring the water contact angle. The wetting properties were examined at three stages: prior to applying a potential (as-deposited), after applying a reductive potential, and after applying an oxidative potential. Fig. 4.4 C shows the wettability change of the PPy film at each stages of the switching cycle when NaDBS and NaDS were used. The as-deposited polymer films were hydrophobic, and the hydrophobicity was enhanced by changing the type of dopant. Actually, water contact angle was 76 ± 3 degrees for NaDS-doped PPy and 86 ± 4 degrees for NaDBS-doped PPy. This observation is in agreement with the fact that wettability of the doped PPy film strongly depends on the types of dopants used [17, 26]. This enhanced hydrophobicity of the NaDBS-doped PPy is due to the long hydrophobic alkyl chain of the dopant NaDBS.

When a reductive potential is applied to the surfactant-doped PPy, the surface becomes more hydrophilic as a result of the reorientation of the dopant molecules with hydrophilic polar sulfonic acid group headed out from the surface, and the charge was neutralized by the incorporation of Na^+ ions [26]. Accompanying this, the water contact angle decreased to 33 ± 4 degrees and 25 ± 6 degrees for NaDS-doped PPy and NaDBS-doped PPy, respectively. The doped-PPy film became hydrophobic again by applying +0.6 V to the reduced film, and water contact angle increased again to 52 ± 4 degrees and 59 ± 3 degrees for NaDS-doped PPy and for NaDBS-doped PPy film, respectively. In this case, the charges of the doped PPy film are neutralized by the expulsion Na^+ ions form the dopant molecules and leaving behind DS- or DBS- molecules which are then coupled to oxidized PPy chains via ionic bonding with polar sulfonic acid group [27]. Because the strongly hydrophilic polar sulfonic acid group is attracted to the polymer backbone and the hydrophobic alkyl group is heading out to the surface, the polymer surface becomes hydrophobic [28]. Fig. 4.4A and 4.4B illustrates the representative example of the wettability changes of the NaDBS-doped PPy film under the application of redox-potential.

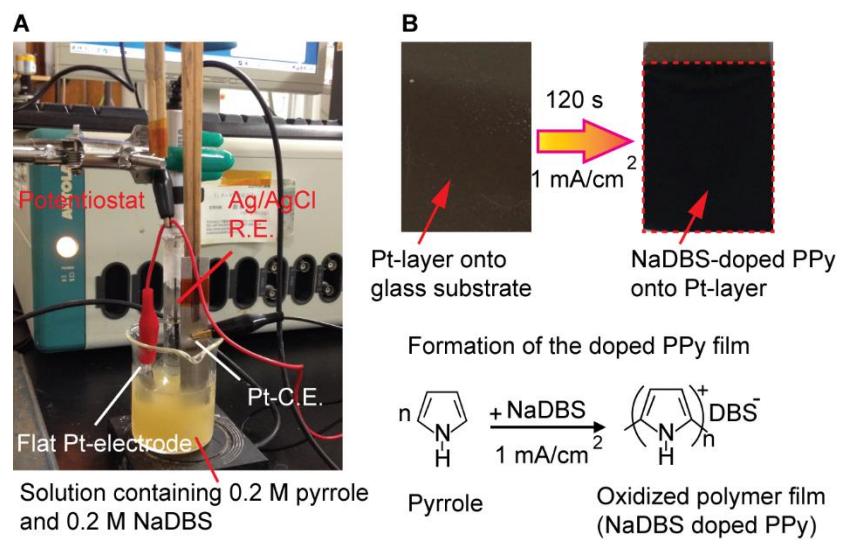


Figure 4.3. (A) Photograph of the experimental set-up for the formation of doped PPy film onto platinum-surface. (B) Platinum-surface is progressively darkened to pitch black as the uniform NaDBS-doped PPy films formed by electrochemically polymerization.

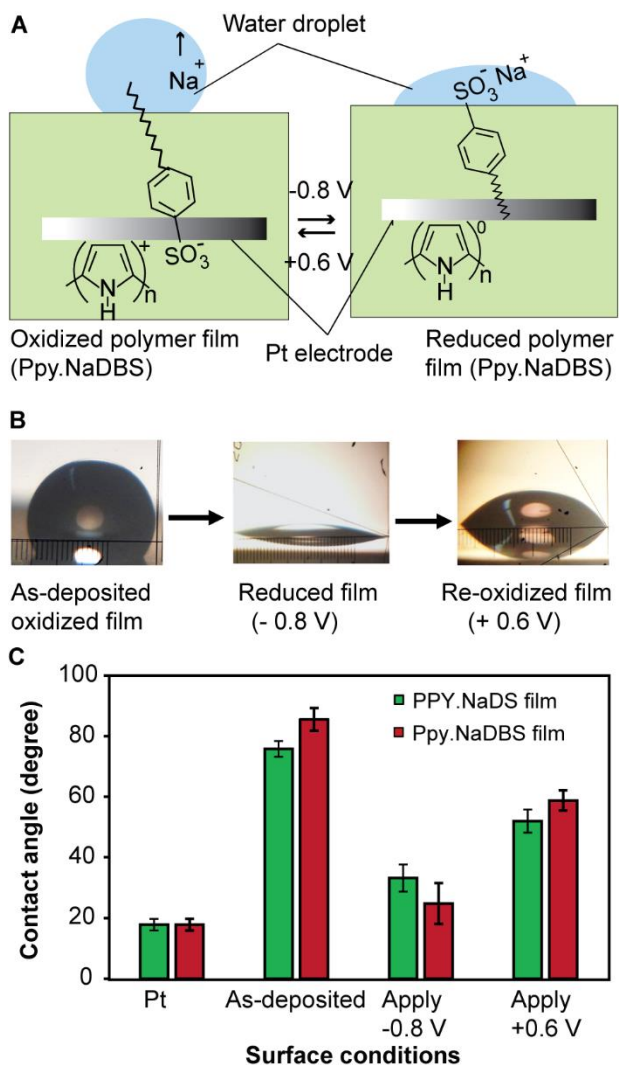


Figure 4.4. Change in wettability of the doped PPy by the application of potential. (A) Schematic illustration of electrical-potential-induced reversible wettability conversion of the NaDBS-doped PPy film (B) Water-droplet on NaDBS-doped PPy coated platinum surfaces at as-deposited film, reduced film and re-oxidized film (C) Surface wettability behavior of the clean flat platinum surface, surfactant doped PPy coated platinum surface (native), reduced and re-oxidized surface of doped PPy coated platinum. Error bar represent \pm standard deviation over 6 replicates.

The length of time for electropolymerization was optimized based on the result of the wettability at each stages of the switching cycle. Although Golabi et al. reported that the wettability is not influenced by the length of time for eletropolymerization [38], our experimental result suggests that wettability depends on the length of time. Fig. 4.5 shows the effect of the polymerization time on wettability changes of the NaDBS-doped PPy film at three stages of the switching cycle. When the polymerization time was longer than 60 s, the contact angle of the as-deposited film tended to saturate at 86 ± 1 degrees, which is close to values reported previously [29, 21, 30]. However, the changes in wettability of the as-deposited, reduced, and re-oxidized films were larger for 120 s polymerization time than that of the other cases. Thus, the polymerization time was 120 s unless otherwise noted.

To investigate the performance of the doped polymer film in wettability switching after extended time storage, the NaDBS-doped PPy films were stored in an air tight box. For checking this, the contact angle of the storage films was measured at three stages: prior to applying a potential, after applying a reductive potential, and after applying an oxidative potential. Fig. 4.6A shows the NaDBS-doped PPy maintained its wettability switching behavior for a longer period, and oxidized (as-deposited) film is highly stable in ambient circumstances [31]. It should be noted that at the room temperature, the reduced film changes its wettability behavior as time elapsed (Fig. 4.6B), and the reduced surface became super hydrophilic (contact angle 5 ± 3 degrees) after 60 min to 90 min and increased again after 90 min. An increased contact angle indicating the reduced film is more susceptible to oxidation in air. The film was kept at open air after applying -0.8 V.

4.4.2 Characterization of the valve

To demonstrate flow control, a 100- μm long valve with a NaDBS-doped PPy layer was formed in a straight flow channel (500 μm wide) (Fig. 4.7A). A solution containing 0.1 M KCl was injected into the solution reservoir. The solution started to move by capillary action and was stopped at the valve edge. When -0.9 V was applied to the platinum electrode, the surface area of the valve that was in contact with the solution became more hydrophilic and the solution passed through the valve region. Once the solution reached the end of the valve, the solution flowed forward in the flow channel by capillary action. It should be noted that the stopped solution immediately started to move after applying a potential to the electrode and the length of time for the solution to cross the 100- μm long valve area was 5s. Without applying the potential, the valve could stop the solution stably for more than 10 min. The 100- μm valve could stop the solution effectively even in a 1-cm wide flow channel.

Switching time of the valve was measured as the length of time for the solution to start moving from one edge of the valve and reach the opposite edge of the valve after the application of the potential. To measure the switching time, valves of different lengths were formed. Here, the length of the valve (L) indicates the length along the flow channel (Fig. 4.2B). Fig. 4.7B shows the switching time of the valves of different lengths. The switching time decreased with the decrease in valve length and was the shortest (5 s) with 50 μm long valves. The effect of applied

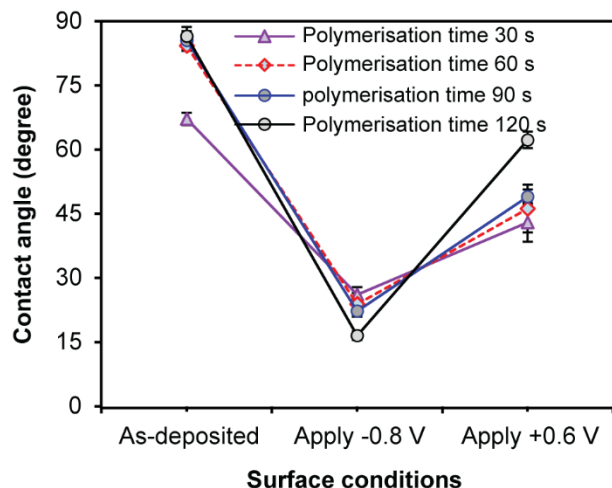


Figure 4.5. Dependence of the wettability changes (contact angle differences) of NaDBS-doped PPy film on polymerization time at three stages switching cycle: as-deposited film, reduced film, and oxidized film. Error bars represent \pm standard deviation over 5 replicates.

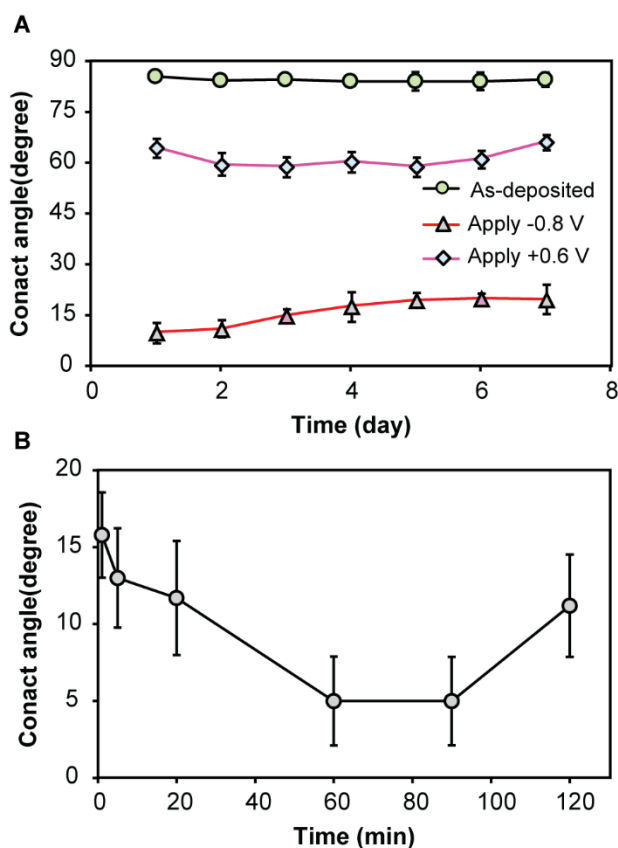


Figure 4.6. (A) Wettability behavior of the NaDBS-doped PPy film with the elapsed time. Error bars represent \pm standard deviation over 3 replicates. (B) Dependence of the water contact angle of the NaDBS-doped PPy reduced (applied -0.8 V) film on the elapsed time. Error bars represent \pm standard deviation over 10 replicates.

potential on the switching time for 100- μm long valves is shown in the Fig 4.8. When potential was more positive than -0.8 V , no influence was observed. However, the switching time decreased to $5 \pm 1\text{ s}$ with potentials more negative than -0.8 V .

The effect of solution pH on switching time was examined using a 100- μm long valve (Fig. 4.9). The switching time became longer in the pH range between 2 and 4, became almost steady in a pH range between 5 and 9, and substantial decrease at the pH of 10. However, at the higher pH range between 11 and 13, the valve did not function properly and the solution moved across the valve area without the application of the potential. The result can be explained by the fact that the polymer chain undergoes deprotonation in higher pH which results of the as-deposited oxidized polymer film to neutral by delocalization of the electron pair over pyrrole ring [24]. As a result, the dopant molecules are reoriented for overall charge neutralization in the doped PPy film and the surface becomes hydrophilic at the higher pH region.

We also examined the storage stability of the valve. For this purpose, 100- μm long valves were formed under the same condition and stored under oxygen free environment in an air tight box. The valve function was tested every 2 days until day 7. The valve showed stable operation until day 5 without any problems. However, the switching time increased after 5 days (Fig. 4.10). This is due to the fact that the doped PPy film may be more susceptible to oxidation in air or after keeping for extend period, the glass substrate may become hydrophobic little bit.

4.4.3 Decreasing the switching time

Dopant and doping level can substantially influence on the wettability of PPy [32]. Therefore, effect of the dopant concentration on the valve switching time was examined using the 100- μm long valves formed with NaDBS of different concentrations. Fig. 11A shows the influence of dopant concentration on the valve function. When the concentration was higher than 0.2 M, the solution never stopped at the valve edge and passed over the valve without the application of potentials. To support this phenomenon, water contact angle of the doped polymer film on the flat platinum surface with different dopant concentration was examined (Fig. 4.11B). When the dopant concentration was 0.4 M, we observed that the smooth film was not formed and an average contact angle of the as-deposited film was 54 ± 3 degrees. On the other hand, the switching time was substantially reduced to 2 s and 1 s when the dopant concentration was 50 mM and 25 mM, respectively and the contact angle of the as-deposited film were 85 ± 0.5 degrees and 86 ± 1 degrees, and the reduced film was 16 ± 2 degrees for both cases.

4.4.4 Controlled operation of the valve in microfluidic systems

In Fig. 4.12, we demonstrate the control of solution transport by integrating valves of different length ($L=100$,

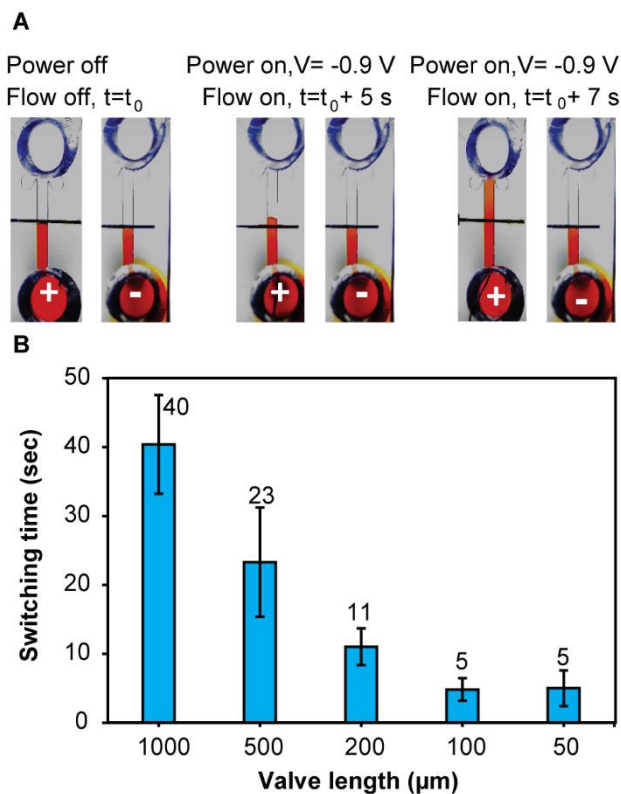


Figure 4.7. (A) Flow control using a 100- μm long valve. Flow channel width: 500 μm . Solution pH: 7.0. The same device structure was used for both cases. In the case of (+), -0.9 V was applied. On the other hand, no potential was applied in the case of (-). (B) Switching times with different length of the valves. Applied potential -0.9 V and solution pH: 7.0. Error bars represent \pm standard deviation over 10 replicates.

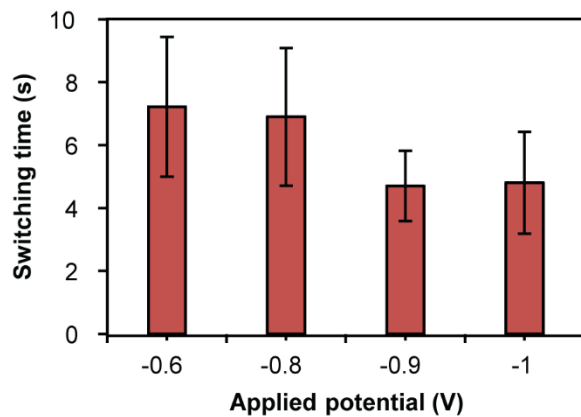


Figure 4.8. Dependence of switching time on applied potential. Valve length: 100 μm . Solution pH: 7.0. Error bars represent \pm standard deviation over 10 replicates.

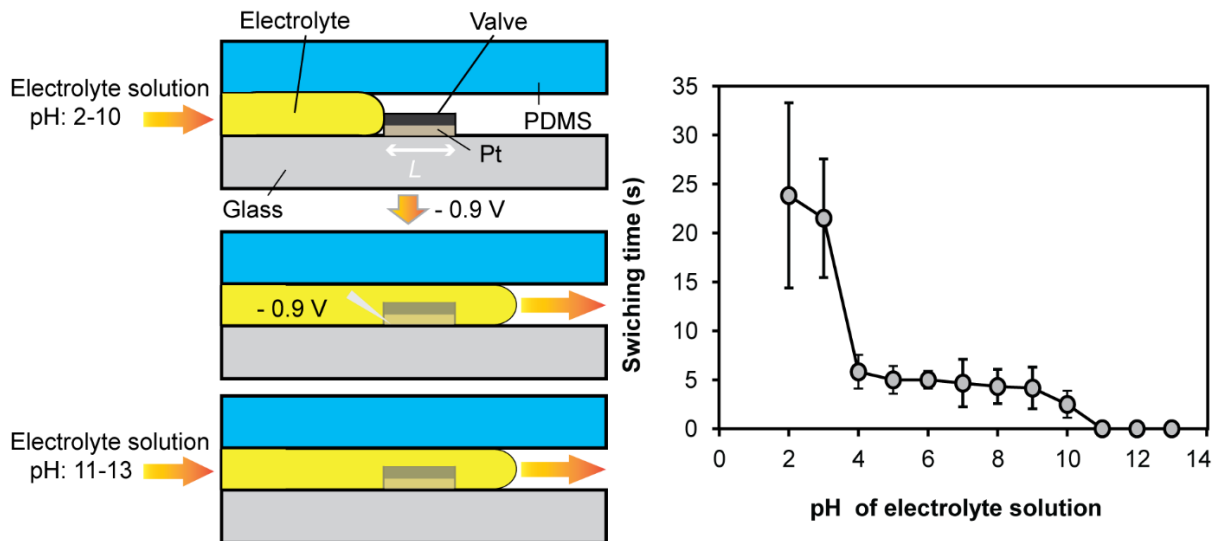


Figure 4.9. (A) Schematic showing the effect of pH on the valve function (100 μm length of valve). (B) Dependence of switching time on the pH of the solution for a 100 μm valve. Error bars represent ± standard deviation over 6 replicates.

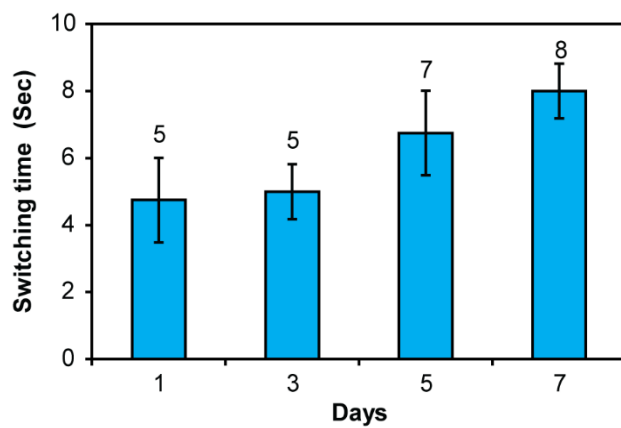


Figure 4.10. Dependence of the switching time on the storage time of the valve. Error bars represent ± standard deviation over 6 replicates.

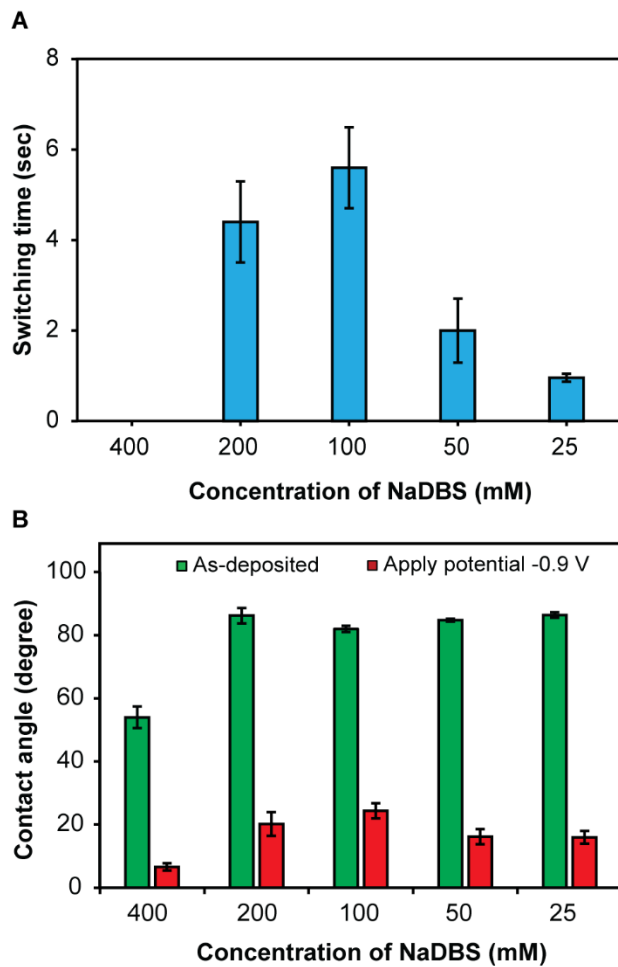


Figure 4.11. (A) Dependence of switching time on the dopant concentration for a 100 μm valve. Solution pH: 7.0. applied potential, -0.9 V ($n=5$). (B) Contact angle changes of the NaDBS-doped PPy film coated platinum with different dopant concentration for as-deposited film and reduced film (applied potential -0.9 V). ($n=5$) Five measurements were carried out for each data point, and the averages and standard deviations are shown

50, 20 and 10 μm) into the straight flow channel. In this case, all valves are connected to a common contact pad. When the solution wets the electrodes, the electrical circuit is completed. Upon the application of an appropriate potential, only the valve that is contact with the solution is opened, and the solution can be passed through the valves step by step. Initially, all the valves were closed, and the loaded solution stops at the edge of 100 μm valve (Fig 4.12 (i)). By applying -0.9 V to the valve electrode, the selective valve is opened and the solution moves forward by the capillary action (Fig 4.12 (ii)-(v)). Therefore, the solution can be moved step by step and the complete on/off flow control is attained by the switching of the electric power “on and off”, respectively.

Fig. 4.13A demonstrates distribution of a solution to multiple flow channels using the valves. In this case, all valves were controlled via the common contact pad. Initially, the potential was applied to open the valves that were in contact with solution, after that the switch was “off” and the switch was “on” again to open the subsequent valves. The injected solution stops at valve 1 and 2 (Fig. 4.13A (i)). By applying potential -0.9 V , the solution is transported by opening the valve 1 and 2 and solution stopes at valves 3 and 4 (Fig. 4.13A (ii)). After that, by applying potential -0.9 V , the valve 3 and 4 are opened and solution stops at the valves 5 and 6. Similarly, the valves are opened 5 and 6 and the solution allows to move forward (Fig. 4.13A (iii)).

Fig. 4.13B shows a radial flow channel structure with eight valves that is operated independently. In this case, the solution can be distributed selectively to the eight different microchannels from the inlet reservoir located at the center. Solutions loaded in the inlet stopped at the valves (Fig. 4.13B (i)). Selected flow channels were opened by applying the potential (Fig. 4.13B (ii-iv)). Fig. 4.13C shows a device with six-valves formed in a comb-shaped flow channel structure. In the same manner, by applying potential -0.9 V to the desired electrode, the solution penetrates into selected flow channels by opening a selected valve (Fig. 4.13C (ii-iv)).

4.4.5 Application to the flow focusing device

We also validated the applicability of the valves in a flow focusing device. The hydrodynamic flow focusing device consisted of the valve with the NaDBS-doped PPy and 500- μm wide PDMS main flow channel, 1000- μm wide sheath flow channel, two inlet reservoirs, and an outlet (Fig. 4.14). Purple color dye solution used to sheath focus of yellow dye solution (Fig 4.14 (right)). The single valve (100 μm long) was integrated into the flow focus device in which valve is formed along the main flow channel (middle) and sheath flow channel. When the valve was closed, the yellow solution containing 0.1 M KCl loaded into the inlet of the main flow channel was stopped at the valve position 1, and subsequently the violet solution containing 0.1 M KCl loaded into the inlet of the sheath flow channel is stopped at the valves 2 and 3 (Fig 4.14). In this case, the electric circuit is completed by wetting the valve electrode with the electrolyte solution at three locations 1, 2, and 3. By applying potential -0.9 V to the valve electrode, all of the stopped solutions started to move forward at a time, and allowed rapid enabling of hydrodynamic focusing in the main flow channel (Fig. 4.14 (right)).

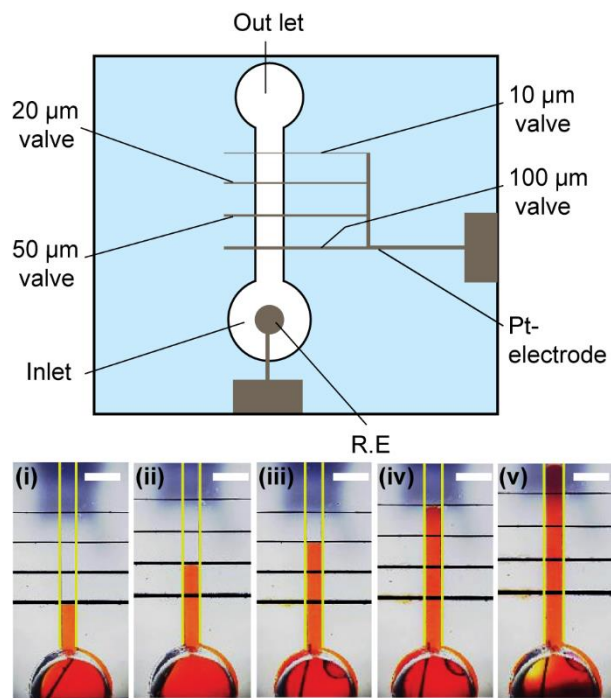


Figure 4.12. Precise solution manipulation and control is demonstrated using multivalves with different length in microchannel. Scale bar: 1mm.

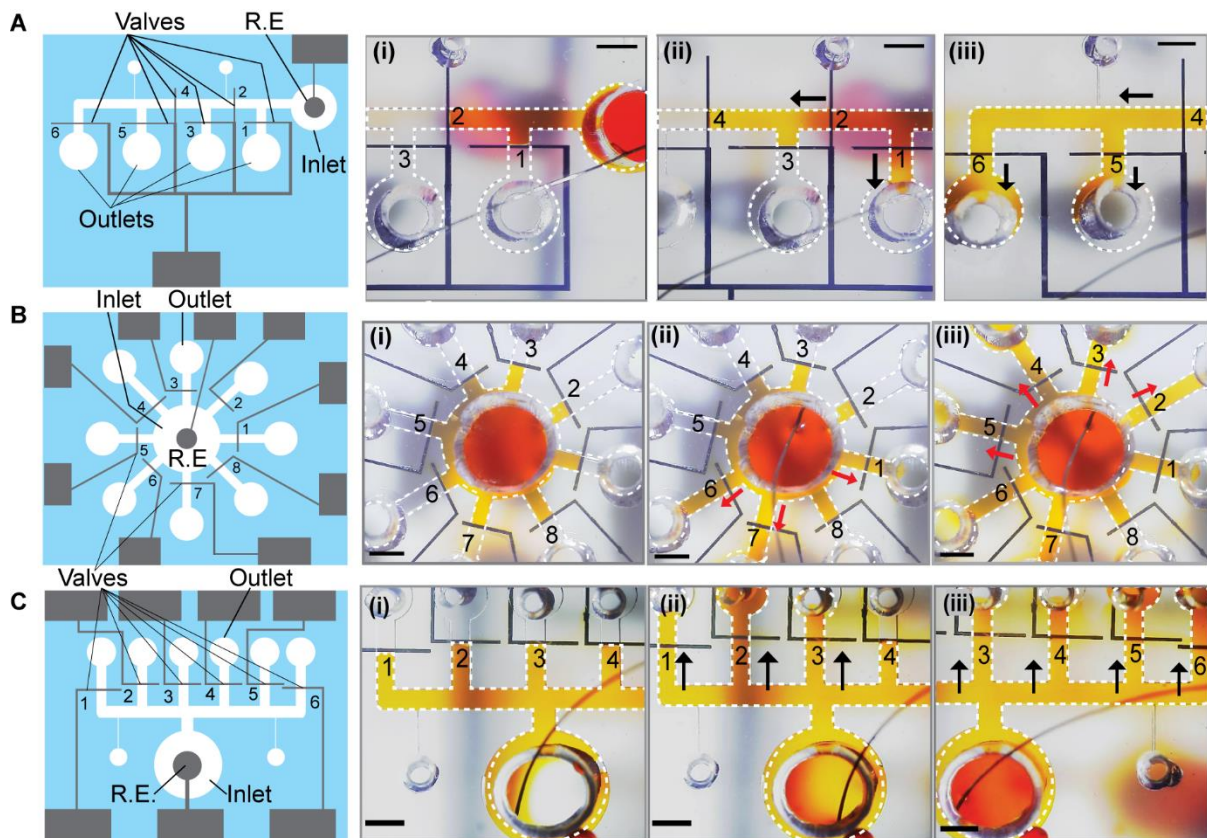


Figure 4.13. Controlled microfluidic transport using multiple integrated valves. (A) Linear multiplexer. (B) Radial multiplexer. (C) comb-shape multiplexer. To aid visualization, a dye solution containing 0.1 M KCl (pH 7) was used. Scale bar: 1 mm. R.E.: reference electrode, μC : microchannel.

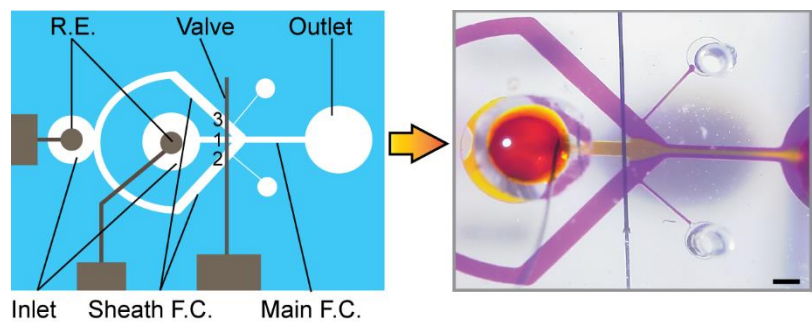


Figure 4.14. PDMS flow focusing device with NaDBS-doped PPy based microvalve. Hydrodynamic focusing state is enabled by opening the valve upon the application of potential. Scale bar: 1 mm. F.C.: Flow channel.

4.4.6 Application the valve to use repeatedly

As the doped PPy film can change the wettability reversibly upon the application of an appropriate potential, we then checked repeatability of the valve function once the valve opened. The regeneration capability of the valve was investigated by integrating the valve in the straight flow channel microfluidic device. When a first solution was injected into the inlet, the solution stopped at the valve. By applying -0.9 V to the valve electrode, the solution passed over the valve region. During this period, $+0.6$ V was applied to the valve electrode to return to the hydrophobic state. After the solution was flushed from the flow channel, the next solution was injected, the solution passed over the valve without stop at the valve. Although the valve surface can change the wettability from hydrophilic to hydrophobic state by the application of $+0.6$ V, the hydrophobicity of the valve surface (water contact angle ~ 60 degree, as shown in Fig. 4.4C) may not be enough to stop the second solution at the valve. Therefore, to use the valve repeatedly for manipulating the solution on demand, two air-vent were formed at the valve in a flow channel for the formation more hydrophobicity at the valve area (Fig. 4.15). The valve with air vent could stop the next solution at the valve once the valve opened (Fig. 4.15). Thus, an air layer (from both sides of the valve due to air vent) along with the hydrophobicity of valve may be created the more hydrophobic barrier at the valve region to stop the next solution effectively at the valve, even if the valve and flow channel were used repeatedly.

4.4.7 Application of the valve into the integrated device

To investigate the exchange of solutions efficiently with minimal user intervention, the valves were integrated at two positions of the previous device as described in chapter 3 (Fig. 4.16A). In the integrated device, one additional glass substrate layer was incorporated and the valves (50 μm long) was formed onto platinum electrode on the glass along the flow channels of the top PDMS layer. Additionally, a through-hole was formed in the glass layer by sand blasting. Another valve was formed onto platinum electrode at the bottom glass layer along the extraction flow channel. The solution exchange was initiated by opening the valve 1 (at the top layer), and the preloaded priming solution (0.1M KCl) in the reservoir starts to move to the polymer disc via a circular through-hole and the polymer disc starts to swell by absorbing the priming solution. Due to swelling of the polymer disc, the diaphragm deflects to downward which then exerts pressure to drive the preloaded sample solution from the inlet reservoir to the reaction chamber. When the priming solution was added to the polymer disc, the preloaded solution in the inlet reservoir was not moved for 60 s and the flow appeared after 60 s. After initiating the flow, the reaction chamber was completely filled with a solution within 1 s. When the solution was injected into the reaction chamber, the solution was stopped at valve 2 in the extraction flow channel that was connected to the main flow channel. After completely full-filling the reaction chamber, the valve 2 (at the bottom layer) was opened and solution started to move forward to the extraction chamber containing the polymer disc. When the polymer disc contact with the solution, the solution was then started to extract from the reaction chamber. In the beginning

the solution was not extracted at all from the reaction chamber, the solution was began to extract after 63 s and the entire solution was extracted within 30 s. The exchange of solution using the integrated device containing a single flow channel is shown in Fig. 4.16C. Using the same mechanism, the sequential exchange of multiple solutions were achieved efficiently using an integrated device with four flow channels Fig. 4.16D.

4.5. Conclusions

A simple PPy-based switchable hydrophobic valve can be realized by forming a hydrophobic NaDBS-doped PPy film on a platinum electrode. The PPy film becomes hydrophilic upon the application of an appropriate potential, and the solution stopped at the valve passes through the valve region. This hydrophobic valve can manipulate the fluid movement on demand in flow channel upon the application of the potential. Without applying the potential, the valve could stop the solution stably for more than 10 min even using the 50- μm long valve. To operate the valve, application of a potential for a short time is sufficient. The valve is easy to fabricate and is suitable for microfluidic systems directed to point-of-care testing.

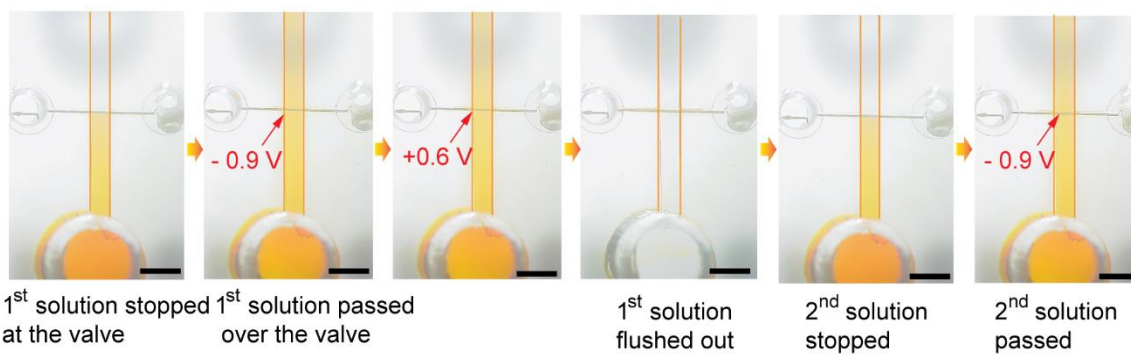
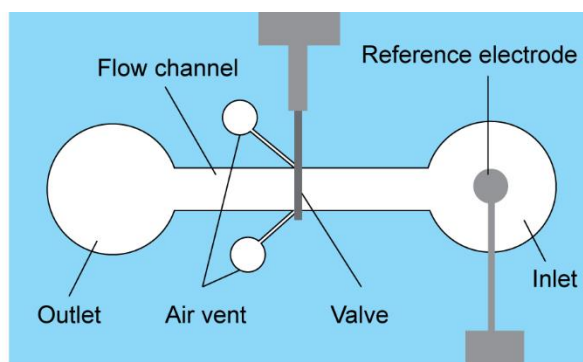


Figure 4.15. Device structure for the regeneration of the valve. The valve is used repeatedly for manipulating the solution on demand. Scale bar 1 mm.

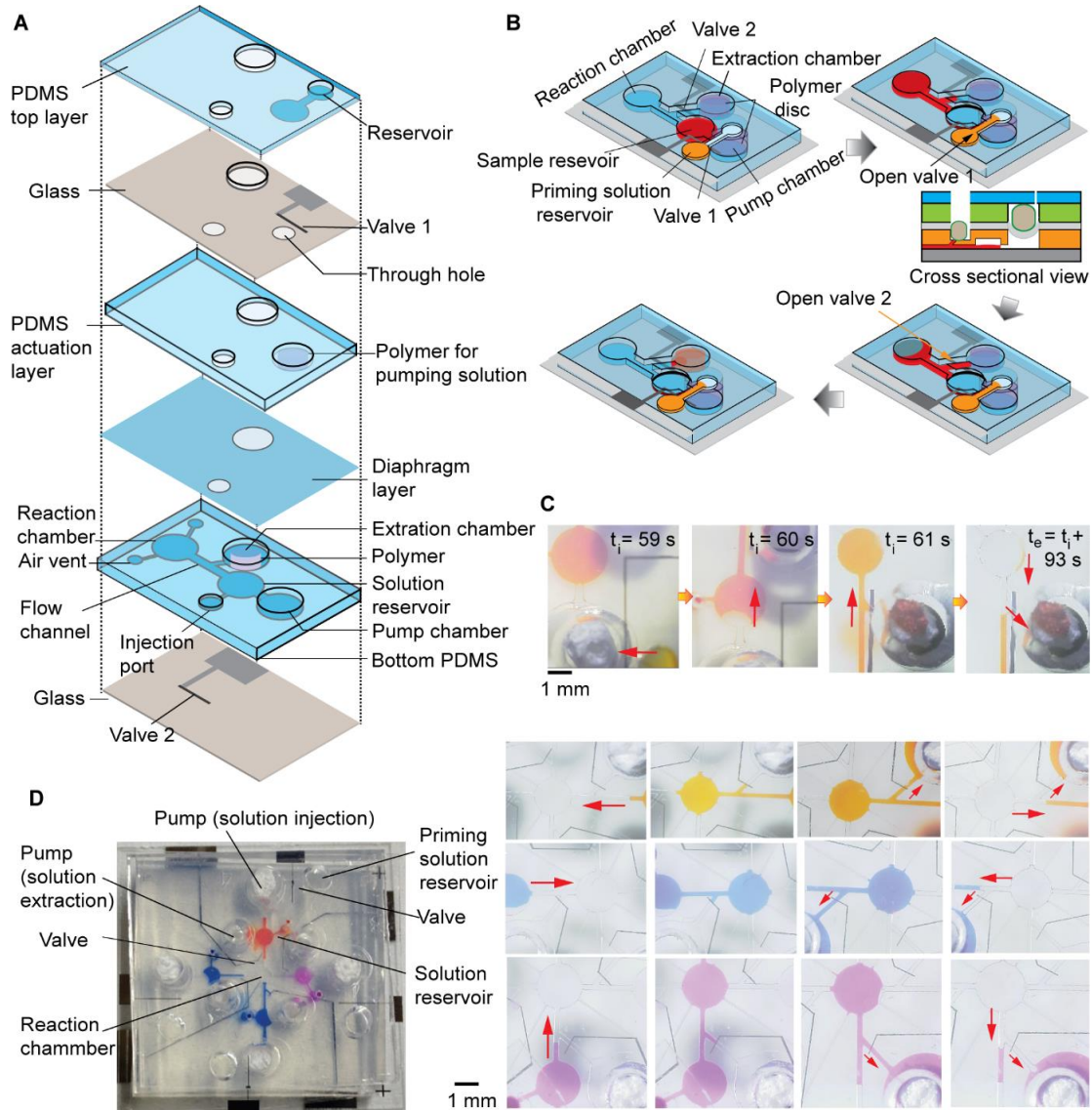


Figure 4.16. Exchange of solutions with minimal user handling steps. (A) Device structure of the integrated device with single flow channel. (B) Mechanism of the exchange of solutions. (C) Images that show exchange of solutions using integrated device with single flow channel. (D) Photograph of the integrated device with four flow channels and images showing the exchange of multiple solutions.

References

1. Lei, K. F., *Journal of laboratory automation*, **2012**, 17(5), 330-347.
2. Henares, T. G., Mizutani, F., & Hisamoto, H., *Analytica chimica acta*, **2008**, 611(1), 17-30.
3. Lei, K.F., Wu, M.H., Hsu, C.W. & Chen, Y.D., *Biosensor & Bioelectronics*, **2014**, 51, 16-21 (2014).
4. Sackmann, E. K., Fulton, A. L., & Beebe, D. J., *Nature*, **2014**, 507(7491), 181.
5. Au, A. K., Lai, H., Utela, B. R., & Folch, A., *Micromachines*, **2011**, 2(2), 179-220.
6. Oh, K. W., & Ahn, C. H., *Journal of micromechanics and microengineering*, **2006**, 16(5), R13.
7. Wang, Y. N., & Fu, L. M., *Microelectronic Engineering*, **2018**, 195, 121–138.
8. Laser, D. J., & Santiago, J. G., *Journal of micromechanics and microengineering*, **2004**, 14(6), R35.
9. Zhang, C., Xing, D., & Li, Y., *Advances and trends. Biotechnology advances*, **2007**, 25(5), 483-514.
1. Jang, L. W., Razu, M. E., Jensen, E. C., Jiao, H., & Kim, J., *Lab on a Chip*, **2016**, 16(18), 3558-3564.
2. Huang, S., Li, C., Lin, B., & Qin, J., *Lab on a Chip*, **2010**, 10(21), 2925-2931.
3. Unger, M. A., Chou, H. P., Thorsen, T., Scherer, A., & Quake, S. R., *Science*, **2000**, 288(5463), 113-116.
4. Lin, S., Wang, W., Ju, X. J., Xie, R., & Chu, L. Y., *Lab on a Chip*, **2014**, 14(15), 2626-2634.
5. Baek, S. K., Yoon, Y. K., Jeon, H. S., Seo, S., & Park, J. H., *Journal of Micromechanics and Microengineering*, **2013**, 23(4), 045006.
6. Kong, L. X., Parate, K., Abi-Samra, K., & Madou, M., *Microfluidics and Nanofluidics*, **2015**, 18(5-6), 1031-1037.
7. Díaz-González, M., Fernández-Sánchez, C., & Baldi, A., *Lab on a Chip*, **2016**, 16(20), 3969-3976.
8. Rogers, C. I., Oxborrow, J. B., Anderson, R. R., Tsai, L. F., Nordin, G. P., & Woolley, A. T., *Sensors and Actuators B: Chemical*, **2014**, 191, 438-444.
9. Cho, H., Kim, H. Y., Kang, J. Y., & Kim, T. S., *Journal of colloid and interface science*, **2007**, 306(2), 379-385.
10. Handique, K., Burke, D. T., Mastrangelo, C. H., & Burns, M. A., *Analytical chemistry*, **2000**, 72(17), 4100-4109.
11. Andersson, H., van der Wijngaart, W., Griss, P., Niklaus, F., & Stemme, G., *Sensors and Actuators B: Chemical*, **2001**, 75(1-2), 136-141.
12. Londe, G., Chunder, A., Wesser, A., Zhai, L., & Cho, H. J., *Sensors and Actuators B: Chemical*, **2008**, 132(2), 431-438.
13. Rios, F., & Smirnov, S. N., *Chemistry of Materials*, **2011**, 23(16), 3601-3605.
14. Biswas, G. C., Watanabe, T., Carlen, E. T., Yokokawa, M., & Suzuki, H., *ChemPhysChem*, **2016**, 17(6), 817-821.
15. Kenanakis, G., Stratakis, E., Vlachou, K., Vernardou, D., Koudoumas, E., & Katsarakis, N., *Applied Surface Science*, **2008**, 254(18), 5695-5699.

16. Hamed, M. M., Campbell, V. E., Rothmund, P., Güder, F., Christodouleas, D. C., Bloch, J. F., & Whitesides, G. M., *Advanced Functional Materials*, **2016**, 26(15), 2446-2453.
17. Xu, L., Chen, W., Mulchandani, A., & Yan, Y., *Angewandte Chemie International Edition*, **2005**, 44(37), 6009-6012.
18. Narahari, T., Dendukuri, D., & Murthy, S. K., *Analytical chemistry*, **2017**, 89(8), 4671-4679.
19. Murray, P., Spinks, G. M., Wallace, G. G., & Burford, R. P., *Synthetic metals*, **1997**, 84(1-3), 847-848.
20. Kim, J. H., Lau, K. T., Shepherd, R., Wu, Y., Wallace, G., & Diamond, D., *Sensors and Actuators A: Physical*, **2008**, 148(1), 239-244.
21. Tsai, Y. T., Choi, C. H., Gao, N., & Yang, E. H., *Langmuir*, **2011**, 27(7), 4249-4256.
22. Bay, L., Jacobsen, T., Skaarup, S., & West, K., *The Journal of Physical Chemistry B*, **2001**, 105(36), 8492-8497.
23. Zhou, M., & Heinze, J., *Electrochimica Acta*, **1999**, 44(11), 1733-1748
24. Sadki, S., Schottland, P., Brodie, N., & Sabouraud, G., *Chemical Society Reviews*, **2000**, 29(5), 283-293
25. Otero, T. F., Marquez, M., & Suarez, I. J., *The Journal of Physical Chemistry B*, **2004**, 108(39), 15429-15433.
26. Mecerreyes, D., Alvaro, V., Cantero, I., Bengoetxea, M., Calvo, P. A., Grande, H., & Pomposo, J. A., *Advanced Materials*, **2002**, 14(10), 749-752.
27. Matencio, T., De Paoli, M. A., Peres, R. C. D., Torresi, R. M., & De Torresi, S. C., *Synthetic metals*, **1995**, 72(1), 59-64.
28. Isaksson, J., Tengstedt, C., Fahlman, M., Robinson, N., & Berggren, M., *Advanced Materials*, **2004**, 16(4), 316-320.
29. Golabi, M., Turner, A. P., & Jager, E. W., *Macromolecular Chemistry and Physics*, **2016**, 217(10), 1128-1135.
30. Xu, L., Wang, J., Song, Y., & Jiang, L., *Chemistry of Materials*, **2008**, 20(11), 3554-3556.
31. Omastova, M., Trchova, M., Kovářová, J., & Stejskal, J., *Synthetic Metals*, **2003**, 138(3), 447-455.
32. Liu, M., Zhang, Y., Wang, M., Deng, C., Xie, Q., & Yao, S., *Polymer*, **2006**, 47(10), 3372-3381.

Chapter 5: Summary

In this thesis, the development of microfluidic device with on-chip solutions exchange facility for immunoassaying is presented. The efficient solutions exchange in microfluidic device are demonstrated by the integration of SP polymer-based micropumps and polypyrrole-based valves.

Chapter 1 explains the present status of the infectious diseases in both developing and developed countries, as the infectious diseases have been emerged a key healthcare concern in developing countries. In this context, the necessity of perfect POCT diagnostics for infectious diseases is a critical factor of clinical developments and general public health. We explained the current constraints of the POCT tools in the application and the state of art of the present solutions of POCT tools were focused for the developing countries. A summary of the current advances of the microfluidics technologies toward POCT for infectious diseases were described. The crucial characteristics of such technologies for the advancement of an entirely integrated POCT tool were presented. The advances of microfluidic components to control the flow in microfluidic technology were also discussed. The aims of this study were mentioned regarding the development of inexpensive and effective microfluidic immunoassay platform for POCT.

Chapter 2 described a valve-less microfluidic device with push-pull sequential solution exchange function for fluorescence immunoassay. In this respect, a simple valve-less microfluidic device consisting of a reaction chamber and eight flow channels was developed to exchange multiple solutions for biochemical analyses. Solutions can be exchanged by only injecting a solution from reservoirs into the reaction chamber and returning the solution to each reservoir. For the efficient solution exchange, the flow channel was optimized by designing a 50- μm constriction in the flow channels at the entrance of the reaction chamber. With this structure, the most reproducible results in the exchange of solutions were attained, and a unique microfluidic design can be retained solutions only in the reaction chamber for more than 30 min during the incubation periods, thereby eliminating the need of integration of micro-valves. Furthermore, the hydrophobicity of the reaction chamber and viscosity effect of the blocking solution were not interrupted to the smooth solution exchange in the microfluidic device. The device is applicable to the detection of proteins. IL-2 could actually be detected within 25 min by consuming minimal volume (nL) sample or reagents. Protein (e.g. IL-2) can be detected with high sensitivity (detection limit 105 pg/mL or 9.0 pM). Reaction surface especially PDMS treated with the oxidative solution, following cAb immobilization and blocking with 0.5% BSA+ 0.01% Tween-20, and subsequent washing with a solution containing 0.01% Tween-20 and PBS can substantially be reduced non-specific binding of the protein. Although the approach can offer a simple solution handling system using disposable syringe with hand pressure, in some cases, the assay was lost reproducibility due to apply uneven pressure during the exchange of solutions or washing steps. Toward integrating the micropumps, the mechanism of the push-pull movement of the diaphragm was applied to manipulate the solution. Solution movement was achieved by applying pressure with the rod to the

solutions through a diaphragm placed on the solution reservoirs. For the application to POCT, automatic assay procedures including exchange of solutions autonomously on-chip is currently desired. The automatic approach could be effective to reduce the variance of the assay results as well as access to end-users.

Chapter 3 presented a polymer-based on-chip micro-pump for the exchange of solutions sequentially in the valve-less microfluidic device. Specifically, a simple micropump based on without external instruments was used to realize automatic solution exchange in the developed immunoassay device. For this purpose, a micropumps were designed using cylindrical freeze-dried polymer discs consisting of superabsorbent polymer (SAP), sodium polyacrylate (SP), and cellulose acetate (CA) for solution injection into and extraction from the reaction chamber. By the swelling property of the polymer disc, SP polymer actuated diaphragm micropump was designed for solution injection from the inlet to the reaction chamber. On the other hand, for the extraction of solution from the reaction chamber, an extraction pump was designed by the super-absorbing property of the polymer disc. When water is added to polymer disc, the diaphragm undergoes deformation to the downward by the volume change of the polymer disc and the pump generates a positive pressure to transport the solution from the solution reservoir into the reaction chamber. After completely full-filling the reaction chamber with the solution, it was extracted from the reaction chamber by the generation of a negative pressure after inserting the polymer disc into the extraction chamber, and the whole solution was extracted from the reaction chamber through the same flow channel.

Initially, the injection pump chamber and extraction pump chamber were optimized to attain an efficient exchange of solution. The injection pump chamber was optimized by measuring the injection flow rate using the pump of different cross-sectional area of the pump chambers, and the highest flow rate was 25.8 $\mu\text{L}/\text{min}$ for the pump chamber of the cross-sectional area of 15.9 mm^2 . The extraction chamber of the extraction pump was optimized based on the solution extraction capability of the polymer disc after inserted into the extraction chamber. And the entire solution could effectively be extracted from the reaction chamber using an extraction chamber of 4 mm in diameter circular chamber with a through-hole of 3 mm in diameter.

The pump performance was then evaluated by the exchange of multiple solutions using the integrated device in which the injection and extraction pump were connected to the reaction chamber through the flow channels. Furthermore, the device performance was characterized by checking the solution exchange capability using the pumps. For this purpose, the injection and extraction flow rates were measured of the aqueous sample solutions containing deionized water (DI), 0.1 M KCl, 0.1% (v/v), 1 M KCl, 0.1% (v/v), Glycerol (2X dilution) and Glycerol (99 %). Other than viscous solutions, an average injection flow rate of sample solutions was the same (25.8 $\mu\text{L}/\text{min}$). The extraction flow rate was highest ($\sim 0.73 \mu\text{L}/\text{min}$) for DI water and no solution was extracted for 99% glycerol solution. The extraction flow rate was substantially low for the other cases.

Both injection and extraction flow rates of the polymer-based pump could be adjusted by selecting an appropriate priming solution and appropriate composition/proportion of the materials used to make the polymer

discs, respectively. The injection flow rate was tuned by using NaCl solutions of different concentrations and the flow rates decreased gradually with the increases NaCl concentration. The best result and optimum extraction flow rate was achieved using a polymer disc when the ratio of SP and CA was 1:1.5, and prepared with DI water.

Chapter 4 illustrated control of microfluidic solution transport by switchable hydrophobic microvalves based on the conducting polymer. The valve structure was made by bonding a poly(dimethylsiloxane) (PDMS) substrate with a flow channel structure and a glass substrate with a thin-film platinum electrode on which a surfactant sodium dodecylbenzene sulfonate-doped polypyrrole film (NaDBS-doped PPy) was formed. NaDBS-doped PPy was deposited on the platinum electrode from a freshly prepared solution containing 0.2 M pyrrole and 0.2 M NaDBS. A constant current (1 mA/cm^2) was applied to the platinum electrode for 120 s. The valve operation was based on the change in wettability of the NaDBS-doped PPy film under the application of the reductive and oxidative potential. First, an appropriate dopant (surfactant) was selected by measuring the water contact angle of the PPy film when NaDBS and the other dopant, sodium dodecyl sulfate (NaDS), were used. The change in the wettability of the PPy film could be enhanced by the addition of a dopant NaDBS as confirmed by contact angle measurement.

To demonstrate flow control, a 100- μm long valve with a NaDBS-doped PPy layer was formed in a straight flow channel (500 μm wide). A solution to be transported (0.1 M KCl in this case) is injected into the solution inlet. The solution immediately moved in the flow channel by capillary action but stops at the edge of the valve. When -0.9 V was applied to the platinum electrode of the valve, the hydrophobic NaDBS-doped PPy film became hydrophilic via reorientation of dopant molecules from the point of contact with the electrolyte solution. Once the solution passed the valve area, the solution moved forward in the flow channel again by capillary action. Without applying the potential, the valve could stop the solution stable for more than 10 min even using the 50- μm long valve. Then, switching time (time for the solution to cross the valve area after the application of the potential) was measured by forming valves with various lengths, L . With a 50- μm long valve, average switching time was 5 s. The effect of solutions pH on switching time were observed using a 100- μm long valve. At higher pH range (11 to 13), the valve did not function properly and the solution moved across the valve area without applying any potential. Also, the switching time decreased with the increase pH of the solutions. After the storage of the valve, the valve can be functioned more than 7 days without any problems.

The dopant concentration had an effect on valve switching time. The switching time could be reduced from 5 s to 1 s by choosing the dopant concentration of 25 mM and the valve could not be functioned properly at the dopant concentrations of higher than 0.2 M. The valve also be used repeatedly once the valve opened. The solutions manipulation and control within the complex microfluidic were achieved by integrating the multivalves. Finally, the valve was integrated to realize the precise exchange of multiple solutions in a microfluidic device with minimum user intervention. The simple structure and operation enabled controlled transport of solutions in a network of flow channels for applications such as biochemical analyses or others.

The studies introduced here are considered an important first step on the road to development of a portable device for immunoassay. A microfluidic device with incorporation of micropumps and valves was demonstrated to realize the exchange of multiple solutions efficiently on-chip. Although excellent performance of the device has already been demonstrated toward an automatic device function, there are still some points to be deliberated for further development of more advanced devices for POCT.

Appendix

Information about the reagents, materials, equipment used for the fabrication, test and evaluation of devices as well as experiments stated in the chapter 2 to chapter 4 are outlined below.

Reagents and materials

- Glass substrate: (wafer of 3 inch diameter) Pyrex glass material, $76.2 \times 0.5 \mu\text{m}$, Corning Japan.
- Positive photoresist: Microposit, S1818, Shipley.
- For a positive resist developing solution: Microposit developer, MF319, Shipley.
- For a thick film negative photoresist: SU-8, Microchem.
- SU-8 for the developer: SU-8 developer, Microchem.
- PDMS (Polydimethylsiloxane) precursor: KE-1300T, ShinEtsu.
- PDMS curing agent: CAT-1300, ShinEtsu.
- Dry film photoresist: A5312-02-B02, Mitsubishi paper mills ltd., Osaka, Japan.
- Negative photoresist (OMR 83) from Tokyo Ohka Kogyo, Kawasaki, Japan
- Potassium chloride: KCl, Wako Pure Chemistry.
- 25% ammonia water: NH_4OH , Wako Pure Chemistry.
- 30% hydrogen peroxide: H_2O_2 , Wako Pure Chemistry.
- Acetone: $\text{C}_3\text{H}_6\text{O}$, Wako Pure Chemistry.
- Toluene: $\text{C}_6\text{H}_5\text{CH}_3$, Wako Pure Chemistry.
- 2-propanol: $\text{C}_3\text{H}_8\text{O}$, Wako Pure Chemistry.
- Sulfuric acid: H_2SO_4 , Wako Pure Chemistry.
- Hydrochloride: HCl, Wako Pure Chemistry.
- Disodium hydrogen phosphate: Na_2HPO_4 , Wako Pure Chemistry.
- Potassium dihydrogen phosphate: KH_2PO_4 , Wako Pure Chemistry.
- Potassium ferricyanide: $\text{K}_3\text{Fe}(\text{CN})_6$, Wako Pure Chemistry.
- Sodium polyacrylate: Sigma-Aldrich, St. Louis, USA.
- Cellulose acetate: Wako Pure Chemistry.
- Hydroxypropyl cellulose: Wako Pure Chemistry.
- Silver nitrate: AgNO_3 , Wako Pure Chemistry.
- Potassium nitrate: KNO_3 , Wako Pure Chemistry.
- Sodium hydroxide: NaOH, Wako Pure Chemistry.
- Bovine serum albumin (BSA): Wako Pure Chemistry.

- (3-aminopropyl)triethoxysilane (APTES): Shin-Etsu Chemical, Tokyo, Japan.
- Etchall® etching crème: B & B Etching Products, Inc., Arizona, USA.
- Amplex Red: 10-acetyl-3,7-dihydroxyphenoxazine, AnaSpec, Inc.
- Silver wire: 0.5 mm (diameter), The Nilaco Corp.
- Food dye red: No 102, KYORITSU FOODS.
- Food dye blue: No 1, KYORITSU FOODS.
- Food dye green: No 1, No. 4, KYORITSU FOODS.
- Food dye yellow: No 4, KYORITSU FOODS.
- Orange G (C₁₆H₁₀N₂Na₂O₇S₂): MERCK, Darmstadt, Germany.
- Methylviolet (C₂₄H₂₈N₃Cl): MERCK, Darmstadt, Germany.
- Sunset yellow FCF (C₁₆H₁₀N₂Na₂O₇S₂): Wako Pure Chemistry.
- Human IL-2 ELISA MAX Deluxe: BioLegend, San Diego, CA
- FITC Labeling kit: Thermo Scientific, Rockford, USA.
- Pyrrole from Sigma-Aldrich, St. Louis, USA.
- Sodium dodecylbenzenesulfonate (NaDBS) from Sigma-Aldrich, St. Louis, USA.
- Sodium dodecylsulphate (NaDS) from Wako Pure Chemical Industries, Osaka, Japan.

Equipment

- Sputter deposition equipment: CFS-4ES-231, Shibaura Eletec.
- Spin coater: 1H-D7, Mikasa.
- Mask aligner: MA-10, Mikasa.
- Dicing equipment: A-WD-10A, Tokyo seimitsu.
- Dry oven: OF-450, AS ONE.
- Hot plate: ND-1, AsOne.
- Basic plasma kit: BP-1, Samco.
- Pure water manufacturing equipment: DirectQ 3 UV with pump, Millipore.
- Potentiostat / galvanostat: HA-151, Hokuto denko.
- Electro meter: HE-104, Hokuto denko.
- Electro meter: PGSTAT12, Autolab, inter Kemi.
- UV irradiation device: ENF-280C / J, Spectronics.
- Laser processing machine: LaserPRO C180, Comnet.
- Thermostatic bath: WBS-80A, AS ONE.
- PH meter: Seven compact S220, METTLER TOLEDO.

- Contact angle meter: Model G-1-1000, ERMA INC., Tokyo, Japan.
- Microscope: SMZ1500, Nikon.
- CCD camera: DCR-SX41, Sony.
- Digital cameras: NEX-5N, Sony.
- Laser microscope: VK-8510, Keyence, Osaka, Japan.
- Entity fluorescence microscope system: VB-G25, Keyence.
- Excitation filter: XF1067, Omega Optical.
- Fluorescent filter: XF3081, Omega Optical.
- Fluorescence microscope: IX-73, Olympus, Japan.
- Filter unit: Cy5-4040C, Olympus, Japan.
- CMOS camera: ORCA-Flash 4.0, Hamamatsu Photonics, Japan.
- Silver / silver chloride reference electrode: # 2080A-06T, HORIBA.
- Punch: Punch no. 1256, Takashiba Gimune Seisakujo, Hyogo, Japan
- Biopsy punch: Kai industries, Gifu pref., Japan.
- Sand blaster: SG 106, Hozan tool industries co. ltd., Osaka, Japan.
- Image analysis software: Photoshop CS4, Adobe, ImageJ.

Fabrication of the device

Glass substrate cleaning

The glass substrate was immersed in the washing solution containing 25% NH₃, 30% H₂O₂ and deionized water at a ratio 1: 1: 4 and boil for 5 min. The glass substrate was then removed and boiled again twice in the ultra-pure water for 5 min. Finally, the substrate was dried by blowing nitrogen.

Fabrication of the PDMS pattern

The PDMS substrate with patterns were formed by replica molding using a template formed with a thick-film photoresist SU-8 25. Briefly, the glass wafer was rinsed for 5 min with a solution containing 25% NH₃, 30% H₂O₂ and ultra-pure H₂O (ratio 1:1:4). Then, SU-8 photoresist was spin-coated onto clean glass substrates and prebaked on a hot plate for 10 min at 65°C and for 45 min at 95°C. After that, using mask aligner, UV light was exposed to the coated substrate across the photomask for 150 s and the substrate was then postbaked for 5 min at 65°C and 95°C for 10 min. Finally, the template with the pattern was obtained by developing the substrates with developer solution. The PDMS prepolymer solution was mixed with the curing agent and was immediately poured onto the

template. After curing in an oven for 30 min at 80°C, the PDMS was peeled from the mold and was cut into chips of appropriate dimensions. Solution inlet and outlet ports were formed by forming through-hole using the puncher.

Fabrication of the electrode pattern

The electrode patterns were formed onto the glass substrate by lift-off method. Briefly, a positive was spin-coated onto a clean glass substrate (500 rpm: 5 s → 2000 rpm: 10 s) and baked in an oven at 80 °C for 30 min. After cooling the substrate UV light was exposed to the coated substrate through the photomask for 45 s using a mask aligner. Then the coated substrate was treated with toluene for 30 s and again baked at 80°C for 15 min. The desired pattern for sputtering was then obtained by developing the exposed coated substrate in developer solution for 1 min, wash with DI water and dry by blowing the nitrogen.

For Pt/Cr sputtering, Dry etch initially the pattern substrate was the dry etched at 200 W for 5 min. Then the Cr layer (5 min) and the Pt layer (15 min × 2) were sputtered subsequently onto the glass substrate using the sputtering machine and RF output power was kept at 100 W.

After sputtering, the substrate with a platinum layer was immersed in the acetone for around 1 h and slowly peeled the Pt/Cr layer other than the electrode region from the glass substrate. Finally, the substrate with the pattern was rinsed again with acetone and dried by blowing nitrogen gas.

For Ag sputtering, the positive photoresist again spin-coated onto the pattern substrate and same steps were followed as explained earlier for the desired Ag layer formation. After that the Ag layer was sputtered (15 min × 2) on the glass substrate by sputtering machine and the output power RF was kept 100 W.

Dicing

Initially, a positive photoresist was spin-coated onto a substrate containing electrode pattern (500 rpm: 5 s → 2000 rpm: 10 s and prebaked at 80 °C for 30 min. Then, the wafer was prepared for dicing (substrate placed onto special polymer sheet) and cut into a desired dimension using a dicing saw. Finally, the chips were immersed in acetone to peel the positive resist and dried by blowing N₂.

Formation of a Ag/AgCl reference electrode

The Ag/AgCl layer was formed onto the Ag-electrode of the substrate by using three electrode set-up, where Ag electrode onto substrate, the commercial Ag/AgCl electrode and the platinum plate are used as working electrode, reference electrode and auxiliary electrode, respectively. All the electrode were immersed into a 0.1 M KCl solution that was stirred with a magnetic stirrer. After that, a constant current of 50 nA to the Ag-electrodes for 15 min using autolab and thin Ag/AgCl layer was formed. Finally, the chip was rinsed with DI water and dried with N₂.

Formation of the through hole onto the glass substrate

To make the dry film photoresist pattern, the substrate was placed on the hot plate and heated at 100°C temperature for around 120s. Then, dry film photoresist was transferred onto the hot substrate by removing the bottom polyethelene (PE) layer. The UV light was then exposed to the coated substrate through the photomask for 12 s using mask aligner. After developing the coated substrate with with 0.2 % Na_2CO_3 at 30°C for 3-5 min, the desired pattern was obtained for making through hole by sand blasting method.

The through hole was formed by blasting the sand to pattern at a constant pressure of 75 kPa, using sand blaster (SG 106, Hozan tool industries co. ltd., Osaka, Japan). In this case, the Al_2O_3 particle of the size of approximately 50 μm was used for the purpose. After making the hole, then the substrate was immersed in a solution containing 3 wt% NaOH (40°C) and removed the dry film photoresist from the substrate. Finally, the substrate was cleaned with the solution containing DI water, 25% NH_3 , 30% H_2O_2 at a volumetric ratio 4:1:1 for 1 h and rinsed with DI water and dried with N_2 .

List of publications

Publication

Shishir Kanti Pramanik and Hiroaki Suzuki, “Microfluidic Device with a Push-pull Sequential Solution-Exchange Function for Affinity Sensing”, *Microfluidics and Nanofluidics*, 2019, 23:19.

International conference proceedings

Shishir Kanti Pramanik and Hiroaki Suzuki, “Valve-less Microfluidic Device for Sequential Exchange of Solutions for Fluorescence Immunoassay”, *International Conference on Solid State Devices and Materials (SSDM) 2017*, PS-11-03, 947-948.

Local conference proceedings

Shishir Kanti Pramanik and Hiroaki Suzuki, “Valve-less Microfluidic Device with a Sequential Solution Exchange Function for Fluorescence immunoassay”, *IEEJ Technical Meeting on Chemical Sensor 2017*, 2017 (12), 35-38.

Shishir Kanti Pramanik and Hiroaki Suzuki, “A Valve-Less Microfluidic Device with a Push-Pull Sequential Solution Exchange Function for Fluorescence Immunoassay” *The 61th Chemical Sensor Symposium 2018*, 34, 43-45.

Shishir Kanti Pramanik and Hiroaki Suzuki, “Control of Microfluidic Solution Transport by Switchable Hydrophobic Microvalves Based on Conducting Polymer” *The 35th "Sensor / Micromachine and Application Systems Symposium 2018*, PS-161.

List of conferences

Shishir Kanti Pramanik and Hiroaki Suzuki, “Valve-less Microfluidic Device with a Sequential Solution Exchange Function for Fluorescence immunoassay”, *IEEJ Technical Meeting on" Chemical Sensor 2017*, IEEJ, Himeji, Japan, June, 2017.

Shishir Kanti Pramanik and Hiroaki Suzuki, “Valve-less Microfluidic Device for Sequential Exchange of Solutions for Fluorescence Immunoassay”, *2017 International Conference on Solid State Devices and Materials (SSDM)*, Sendai, Japan, September, 2017.

Shishir Kanti Pramanik and Hiroaki Suzuki, “A Valve-Less Microfluidic Device with a Push-Pull Sequential Solution Exchange Function for Fluorescence Immunoassay” *61th Chemical Sensor Symposium*, Tokyo, Japan, March, 2018.

Shishir Kanti Pramanik and Hiroaki Suzuki, “Control of Microfluidic Solution Transport by Switchable Hydrophobic Microvalves Based on Conducting Polymer” *The 35th "Sensor / Micromachine and Application Systems Symposium*, Sapporo, Japan, October, 2018.

Acknowledgement

It was my pleasure during the last three years and six months as I had an opportunity to work within the Bio-microsystem laboratory in the Department of Nano-science and Nano-technology, University of Tsukuba. I would like to express my gratitude to those peoples who helped me at several stages of the experimental period.

First of all, I would like to express my sincere gratitude to my academic advisor Prof. Hiroaki Suzuki, Graduate school of pure and applied science, Institute of Materials Science, University of Tsukuba, Japan, who gave me an opportunity to do the study in his famous research group. Furthermore, I am indebted to Prof. Hiroaki Suzuki for his encouragement, kind cooperation and scholastic supervision that helped me to finish this thesis. He advised me throughout the project in both theoretical and experimental aspects of the bio-microsystem system. I firmly believe that this thesis could not be possible without his cordial support.

I would also like to thanks to the Japanese government for providing me the financial support such as MONBUKAGAKUSHO (MEXT) fellowship for my study at Japan.

I would also like to thanks to Prof. Masatoshi Yokokawa, Dr. Gokul Chandra Biswas and Dr. Isa Anshori for their valuable discussions.

I am also very grateful to my tutor Tanabe who helped initially to introduce me with many of the laboratory facilities, and thanks to Shinnosuke Tsuchiya, Koki Kariya, Kinari Yokote, and Tabata for their support to fabricate the complete device. I would like to special thanks to all the lab members, former and present for their cordial support at several stages of my experiment.

Last but not least, I am also grateful to my wife, son, daughter, mother, sister, and brother who's sacrificed and encouragement to bring me at the final stage of the research.